

Durham E-Theses

A Chemo-enzymatic Route Towards Nucleoside Triphosphate Synthesis

SIMS, HELEN,PATRICIA,GRETA

How to cite:

SIMS, HELEN,PATRICIA,GRETA (2019) *A Chemo-enzymatic Route Towards Nucleoside Triphosphate Synthesis* , Durham theses, Durham University. Available at Durham E-Theses Online: <http://etheses.dur.ac.uk/13274/>

Use policy

The full-text may be used and/or reproduced, and given to third parties in any format or medium, without prior permission or charge, for personal research or study, educational, or not-for-profit purposes provided that:

- a full bibliographic reference is made to the original source
- a [link](#) is made to the metadata record in Durham E-Theses
- the full-text is not changed in any way

The full-text must not be sold in any format or medium without the formal permission of the copyright holders.

Please consult the [full Durham E-Theses policy](#) for further details.

UNIVERSITY OF DURHAM

**A Chemo-Enzymatic Route
Towards Nucleoside Triphosphate
Synthesis**

Helen Patricia Greta Sims

Supervised by
Dr. David R.W. Hodgson

July 2019

Abstract

Nucleoside 5'-triphosphates (NTPs) are ubiquitous throughout the natural world. As such investigations into their interactions within organisms is essential. Currently, commercially available NTPs are expensive due to the synthetic challenges associated with the formation of phosphoanhydride bonds.

Chemo-enzymatic approaches to NTP synthesis are readily applicable to naturally occurring NTPs, as such these methods have gained traction over recent years. We have investigated a nucleoside diphosphate kinase (NDPK H122G) mediated chemo-enzymatic method for the phosphorylation of nucleoside- 5'-diphosphates (NDPs), using phosphoimidazole as a phosphoryl donor. We developed a synthetic route and a purification procedure, which allowed for the production and partial purification of phosphoimidazole using inexpensive chemical precursors. The optimisation investigations undertaken during the development of the phosphoimidazole synthetic protocol resulted in an increase in phosphoimidazole production from 45% to 55% in the crude reaction solution. Optimisation of the purification procedure led to the production of phosphoimidazole of 98% purity.

NDPK H122G catalysed phosphorylation reactions of adenosine 5'-diphosphate (ADP), were investigated over a range of conditions. The effect of both acetonitrile and imidazole impurities on the total conversion of ADP to adenosine 5'-triphosphate (ATP) was investigated. It was found that both acetonitrile and imidazole impurities prompted a decrease in the % conversion to ATP of 17% and 22%, respectively. The effect of phosphoimidazole concentration on the initial rate of phosphorylation and total % conversion after 24 h was also investigated. The initial rate of phosphorylation and the % conversion to ATP after 24 h, were both found to increase with the initial concentration of phosphoimidazole. Initial phosphoimidazole concentrations of 5, 10, 20 and 50 mM were investigated; total % conversion to ATP after 24 h was found to be 12%, 14%, 30% and 43%, the initial rate of phosphorylation was 0.752×10^8 , 1.263×10^8 , 1.627×10^8 and 2.588×10^8 M s⁻¹, respectively.

The kinetics of the NDP phosphorylation reactions were monitored using high performance liquid chromatography (HPLC). Phosphorylation of ADP was monitored on a SUPELCOSIL-LC-18-T reversed-phase analytical column, while GDP phosphorylation was monitored on a SIELC-Primesep SB mixed mode analytical column. Protocols were developed for both of the columns to ensure that the nucleotides had significant retention times and the peaks were well separated with little tailing.

Acknowledgements

I would like to thank Dr Hodgson for all the support and guidance that he gave over the course of my project. In addition I am also very grateful to Dr Congreve for all of her help with HPLC.

I would also like to thank all of the members of the office; Niamh, Vicki, Sritama and Chris, for all of the laughs, cake and general distractions.

Thank you to both my parents and grandparents for all of the help and support they have given me over the years. Particular thanks to my dad for providing copious amounts of biscuits, while I wrote up.

Contents

Overview	i
Acknowledgments	ii
Abbreviations	vi
List of Figures	vii
List of Tables	viii
1 Introduction	1
1.1 Nucleotides in Biological Systems	1
1.1.1 Glycosylation Processes	2
1.2 Kinase Enzymes	3
1.2.1 Nucleoside Diphosphate Kinase	6
1.3 Methods of Nucleotide Synthesis	6
1.3.1 Chemical Synthesis	7
1.3.2 Chemo-Enzymatic Synthesis	14
1.4 Biocatalysis for Cofactor Regeneration	18
1.4.1 ATP Regeneration via Acetate Kinase	19
1.4.2 ATP Regeneration via Pyruvate Kinase	20
1.4.3 ATP Regeneration via Polyphosphate Kinase	20
1.4.4 Comparison of ATP Regeneration Systems	22
2 Protein Production	24
2.1 Introduction to Molecular Cloning	24
2.1.1 Isolating DNA fragments	24
2.1.2 Cloning Recombinant DNA	25
2.2 Protein Expression	26
2.2.1 Step 1: Insert Generation	26
2.2.2 Step 2: Linearise Expression Vector	27
2.2.3 Step 3: Vector-Insert Annealing	27
2.2.4 Step 4: Protein Overexpression	28
2.3 Protein Purification	28
2.3.1 Purification of NDPK H122G	28
2.3.2 Confirmation of NDPK H122G Purification	30
2.4 Chapter Summary	30
3 Phosphorylation of Imidazole	32
3.1 Introduction	32
3.1.1 Known Methods for the Synthesis of Phosphoimidazole	32

3.1.2	Aqueous Phosphorylation Methods	33
3.2	Synthesis of Phosphoimidazole	34
3.3	Optimisation	36
3.3.1	Aqueous Phosphorylation of Imidazole	36
3.3.2	Purification Procedure	37
3.4	Conclusions	39
4	Enzyme Assays and Analysis	40
4.1	HPLC Analysis	40
4.1.1	HPLC Columns	40
4.1.2	Enzymatic Assay Analysis	42
4.2	Enzyme Assays	44
4.2.1	Pilot Experiment: Dephosphorylation of ATP	45
4.2.2	Initial Enzymatic Phosphorylation Reaction of ADP to ATP	46
4.2.3	Effect of Impurities and [PIm] on % Conversion	47
4.2.4	Enzymatic Phosphorylation of GDP	51
4.2.5	Bioluminescence Studies	52
4.3	Conclusions	57
5	Conclusions and Future Work	59
5.1	Conclusions	59
5.1.1	Optimised Synthesis of Phosphoimidazole	59
5.1.2	Use of Phosphoimidazole in Biocatalytic Reactions	60
5.2	Future Work	60
5.2.1	Further Optimisation of the Production of PIm	60
5.2.2	Thiophosphorylation of Imidazole	61
6	Experimental	63
6.1	General Instrumentation and Materials	63
6.2	Enzyme Expression	63
6.2.1	Protein Expression	63
6.2.2	Protein Purification	67
6.3	Chemical Synthesis	69
6.3.1	Synthesis of Phosphoimidazole 62	69
6.3.2	Synthesis of Potassium Thiophosphodichloridate 90	69
6.3.3	Synthesis of Thiophosphoimidazole 91	70
6.4	Enzyme Assay	70
6.4.1	Reactions involving Adenosine Nucleotides	70
6.4.2	Bioluminescent Assays	72
6.5	HPLC Conditions and Retention Times	73
6.5.1	Buffer Preparation	73
6.5.2	SUPELCOSIL-LC-18-T Column Protocol	74

6.5.3 SIELC-Primesep SB Column Protocol 75

Abbreviations

ACN	Acetonitrile
ADP	Adenosine 5'-diphosphate
AMP	Adenosine 5'-monophosphate
ATP	Adenosine 5'-triphosphate
CPG	Controlled pore glass
DCC	<i>N,N'</i> -Dicyclohexylcarbodiimide
DMF	Dimethylformamide
FPLC	Fast Protein Liquid Chromatography
HEPES	4-(2-Hydroxyethyl)-1-piperazineethanesulfonic acid
HPLC	High Performance Liquid Chromatography
NDP	Nucleoside 5'-diphosphate
NDPK	Nucleoside diphosphate Kinase
NMP	Nucleoside 5'-monophosphate
NTP	Nucleoside 5'-triphosphate
PCR	Polymerase chain reaction
PEG	Poly(ethylene glycol)
PI _m	Phosphoimidazole
PS	Polystyrene
PVA	Poly(vinyl alcohol)
SOB	Super optimal broth

List of Figures

1	DNA Structure	1
2	ATP Structure	1
3	NTP and NDP Structure	4
4	NDPK Conserved Catalytic Core	5
5	ATP Binding in NDPK Catalytic Core	5
6	Retro-synthetic Disconnection	8
7	Psuedo-ATP Intermediate	9
8	By-products of the Ludwig Scheme	9
9	Reversibility of Im rescue of NDPK activity	17
10	Generalised Scheme for Enzyme Catalysed ATP Regeneration	19
11	Two Enzyme Coupled Systems for ATP Regeneration based on Poly(P)	21
12	Agarose Gel of linearised pOPINF	27
13	Agarose Gel of PCR Products for Fusion Product Colonies	28
14	Chromatograph showing the elution of proteins via FPLC	29
15	SDS-PAGE Gel of Fractions Collected during NDPK H122G Purifi- cation	30
16	POCl ₃ Potential Hydrolysis and Aminolysis Reactions	34
17	log k_{obs} -pH Rate Profile for the Hydrolysis of Phosphoramidate	35
18	³¹ P NMR Spectrum of PIm after Various Purification Steps	36
19	PIm Synthesis % Product Distribution	37
20	³¹ P NMR Spectrum of PIm after Various Purification Steps	39
21	Mixed Mode Reverse-Phase/Ion Exchange Column Media	42
22	Chromatograph of Separation of Adenosine Nucleotides	43
23	Chromatograph of Separation of Guanine Nucleotides	44
24	PIm rescue of H122G activity	44
25	Pilot Experiment: Dephosphorylation of ATP	45
26	Initial Enzymatic Reactions	46
27	Effect of Impurities on % Conversion	48
28	% Conversion to ATP after 24 h	49
29	% Conversion to ATP after 5 h	50
30	Initial Rate of ATP formation at various PIm Concentrations	50
31	% Conversion to GTP after 47 h Experiments	52
32	Graph of Luminescence Signals for Reaction XII	54
33	Graph of Luminescence Signals for Reaction D	55
34	Graph of Reaction XIII After 0.25 h	56
35	Next Day Luminescence Signals for Reaction D	57

List of Tables

1	RCP Temperature Cycle	26
2	% of Compound with Purification Procedure	38
3	Composition of the 3 Parallel Initial Enzymatic Experiments	46
4	Composition of the 3 Parallel Impurities Enzymatic Experiments	47
5	Composition of the 2 Parallel Enzymatic Experiments of GDP	51
6	Composition of the bioluminescent assays	53
7	Overnight Luminescence Signals for Reactions	56
8	% of Compound with Imidazole Concentration	59

1 Introduction

This thesis discusses the use of a chemo-enzymatic route towards the synthesis of NTPs via the use of a kinase enzyme. Through the use of inexpensive chemical precursors, our aim was to develop and optimise a simple, cost-efficient chemo-enzymatic method to synthesize NTPs and their analogues. Thus avoiding difficult and complex synthetic challenges and costs.

1.1 Nucleotides in Biological Systems

Nucleotides and in particular NTPs are ubiquitous throughout the natural world, and they are integral to many of the most fundamental processes in living systems. From the inheritance of genetic information through nucleic acids such as DNA (Figure 1), to the phosphoryl transfer of the γ -phosphate of ATP (Figure 2), which releases the chemical energy necessary for thermodynamically unfavourable processes such as cellular construction and maintenance, NTPs play a vital role.¹

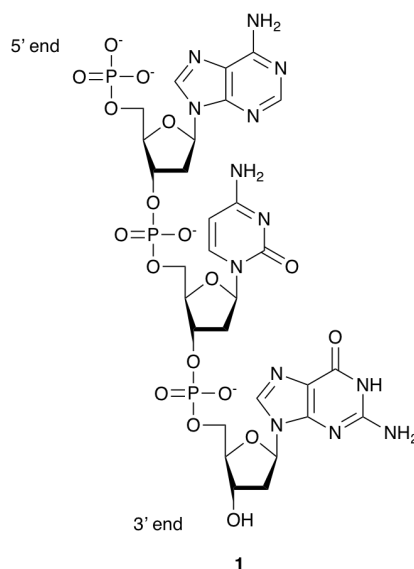


Figure 1 Structure of a three nucleoside strand of DNA

The abundance of nucleotides in nature, means that research into their interactions within organisms is essential. Currently, commercial NTPs and their available analogues are expensive owing to the synthetic difficulties associated with the formation of phosphoanhydride bonds².

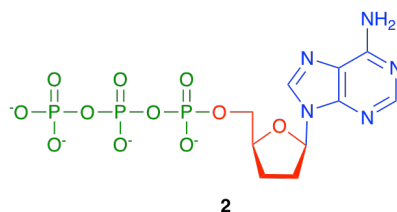


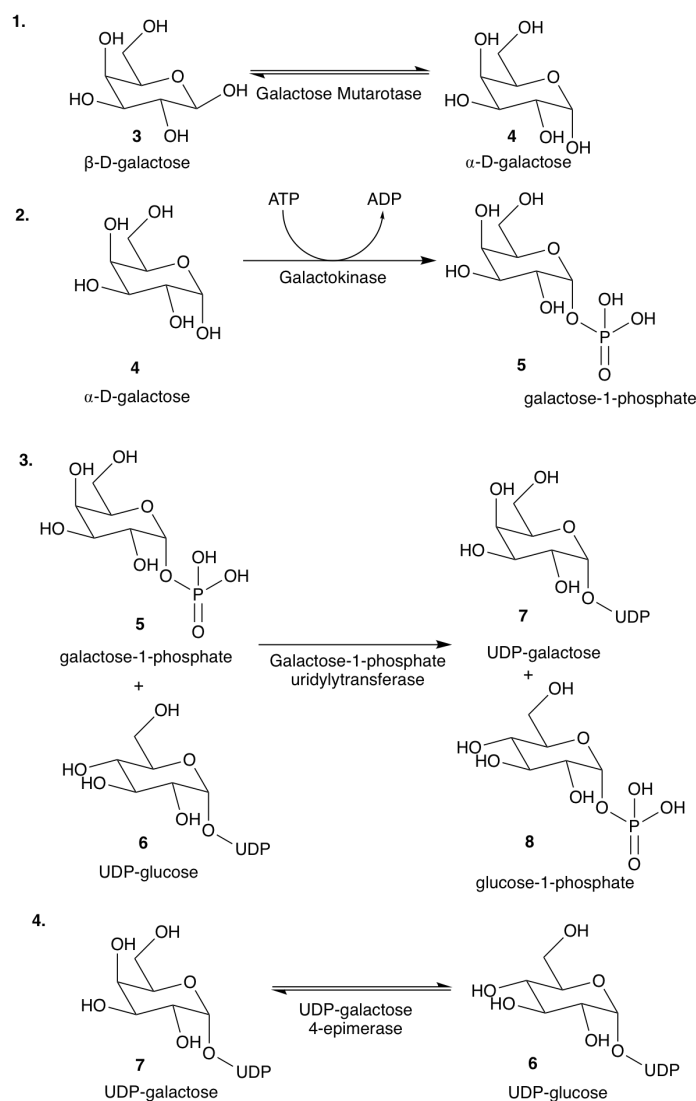
Figure 2 Structure of ATP: green moiety - triphosphate group, red moiety - deoxyribose sugar, blue moiety - adenosine nucleobase

1.1.1 Glycosylation Processes

In nature all cells have an array of covalently bound monosaccharides and oligosaccharides, these sugar moieties are commonly referred to as glycogens.³ Glycogens can be found on the surface of cells and macromolecules mediating; cell-cell, cell-matrix and cell-molecule interactions, as such they are critical to the development of multicellular organisms. Glycogens often conjugate with other biological molecules such as protein and lipids, thus forming glycoproteins and glycolipids. Glycoproteins are predominantly found in the cytoplasm and nucleus of cells, where they serve as regulatory switches.³

Common classes of eukaryotic conjugate glycogens are categorised based on the linkage between the glycogen and the conjugate unit. Proteins in glycoproteins are covalently bound to the glycogens molecules via O- or N- linkages to the polypeptide backbone.³ Most conjugate glycogens, such as glycoproteins, are produced in the endoplasmic reticulum (ER) and the golgi apparatus, new proteins are produced in the ER and undergo glycosylation, a post translational modification which covalently binds glycogens (usually monosaccharides) to the protein.⁴ Glycosylation reactions use activated forms of monosaccharides, typically in the form of nucleotide sugars which act as high energy donors, these reactions are catalysed by glycosyltransferase enzymes.³ The process of forming activated nucleotide sugars requires a NTP, typically UTP or GTP, and a monosaccharide with a phosphate group bound to the anomeric carbon.⁵ There are two methods used to make these nucleoside sugars, (1) monosaccharide-1-phosphate utilises a kinase enzyme, forming an activated sugar nucleotide and a inorganic pyrophosphate.⁵ (2) nucleotide sugars can also be formed by the exchange of the nucleotide from one sugar to another, an example of this is the leloir pathway.

The leloir pathway (Scheme 1) is responsible for the conversion of UDP-galactose to UDP-glucose, it also produces the more metabolically useful glucose-1-phosphate from β -D-galactose^{6,7} The pathway consists of four enzymatic reactions; in the first reaction galactose mutarotase, catalyses the epimerisation of D-galactose from the β to the α form.⁷ α -D-galactose is phosphorylated by a galactokinase (ATP dependant) in the second reaction, resulting in the production of galactose-1-phosphate.⁷ The third enzymatic reaction uses galactose-1-phosphate uridylyltransferase, to mediate the transfer of UMP from UDP-glucose to galactose-1-phosphate, producing glucose-1-phosphate and UDP-galactose. The fourth and final reaction, converts UDP-galactose to UDP-glucose via UDP-galactose 4-epimerase.⁸ The UDP-glucose produced is a high energy nucleotide sugar, which can act as a donor to form conjugate glycogens such as glycoproteins, an enzymatic reaction mediated by glycosyltransferase.



Scheme 1 Schematic showing the four enzyme catalysed reactions with make up the leloir pathway. **1** Conversion of β -D-galactose to the α form. **2** Kinase mediated reaction using ATP as a phosphate donor to produce galactose-1-phosphate. **3** Reaction between UTP-glucose and galactose-1-phosphate producing glucose-1-phosphate and UDP-galactose. **4** UDP-galactose is epimerised to produce UDP-glucose.

1.2 Kinase Enzymes

Protein kinases are one of the largest classes of enzyme, there are estimated to be over 2000 protein kinases in the vertebrate genome, which are involved in a plethora of biochemical processes.⁹ Humans have 518 protein kinase genes, which account for $\sim 1.7\%$ of all human genes.¹⁰

Kinases catalyse the transfer of a phosphoryl group from a phosphate donor to a substrate, thus phosphorylating the substrate.¹¹ Phosphorylation is one of the most prevalent post-translational modifications found in the cell. Protein kinases regulate a wide range of biochemical processes, including the metabolism of both lipids and proteins, neurotransmitter biosynthesis, DNA transcription and replication as well as cell differentiation.⁹

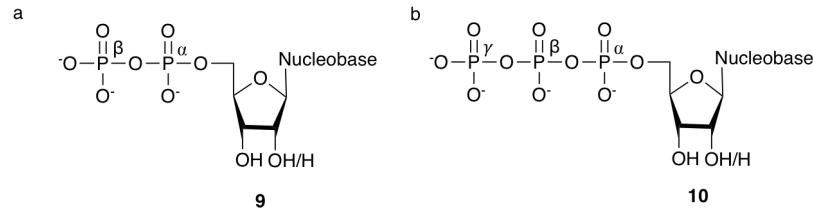


Figure 3 **a** structure of NTP, **b** structure of NDP. Green moiety is the phosphate group, the red moiety is the ribose sugar and the blue moiety is the nucleobase

Kinases are ATP-dependant phosphotransferases that catalyse the transfer of the γ - phosphoryl group of the ATP. There are several varieties of categories of protein kinases; (1) serine/threonine, (2) tyrosine and (3) histidine.¹² Both serine/threonine and tyrosine protein kinases are primarily used for signal transduction, they catalyse phosphorylation by transferring the phosphoryl group to the hydroxyls of serine, threonine or tyrosine.¹² Histidine protein kinases (NDPK) catalyse the transfer of the phosphoryl group onto a histidine residue, which then transfers the phosphoryl group to an NDP. The most common NTP used for phosphorylation by nature is adenosine triphosphate (ATP), but NDPKs are promiscuous and as such they are capable of utilising all NTPs irregardless of nucleobase as phosphoryl donors.¹²

There are myriad histidine protein kinases which differ in size, substrate specificity, and subunit composition, despite these differences all histidine protein kinases known to date share at least 40% of their genetic sequence and contain a homologous catalytic core, thus implying that similar phosphorylation mechanisms will be employed by all protein kinases,¹³ eukaryotic enzymes tend to present as hexamers (trimer of dimers with D3 dihedral symmetry), while a number of bacterial enzymes are tetramers (pair of dimers with D2 pyrimidal symmetry).¹⁴ The dimers which make up the tertiary structure of the NDPK enzyme are all identical, and form the conserved catalytic core of NDPK enzymes.¹⁴

The conserved catalytic core of protein kinases consists of two regions separated by a large cleft, a *N*-region, used for the binding of ATP, and a larger *C*-region which is responsible for catalysis and substrate binding (Figure 4)^{13,15} The *N*-region is made up of a 5-strand antiparallel β -sheet and a α helix. The α and β -phosphate groups of ATP bind to a phosphate anchor, situated between $\beta 1$ and $\beta 2$ in the *N*-region.¹⁵

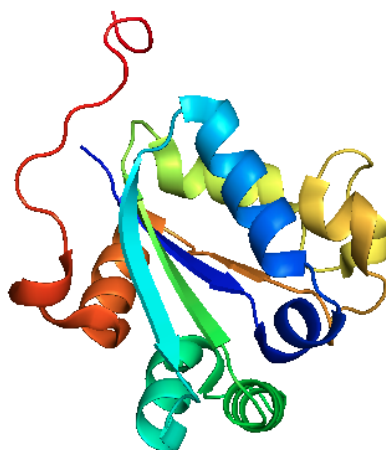


Figure 4 Conserved catalytic core of NDPK, made in MacPyMOL using PDB entry 1NDK.¹⁶

The *C*-region consists of four β strands and a two α helices.¹⁵ The arrangement of the β sheets and α helices forms an α - β sandwich (ferredoxin fold), a motif commonly found in nature. The two α helices connect $\beta 1$ to $\beta 2$ and $\beta 3$ to $\beta 4$, respectively. The geometrical conformation of the $\beta \alpha \beta \beta \alpha \beta$ arrangement results in the formation of a hydrophobic core, which is highly conserved between all known NDPKs. These two regions not only provide and position the essential amino acids needed to catalyse the phosphoryl transfer reaction but also coordinate to Mg^{2+} ions, which assist ATP binding and expedite the phosphoryl transfer reaction.¹⁵

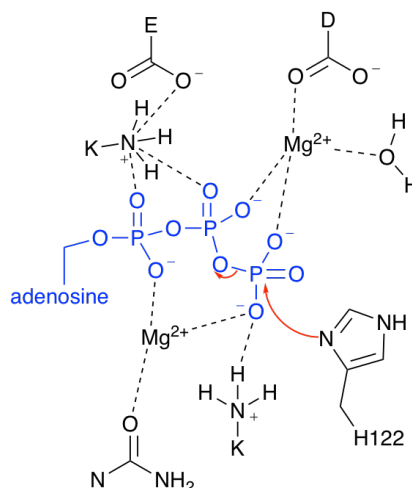
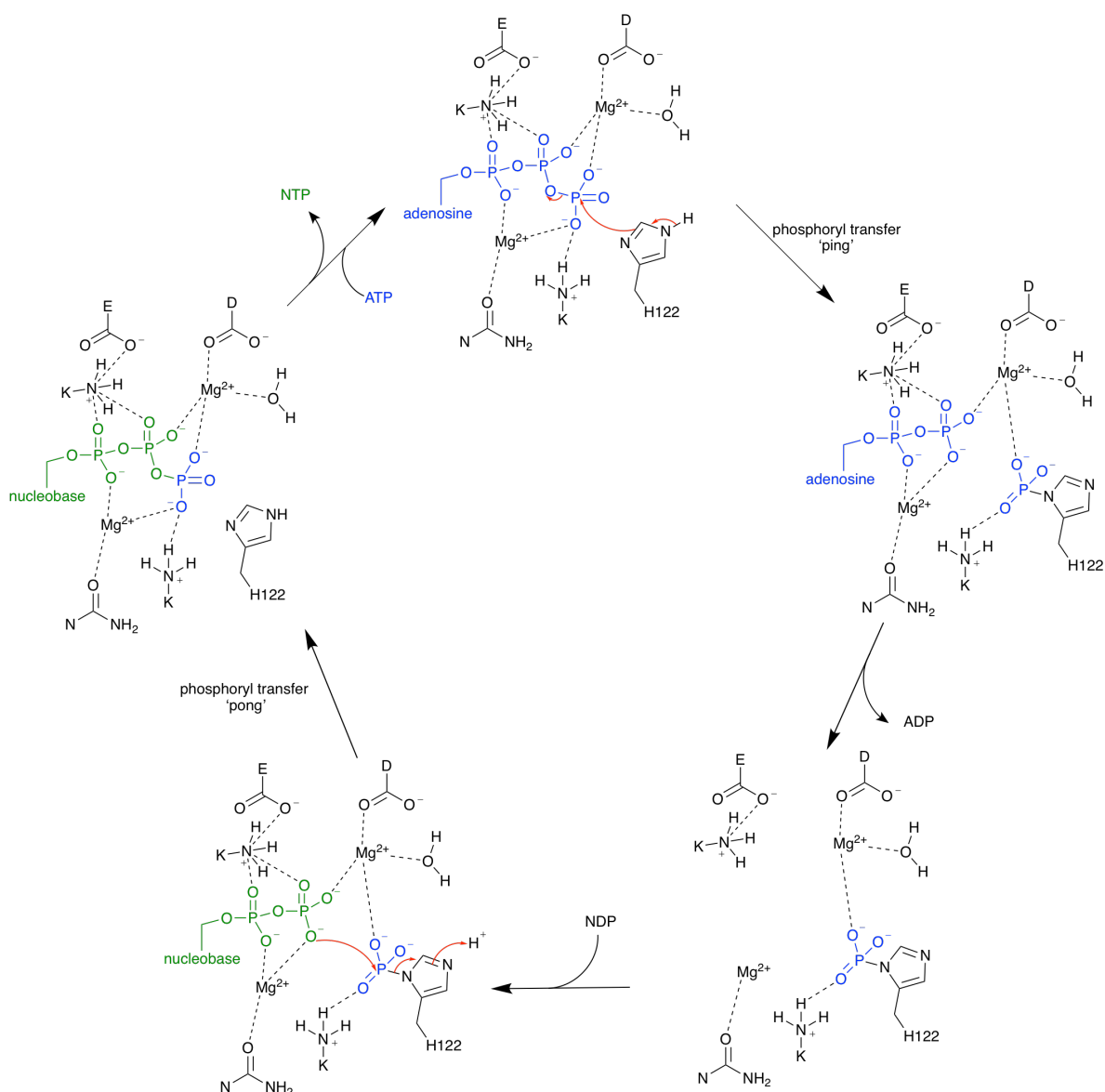


Figure 5 NDPK binding ATP in the catalytic core with Mg^{2+} cations in preparation for phosphoryl transfer, adapted from¹⁵

The first Mg^{2+} optimises the positioning of the γ -phosphoryl group of ATP, Mg^{2+} also neutralises charges on the γ -phosphate group thus facilitating nucleophilic attack.¹⁵ The second Mg^{2+} ion is bound to amino acid residues asparagine and aspartic acid and a water molecule. It is thought to act as a lewis acid, stabilising the negative charge which develops on the oxygen between γ and β phosphate groups during the transition state.¹⁷

1.2.1 Nucleoside Diphosphate Kinase

Nucleoside diphosphate kinase (NDPK) enzymes catalyse the reversible transfer of a γ -phosphoryl group from a nucleoside 5'-triphosphate (NTP) to a nucleoside 5'-diphosphate (NDP), via a covalent intermediate.¹⁸ NDPKs utilise a 'ping-pong' mechanism to bring about the phosphorylation of the NDP substrate, a histidine group in the NDPK active site is phosphorylated by the NTP.¹⁹ The phosphoryl group is subsequently transferred onto a NDP molecule (Scheme 2).²⁰



Scheme 2 NDPK 'ping-pong' mechanism. Adapted from¹⁵

1.3 Methods of Nucleotide Synthesis

Nucleotides are difficult to synthesis, purify and store owing to a range of factors. Firstly, one of the major challenges to the production of NTPs and their analogues lies in the extensive and laborious purification procedures that are necessary to separate the complex crude reaction mixture of nucleotides (NMP, NDP and NTPs)

and by-products (predominantly inorganic phosphates) that often arise from phosphorylation procedures.

Nucleotides and inorganic phosphate by-products often have similar characteristics, thus making the isolation of nucleotides and their analogues particularly difficult, and so purification of the nucleotides via chromatography remains a limiting step, due to crude reaction mixtures being contaminated with a variety of anionic by-products.²¹

NTPs have been shown to be relatively stable in aqueous solutions at neutral pH.²² The rate of spontaneous hydrolysis of both ATP and ADP appears to be insensitive to pH changes in the neutral range.²³ Stockbridge and Wolfenden found that half-life for the spontaneous hydrolysis of ATP⁴⁻ when bound to Mg²⁺ was 17.5 days at 25 °C.²⁴

In this section both the current chemical synthetic methods and chemo-enzymatic methods of nucleotide synthesis will be discussed in detail. These examples will serve to illustrate some of the challenges which are commonly found in NTP production. After which, this section will focus on the use of imidazole to rescue activity of genetically modified NDPKs, and how the reverse of this reaction can be utilised as a chemo-enzymatic route towards nucleotides.

1.3.1 Chemical Synthesis

Nucleoside triphosphates, are rich with polar functional groups, it is this essential polarity which determines and controls the molecular recognition properties of biological systems. It is this essential polarity which makes chemical synthesis methods so laborious. Chemical synthesis requires dry reaction conditions and, due to the polarity of the NTPs they are not soluble in organic solvents. To counter this, alkylammonium salts are used to aid solubility. Alkylammonium salts are extremely hygroscopic, to the point of deliquescence, thus increasing the chance of water ingress into reactions and destroying reagents.

There are a variety of chemical synthesis methods that have been used in the production of NTPs, this report will look in detail at solution-phase syntheses, concentrating on syntheses via nucleophilic attack of pyrophosphate on activated NMPs. The use of solid-supports in the synthesis of nucleoside 5'-triphosphates, has become more prevalent in recent years and as such a section on solid-phase synthesis of nucleotides has been included for completeness.

1.3.1.1 Solution-Phase Synthesis of Nucleoside Triphosphates

The most common method of chemical synthesis of nucleoside 5'-triphosphates utilises the nucleophilic attack of pyrophosphate on activated NMPs, the disconnection for this reaction is shown in Figure 6.

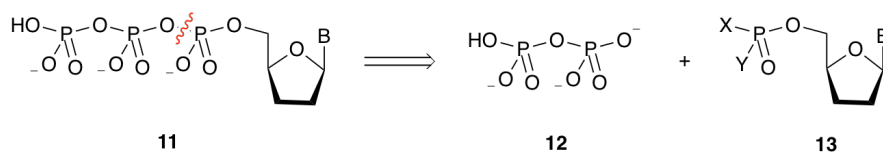
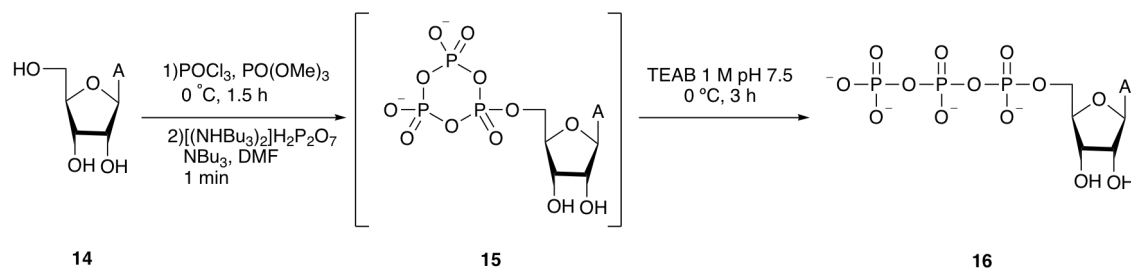


Figure 6 Disconnection for nucleophilic attack of pyrophosphate on activated NMPs

These reactions require the use of pyrophosphate salts, such as tri-*n*-butylammonium pyrophosphate, which are commercially available. The activated NMPs are not available commercially and so must be prepared. This section will discuss NTP formation via the nucleophilic attack of pyrophosphate on firstly phosphorodichloridate intermediate, then phosphoramidate intermediate.

1.3.1.1.1 *NTP Formation via Phosphorodichloridate Intermediate*

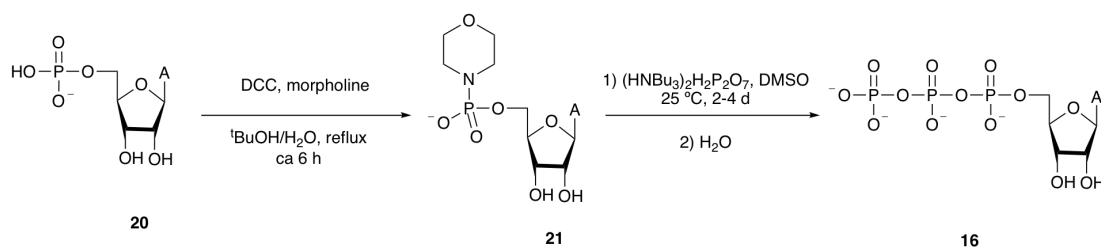
Nucleosides were successfully reacted with phosphorus oxychloride to form phosphorodichloridate intermediates by Yoshikawa's group in 1967, (reaction is 5' selective) they achieved this by using trialkylphosphate solvents, typically trimethyl- or triethylphosphate. The rate of phosphorylation is increased in trialkylphosphate solvents, unlike earlier solvents trialkylphosphate is able to dissolve both the nucleoside and the reactive reagents^{25, 26}. Ludwig utilised Yoshikawa's method for the formation of phosphorodichloridate intermediates, and adapted it to create a three-step, one-pot synthesis method for NTPs, which is one of the most prevalent chemical methods for NTP synthesis. Once produced, the phosphorodichloridate intermediate was reacted with tributylamine and a 5-fold excess of bis(tris-*n*-butylammonium) phosphate in dry DMF for 1 minute, leading to the formation of a cyclic alkyl trimetaphosphate intermediate (**15**), which is then hydrolysed resulting in the production of NTPs, ATP produced by this method typically gives moderate to low yields^{21, 27}.



Scheme 3 Scheme of the three-step, one-pot synthesis devised by Ludwig to produce NTPs, this scheme relates to ATP specifically.

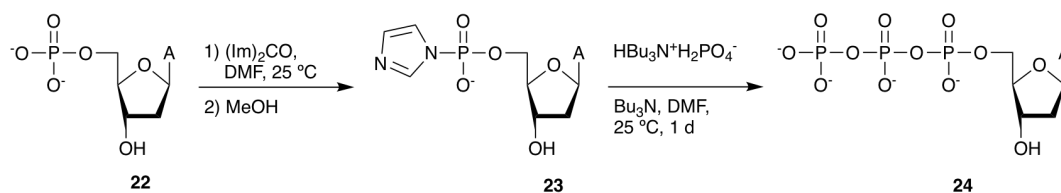
Adenosine 5'-triphosphate (**2**) produced as the major product when there is a large excess of POCl_3 and tris-*n*-butylammonium. Currently, the suggested mechanism utilises a pseudo-ATP intermediate (**16**), which undergoes a rearrangement to form the cyclic alkyl trimetaphosphate intermediate (**15**) shown in Scheme 3^{26, 28}.

pathway for ATP via this procedure, yields of between 73 -80 % were obtained for NTPs made via this method^{26, 30}



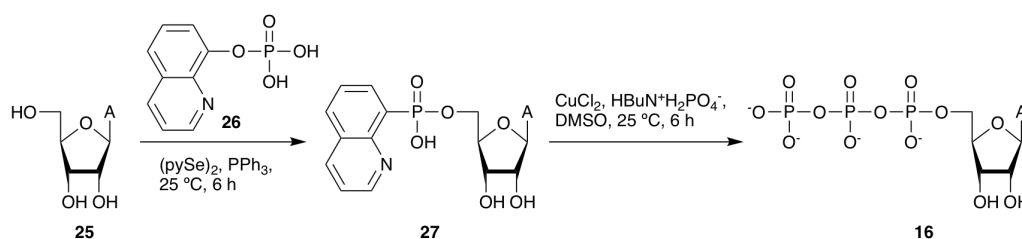
Scheme 4 Reaction scheme of Moffat and Khorana ATP synthesis protocol using a phosphoramidate intermediate³⁰

Phosphoroimidazolates are phosphoramidate intermediates, first utilised by Hoard and Ott in the production of dNTPs.^{26,31} The nucleoside monophosphates are activated by 1,1'-carbonyldiimidazole (CDI) in DMF (Scheme 5), yields ranged from 20 -70% depending on the dNTP being produced.^{26,31} The use of this method for the synthesis of NTPs initially had some issues as CDI and the activated NMPs reacted to form cyclic carbonate impurities, which were carried through to the triphosphate products.²⁶ The carbonyl group can be removed via the use of ammonia.



Scheme 5 Reaction scheme of Hoard and Ott's dNTP synthesis protocol, which was the first method to utilise phosphoroimidazolates as phosphoramidate intermediates^{26,31}

Metal ions have been coordinated to phosphoroimidazolates, this results in an increase in the electrophilicity of the phosphoroimidazolite. ATP (**16**) was synthesised from 8-quinolyl phosphate using a metal mediated method.²⁶ The intermediate **27** was activated by CuCl_2 in DMSO, **16** was produced with a yield of 77%.³²



Scheme 6 Metal mediated synthesis of ATP, copper ions increase the electrophilicity of the phosphoramidate intermediate

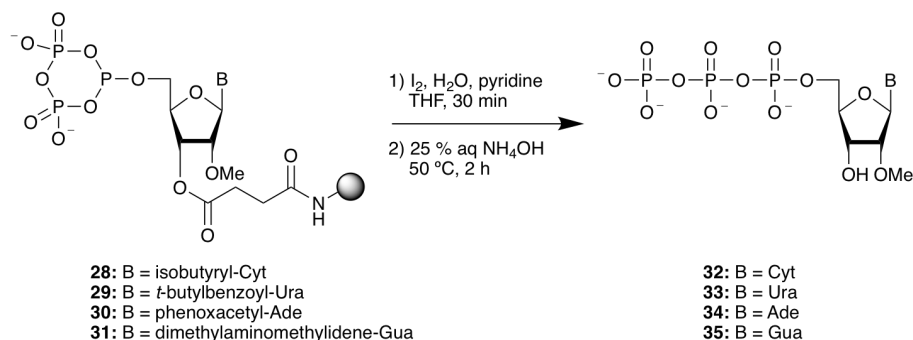
1.3.1.2 Solid-Phase Synthesis of Nucleoside Triphosphates

Solid-phase synthesis was first used in the 1960s, when the Merrifield method was used to synthesise a tetrapeptide using a chloromethylated copolymer of styrene and divinylbenzene.³³ Solid-phase synthesis allows for reaction equilibria to be pushed towards completion via the use of excess reagents.²¹ Reaction products are anchored onto a solid insoluble support, which makes purification of the crude reaction mixture much simpler as soluble by-products and excess reagents may be removed via filtration.^{21,34} The loading capacity of the support (number of binding sites per gram of support), is an important feature of the support bead. Linkers are often used to bond the reagent to the support, this is done to increase the ease of product recovery by providing an easily cleaved bond.²¹

Controlled pore glass (CPG) and polystyrene (PS) are the two most common forms of insoluble solid support, used in nucleotide synthesis. CPG is a nonswelling insoluble material which contains large pores where nucleotide synthesis can occur.²¹ PS beads are highly crosslinked and exhibit hydrophobic properties, as such they can be used for nucleotide synthesis.²¹ The use of insoluble beads gives heterogeneous reaction conditions, which can give rise to non-linear reaction kinetics and inefficient coupling rates both of which are disadvantageous to effective nucleotide synthesis.²¹ Soluble polymer-supported synthesis of nucleotides allows for the easy separation of by-products and product, while maintaining homogeneous reaction conditions, the two most widely used polymer-supports are poly(vinyl alcohol) (PVA) and poly(ethylene glycol) (PEG).²¹

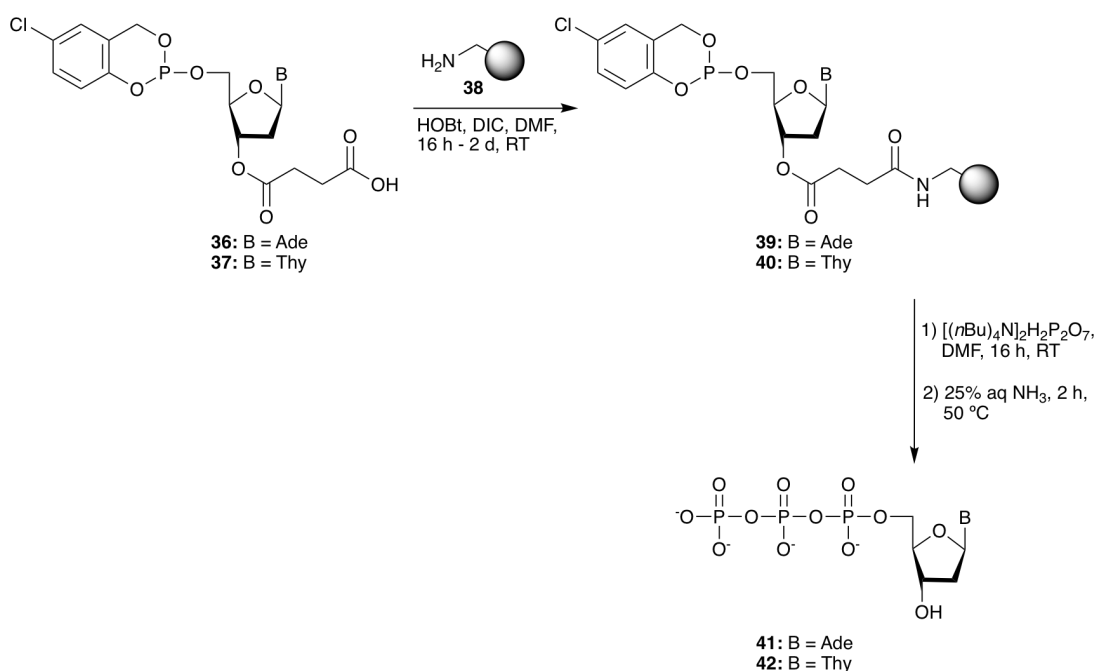
1.3.1.2.1 NTP Formation with Sugar Moiety Bound to the Support

The Gaur group adapted Ludwig's three-step, one-pot method in the early 1990s to make it suitable for solid-phase synthesis.²¹ The method (Scheme 7) used a succinimide linker attached to an aminopropyl-CPG to synthesis 2'-O-methylribonucleoside 5'-triphosphates.³⁵ All 2'-O-methylribonucleoside 5'-triphosphates produced achieved yields of between 60-65%, the resulting NTP analogues were removed from the support via the use of hot aqueous ammonia.³⁵



Scheme 7 Scheme of the three-step, one-pot synthesis adapted by the Gaur group for solid-phase synthesis of NTPs

The Meier group devised a solid state method for the synthesis of NTPs, via the use of *cycloSal*-phosphate triesters as active ester reagents.²¹ The method used utilised three distinct steps (Scheme 8), firstly the 2'-*O*-succinyl-*cycloSal*-nucleotides (**36**, **37**) were attached to aminomethyl-PS (**38**) via an amide bond.³⁶ Conversion of the immobilised 2'-*O*-succinyl-*cycloSal*-nucleotides to NTPs (**41**, **42**) required the use of a reactive nucleophile. The pyrophosphate nucleophile was prepared via ion exchange of phosphoric acid, $\text{Na}_2\text{H}_2\text{P}_2\text{O}_7$, using an ion-exchange resin; the product of which was titrated with $[(n\text{Bu})_4\text{N}]\text{OH}$, to form the tetra-*n*-butyl ammonium salt ($[(n\text{Bu})_4]\text{H}_2\text{P}_2\text{O}_7$).³⁶ The resin (**39**, **40**) and the nucleophilic pyrophosphate salt were both rigorously dried, as the presence of water can result in the formation of unwanted by-products.³⁶ Removal of the produced salicyl alcohols and the excess pyrophosphate from the polymer bound dNTPs was done via washing.³⁶ Nucleoside triphosphates **39** and **40** were both cleaved from the solid support via the use of hot aqueous ammonia, the resulting products **41** and **42** had purities of 79% and 90%, respectively.³⁶



Scheme 8 Scheme of the three-step protocol developed by the Meier Group for the solid-phase synthesis of NTPs

1.3.1.2.2 NTP Formation with Base Moiety Bound to the Support

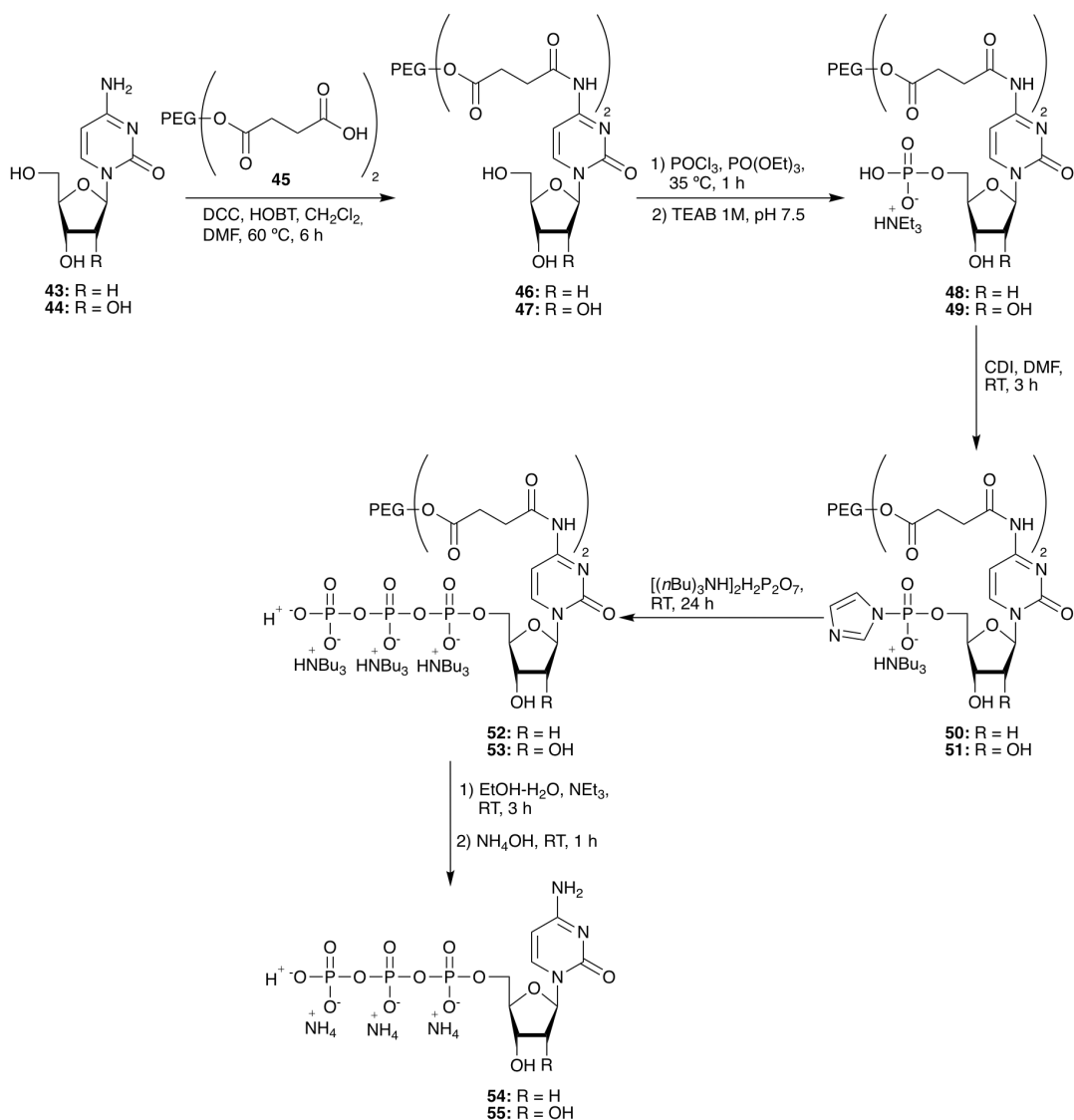
In 2009, Peyrottes group devised a method for the synthesis of dCTP (**54**) and CTP (**55**) via the use of a PEG soluble support (Scheme 9).^{21,37} Nucleosides **43** and **44** were bound to the soluble PEG support by a basolabile succinimide linker, which reacted with the exocyclic amino group of the nucleobase.^{37,38} The % yield of **46** and **47** was 87% and 83% respectively, both reactions gave a conversion rate of 100%. The phosphorylation of the two NMPs; **48** and **49** was done using Hoards method which requires the activation of NMPs via CDI to generate a phospho-

ramidate intermediate.^{31,37} The phosphoramidate intermediate (**50** or **51**) was then condensed with inorganic pyrophosphate, resulting in the formation of the desired NTP derivative (**52** or **53**).³⁷ The crude NTPs (**54** and **55**) produced gave yields of 70% and 90%, respectively. The purity of the crude products was determined via HPLC, **54** had a purity of 84% and **55** a purity of 76%.³⁷

Cleavage of the basolabile succinimide linker during the final step of the reaction resulted in the formation of succinimide.³⁹ The presence of succinimide and phosphate salts as by-products resulted in two purification steps, reverse phase HPLC and dialysis.^{38,39}

In 2018, the Peyrottes group investigated the effect of using a carboxylethoxy linker instead of a succinimide linker.³⁹ The linker anchoring the nucleoside to the soluble PEG support must have a carboxylic acid group to allow the formation of an amide bond between the exocyclic amine of the nucleobase and the linker.³⁹ To avoid the formation of by-products, such as succinamide from the succinimide linker, the bond between PEG and the linker must be stable throughout both phosphorylation and the cleavage reaction. Work done by Hölzl et al suggested that an ether bond would be stable throughout the synthesis of the NTPs, as such a carboxylethoxy linker was used.^{39,40}

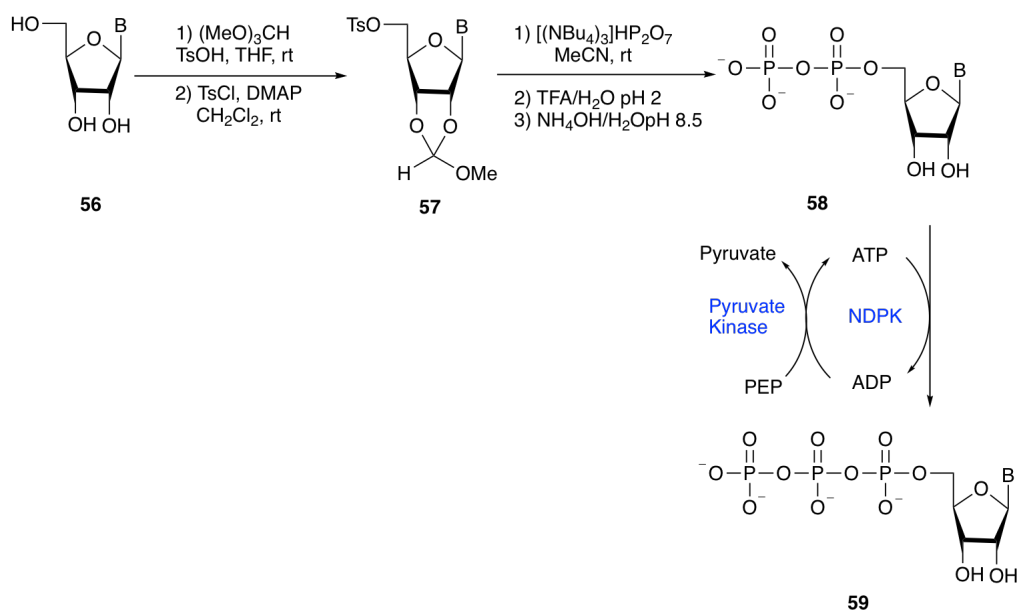
The use of the carboxylethoxyl linker instead of the succinimide linker, eliminated the need for the dialysis step of the purification procedure thus reducing both the complexity and the time required for the synthesis of **50** and **51**.³⁹



Scheme 9 Scheme for the synthetic protocol devised by the Peyrottes group for the synthesis of dCTP (**54**) and CTP (**55**)

1.3.2 Chemo-Enzymatic Synthesis

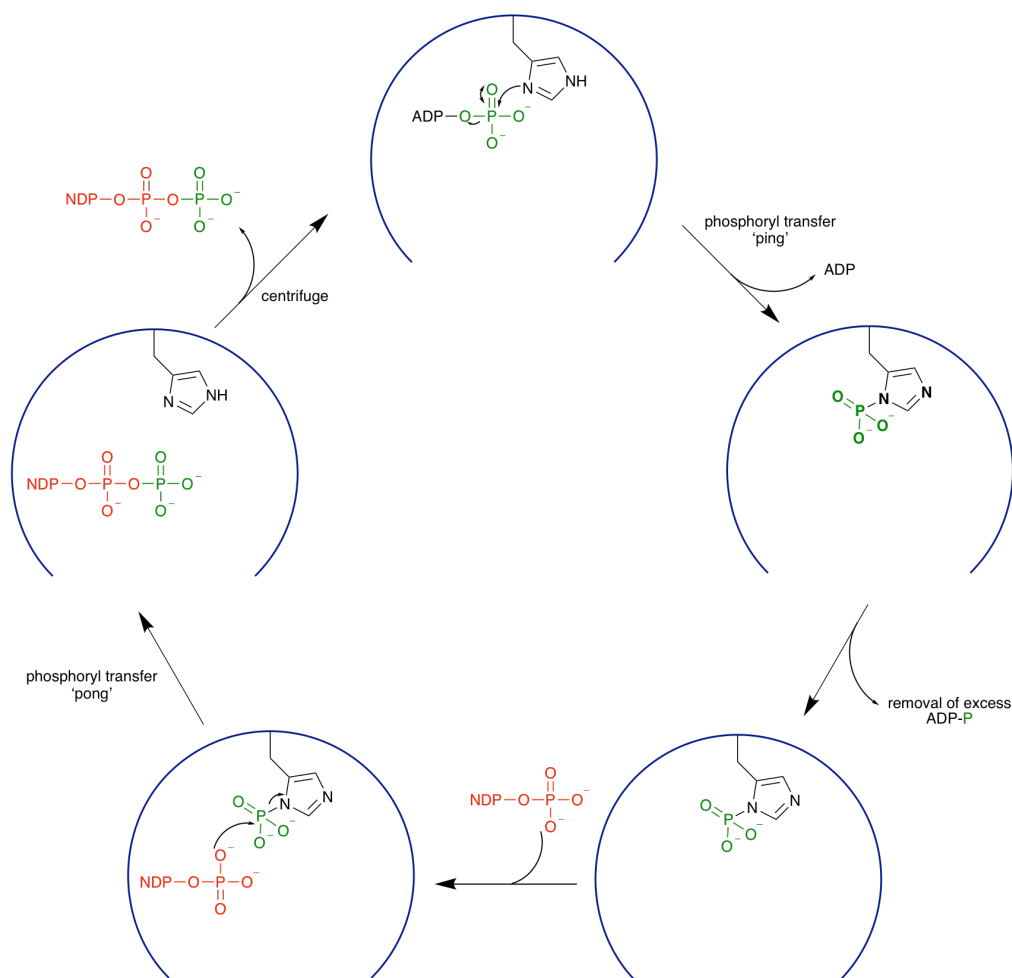
Chemo-enzymatic approaches to NTP synthesis are often readily applicable to naturally occurring NTPs, especially if the product can be used as part of a crude mixture, when it can be coupled to another enzyme system for immediate use. In 2003, work done by the Davisson group combined chemical and enzymatic processes to produce dNTPs, the same enzymatic process was able to be used for all of the dNTPs produced, regardless of nucleobase due to the promiscuity of NDPK enzymes^{41, 42} The production of NTPs utilised pyruvate kinase for the phosphorylation reaction, with PEP serving as the phosphate donor.



Scheme 10 Scheme showing pyruvate kinase controlled synthesis of NTPs

1.3.2.1 NDPK Mediated NTP Synthesis

NDPKs react via a ‘ping-pong’ type mechanism allowing the transfer of the phosphoryl group from NTPs to NDPs. In the production of NTPs, it is ATP which acts as the phosphoryl donor. The histidine residue in the active site is phosphorylated during the ‘ping’ step of the mechanism, at this stage the excess ATP is washed away. The phosphorylated NDPK is then exposed to the substrate NDP, the phosphoryl group is transferred to the NDP during the ‘pong’ step of the mechanism, after which the reaction solution is subjected to centrifugation and the new NTP is collected. The use of ATP as the excess phosphoryl donor is one of the most prohibitive factors to this procedure, ATP is a very expensive reagent and at present is it washed away after the ping step and cannot be recovered.



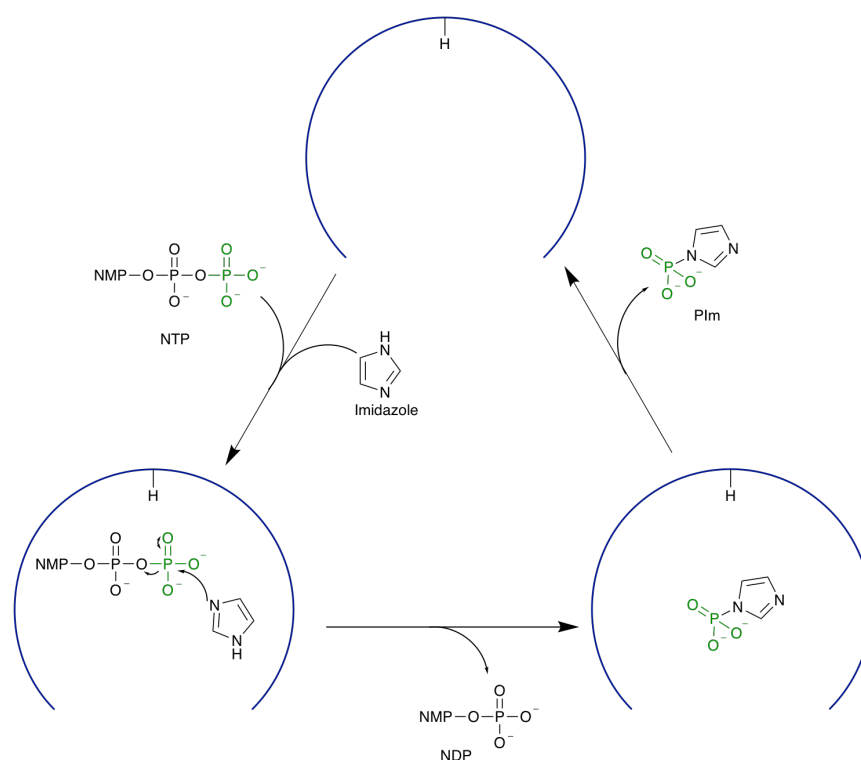
Scheme 11 Scheme showing the WT-NDPK mediated synthesis of NTP

1.3.2.1.1 *Genetically Modified NDPK for NTP Synthesis*

In the late 1990's Herschlag, began investigating whether a small molecule nucleophile, such as imidazole could rescue activity of a mutated enzyme. The genetically modified enzyme chosen was H122G, a site-directed mutant of NDPK in which the His residue at position 122 had been changed to a Gly residue.⁴³

Crystals of H122G in the presence of ATP were grown and were found to be very similar in structure to WT-NDPK crystal structures, they were also found to have the same space group as crystals grown with ADP·AlF₃ which is the transition state analogue.⁴³ This ablation of the His 122 residue has little effect on the surrounding residues, with the main-chain conformation of adjacent amino acid residues in strand β 4 remaining unchanged.⁴³ In WT-NDPK His 122 hydrogen bonds to Glu 133, securing the position of the His group into the correct orientation. In the H122G NDPK mutant, Glu 133 maintained its orientation despite the loss of the hydrogen bond from the His residue, this is thought to be due to an interaction between the carboxylate group of 133 Glu and the hydroxyl group of 124 Ser.⁴³ These studies found that in the absence of the His residue ATP dephosphorylation could be rescued by the presence of imidazole, with the k_{cat}/K_M value 50 times lower than the

WT-enzyme at ATP saturation.⁴³



Scheme 12 Herschlag's work on using imidazole to rescue activity of the H122G NDPK mutant

Rescuing activity of the mutated enzyme with imidazole produces ADP (**61**) and PIm (**62**); due to the principle of microscopic reversibility this is a reversible reaction. Under Herschlag's conditions imidazole (**60**) is in excess and so the equilibrium is pushed far towards the right (Figure 9), thus if **62** could be provided to the NDPK in excess then this could potentially allow for NTP generation, using a cheap phosphoryl donor such as PIm. This concept forms the core basis of this MSc project.

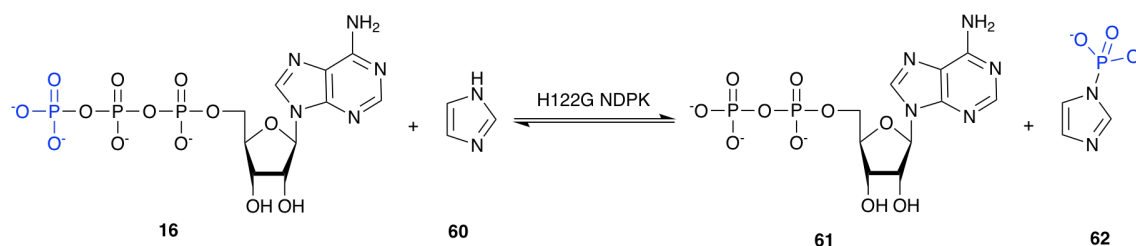
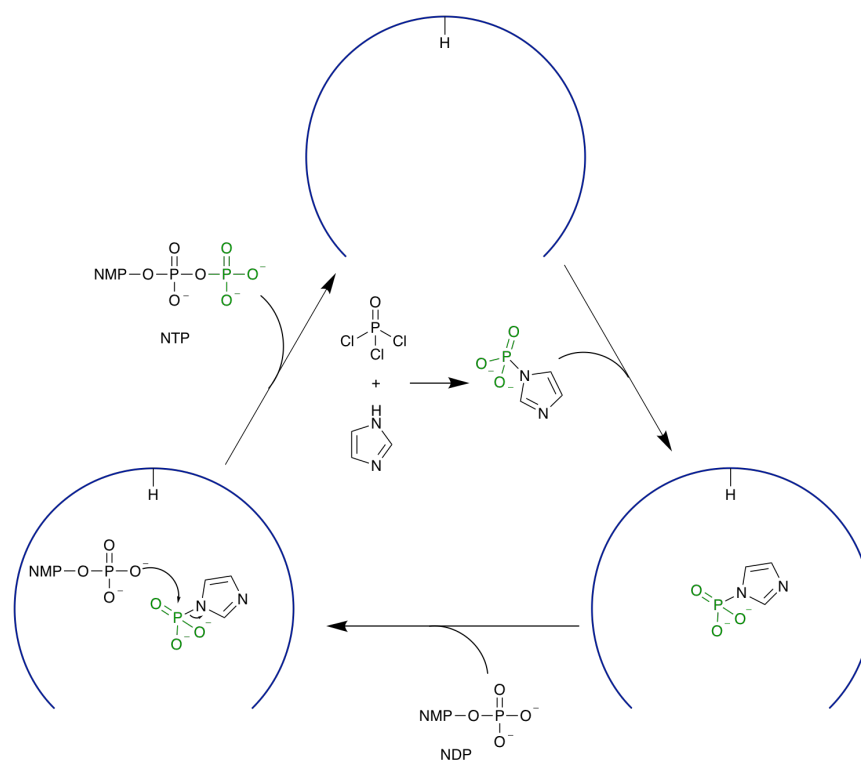


Figure 9 Equation showing the potential reversibility of Im rescue of NDPK activity.

Enzymatic Scheme 13 below, shows the synthesis of **62** and how it can potentially be exploited as a phosphoryl donor in the NDPK reaction. The synthesis and subsequent optimisation of a synthetic route towards phosphoimidazole will be discussed in detail in Section 3.



Scheme 13 Mutant NDPK scheme which allows the generation NTPs, using a cheap phosphoryl donor

1.4 Biocatalysis for Cofactor Regeneration

In recent years biocatalysis as a synthetic route, has become more prevalent in both academia and industry. While some enzymes (hydrolases) operate without the use of cofactors, most enzymes that carry out complex chemical reactions require a range of cofactors. Some cofactors such as, flavins and pyridoxal phosphate are bound tightly to the enzyme active site and remain in place throughout the catalytic cycle, these cofactors are self-regenerating and as such impart no economic burden onto the use of these enzyme in biocatalysis. Cofactors such as ATP and nicotinamide (NADPH) are dissociable, and work by providing functional groups that are transferred to substrate molecules, as such these cofactors must be used in stoichiometric amounts. The financial cost of these cofactors prevents them from being used stoichiometrically and instead they must be regenerated *in situ*⁴⁴. Regeneration can be done in one of three ways via; a coupled enzyme system, a coupled substrate system or electrochemically. When compared with enzyme-coupled regeneration, electrochemical strategies have been found to often be incompatible with other components of the enzymatic reaction, as well as not being able to achieve a high 'total turnover number' (TTN: the total number of moles of product formed per mole of cofactor over the course of the reaction).⁴⁵ The lower TTN for electrochemical strategies is often due to their lack of selectivity when compared with enzymatic regeneration methods.

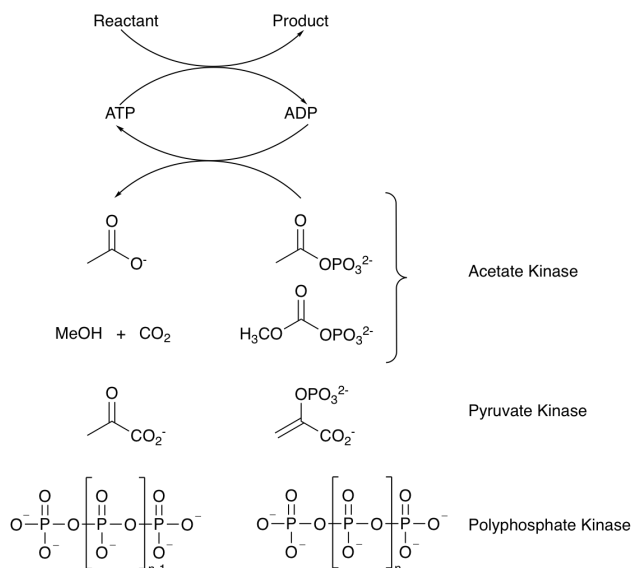


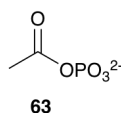
Figure 10 Four most common enzyme catalysis methods of ATP in situ regeneration

At present ATP can only be regenerated via coupled enzyme systems, there are three different types of kinase enzyme which have been found to be effective in the regeneration of ATP: acetate kinase, pyruvate kinase and polyphosphate kinase. It is important to note that while this project focuses on the regeneration of ATP, due to the promiscuity of both the acetate and pyruvate kinase other NTPs such as GTP, UTP and CTP have also been regenerated through the use of these kinase enzymes. Each of the three mentioned kinase enzymes will be discussed in detail in this section.

1.4.1 ATP Regeneration via Acetate Kinase

Acetate kinase (Figure 10), has been shown by Whitesides to be capable of being used with two different phosphoryl donors; acetyl phosphate and methoxycarbonyl phosphate.⁴⁶ Both of these phosphoryl donor possess their own individual strengths and weaknesses, which will be detailed below.

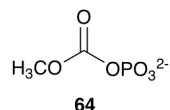
1.4.1.1 Phosphoryl Donor: Acetyl Phosphate



Acetyl phosphate (**63**) is stable in solution and is a phosphoryl donor of intermediate strength. The ease of synthesis of **63** is main factor that has enabled it to become one of the most commonly used phosphoryl donors in ATP regeneration enzyme systems.⁴⁶ There are two major drawbacks for the use of **63**, firstly it has a hydrolysis half life (25 °C, pH 7.5) of 21 h, secondly the acetate ion produced as a by-product of the ATP regeneration reaction acts as an inhibitor of the acetate

kinase.⁴⁷ Inhibition by the acetate ion has been found to only be of real import once in solutions containing in excess of 1 M acetate, and so **63** has been used successfully in ATP regeneration systems.⁴⁶

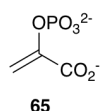
1.4.1.2 Phosphoryl Donor: Methoxycarbonyl Phosphate



Methoxycarbonyl phosphate (**64**) is a high strength phosphoryl donor, and similarly to **63** is relatively simple to produce. The by-product of phosphorylation is methyl carbonate, which undergoes rapid hydrolysis in solution to produce carbon dioxide and methanol. Immediate decomposition of the methyl carbonate helps to avoid by-product inhibition, as seen in both acetate kinase with **63** and pyruvate kinase with phosphoenolpyruvate, as well as diminishing the potential for problems arising during product isolation.⁴⁶ The only major drawback of **64** is its half life (25 °C, pH 7.5) of 0.3 h, which is inconveniently short.⁴⁶

1.4.2 ATP Regeneration via Pyruvate Kinase

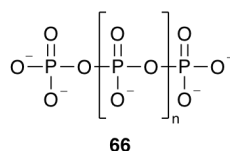
Pyruvate kinase can be used as a coupled enzyme in the *in situ* regeneration of ATP. Pyruvate kinase utilises phosphoenolpyruvate (**65**), which is a very strong phosphoryl donor, unlike the synthesis of both **63** and **64**, production of **65** is complex.



Pyruvate produced as a by-product of the ATP regeneration reaction is an effective inhibitor of the pyruvate enzyme, thus the reaction must be carried out in dilute solutions to ensure pyruvate concentration is low, and pyruvate must be removed upon formation to enable efficient ATP regeneration. The half-life (25 °C, pH 7.5) of **65** is 40 days.

1.4.3 ATP Regeneration via Polyphosphate Kinase

Regenerating ATP from AMP instead of ADP is highly desirable, as many ATP dependant enzymatic reactions produce AMP as opposed to ADP. The use of inorganic polyphosphates (Poly(P)), (**66**) to regenerate ATP from AMP is a recent development, polyphosphates are linear polymers made up of orthophosphate monomers linked together by high energy phospho-anhydride bonds.⁴⁵



In 2000, Resnick and Zehnder were the first to show that AMP could be used as an initial reagent, for the production of glucose-6-phosphate with hexokinase.⁴⁸ Hexokinase produces glucose-6-phosphate from glucose and ATP, producing ADP as a by-product. Resnick used a polyphosphate:AMP phosphotransferase (PAP) from *Acinetobacter johnsonii* to convert AMP to ADP, which was then converted to ATP by adenylate kinase. The ATP produced was then used by hexokinase to produce glucose-6-phosphate. The substrate specificity of PAP was probed, and it was found that only AMP showed significant phosphorylation to its relevant nucleoside 5'-diphosphate, the rate of GMP phosphorylation by PAP was shown to be 4 % of the rate measured for AMP, while no phosphorylation was found to have occurred for CMP or UMP.⁴⁸ While this use of PAP was an innovative leap forward in ATP regeneration, the method was marred with drawbacks such as a low TTN; and no cloned gene encoding for PAP.⁴⁵

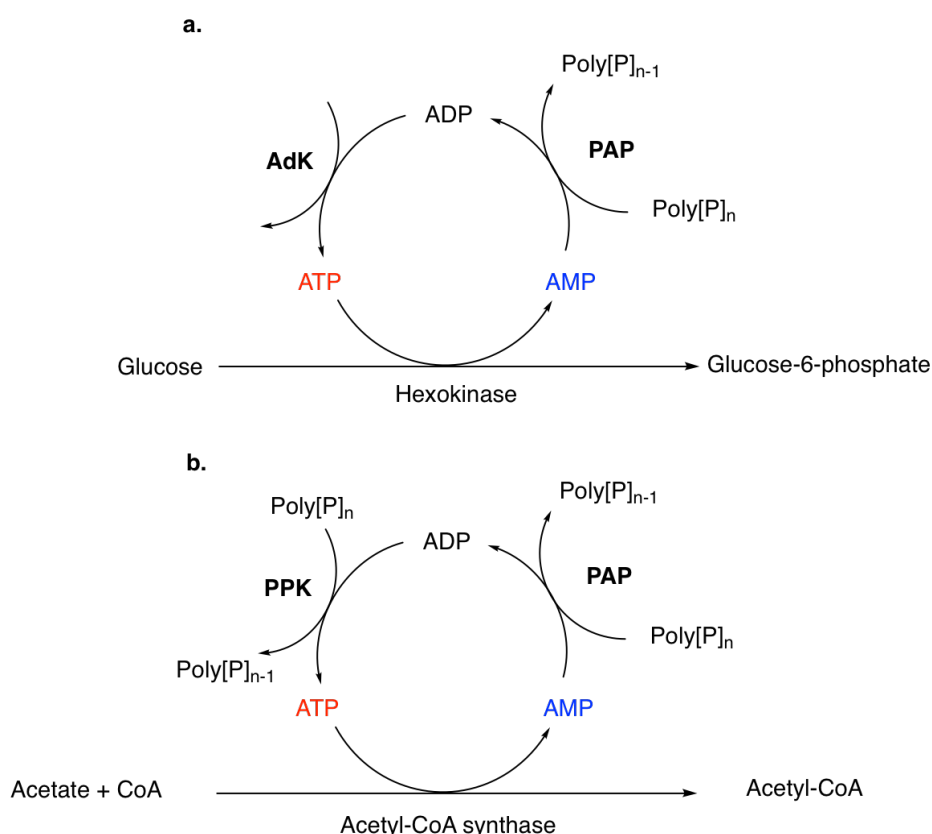


Figure 11 a. Resnick system for the production of glucose-6-phosphate using **66** as a phosphoryl donor for PAP. **b.** Shiba ATP regeneration, used in the production of acetyl-CoA, using **66** as the phosphoryl donor for both PAP and PPK reactions

In 2001, Shiba used polyphosphate:AMP phosphotransferase and polyphosphate kinase (PPK), to show that ATP could be regenerated from AMP using polyphos-

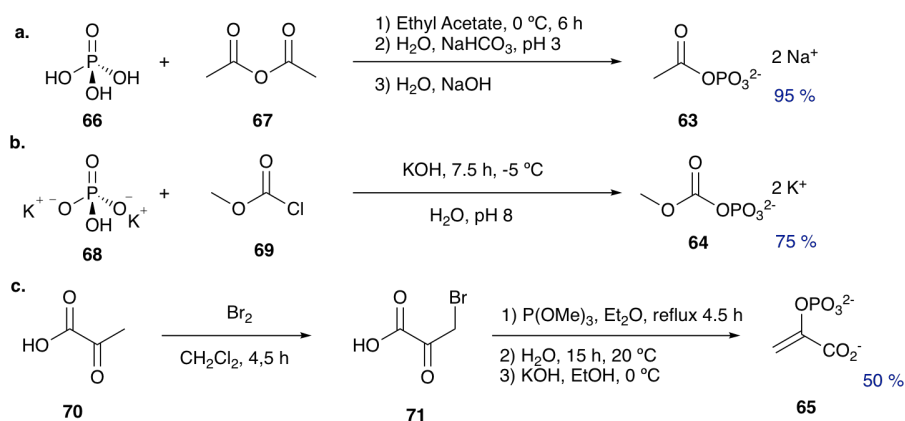
phate as a phosphoryl donor in both enzymatic reactions (Figure 11 b).⁴⁹ This system was subsequently used in the synthesis of acetyl-CoA from CoA, catalysed by acetyl-CoA synthase.⁴⁹ The production of acetyl-CoA required a source of ATP and generates AMP as a by-product, PAP was used to convert AMP to ADP using polyphosphate as a phosphoryl donor, PPK then converted ADP to ATP, again utilising polyphosphate as a phosphoryl donor.⁴⁹

The initial concentration of **66** is critical as both PAP and PPK use it as a phosphoryl donor, as such **66** concentration is the limiting factor in both reactions. At high concentrations **66** was shown to chelate Mg^{2+} ions, these divalent metal ions are essential for enzymatic catalysis, thus resulting in a decrease in the rate of ATP production. During the synthesis of acetyl-CoA, the amount of acetate decreased steadily over 16 h, and after 18 h all of the CoA had been converted into acetyl-CoA.⁴⁹ Initially only 0.25 mM AMP was added to the reaction, thus over the course of the 18 h ATP was regenerated 39.8 times, this is significantly higher than the degree of ATP regeneration in Resnick's method where ATP was regenerated between 3 and 4 times.⁴⁹ Regeneration from GMP was investigated and the dual enzyme system was found to be capable of regenerating GTP.⁴⁹

1.4.4 Comparison of ATP Regeneration Systems

At present, acetate kinase utilising **63** as a phosphoryl donor is the most commonly used method of *in situ* ATP regeneration.⁵⁰ This subsection will discuss and compare the advantages and disadvantages of acetate kinase, pyruvate kinase and the polyphosphate donor systems developed by Resnick and Shiba.⁴⁹

The pyruvate kinase system is one of the most efficient, due to the use of **65**, which behaves as a strong phosphoryl donor. Pyruvate kinase has a half-saturation constant (K_m) for ADP of 0.1 mM, while acetate kinase has a K_m [MgADP] of 0.4 mM, thus meaning that pyruvate kinase is capable of regenerating ATP at lower concentrations of ADP.^{46, 48} The K_m of PAP is 0.26 mM for AMP, while polyphosphate kinase has $K_m = 0.8 \mu\text{M}$ for ADP, meaning that **66** is tightly bound to the active site of the kinase and, is used until it decomposes.⁴⁸



Scheme 14 Synthetic pathways for the production of (a) **63**, (b) **64** and (c) **65**.⁴⁶

A key factor in determining the most industrially useful method of ATP regeneration lies in the ease of production of the phosphoryl donor. Figure 14 shows that synthetic pathways for both **63** and **64** are simple, while **65e** has a much more complex pathway. Unfortunately due to the very short half life of **64** (0.3 h), it is inconvenient for use in ATP regeneration. Both **63** and **65** have been used successfully in ATP regeneration systems, but both come with their own individual disadvantages, the pyruvate by-product acts as an inhibitor of the pyruvate enzyme while **63** has a relatively short half life of 21 h. The use of **66** as a donor in ATP regeneration systems has been shown to be effective, but is not currently widely used, though **66** is cheap to purchase and could allow phosphorylation from AMP as opposed to ADP, the strict substrate specificity of polyphosphate kinases means that only ATP can be effectively regenerated by these kinase enzymes. Our chemo-enzymatic route towards NTP production, uses inexpensive reagents to produce the phosphoryl donor and uses a promiscuous NDPK. As such our pathway has the potential to be used for the regeneration of a range of NTPs.

2 Protein Production

This chapter describes and discusses the initial production, transformation and expression of NDPK H122G which was developed by Dr Stefanie Freitag-Pohl, before moving on to discuss the subsequent purification of the protein. Protein over expression and purification were originally preformed by Dr Freitag-Pohl during the first iteration of this project. BL21(DE3) *E. coli* competent cells were produced by Dr Freitag-Pohl and frozen, the frozen cells where defrosted by the author then overexpressed and purified using the methods outlined in Sections 2.2.4 and 2.3.

Firstly, background information relating to the biochemical technologies used throughout this project will be discussed, after which the methods used to express and purify the H122G NDPK mutant will be discussed in detail.

2.1 Introduction to Molecular Cloning

The discovery of DNA's structure by Watson and Crick in the 1950's, led to an understanding of the physical basis of genetics ⁵¹. Since this fundamental discovery, advances in genetic engineering have enabled scientists to alter and manipulate the genetic code, allowing insight into how altering even a single nucleotide can alter behaviour.

Molecular cloning, the ability to cut, alter and combine DNA molecules together *in vivo*, and the use of vector systems to mass produce recombinant DNA, together form the basis of recombinant DNA technology. This project has utilised both of these strategies, and so the biochemical background of both will be explored below in Sections 2.1.1 and 2.1.2.

2.1.1 Isolating DNA fragments

DNA fragments are primarily amplified via one of two methods, restriction enzymes or the polymerase chain reaction (PCR). This project only utilised PCR, and as such restriction enzymes will not be discussed in this report.

2.1.1.1 *Polymerase Chain Reaction*

The polymerase chain reaction (PCR), is a process which utilises specific heating and cooling cycles in the presence of a thermostable DNA dependant DNA polymerase to amplify small DNA fragments. There are several essential components in PCR, firstly a template containing the target sequence, which will be amplified, two primers (forward and reverse primer) are also present in large excess in the reaction solution.⁵² The primers are essential as they specify which fragment of DNA will be amplified by binding to the template on either side of the fragment. All four varieties of NTP (A, G, C and T) are present in the reaction solution, as well as

a thermally stable DNA polymerase, which is responsible for the addition of the dNTPs onto the forming DNA strands.

There are three stages to the PCR cycle, the first is strand separation; template DNA is heated to ~ 95 °C causing the two complementary strands of template DNA to separate, thus each strand may serve as a template.⁵² The reaction solution is then cooled to ~ 55 °C which allows hybridisation of the primers to the DNA templates, the second stage of PCR. One primer will hybridise to the 3'-end of the target sequence on one strand, while the second primer will hybridise to the 3'-end of the complementary strand, since DNA synthesis occurs in a 5' to 3' direction new NTPs are added to the 3'-end and the two primers are directed towards one another, thus amplifying the region between the two primers.⁵² The reaction solution is heated to ~ 75 °C, and the DNA polymerase elongates both primers across the target sequence, thus generating two additional copies of the target sequence. These three stages constitute one PCR cycle, with each cycle the amount of DNA doubles. Typically between 20-30 cycles are required, after which the main species present in solution is a DNA fragment whose length is equal to the distance between the two primers.

2.1.2 Cloning Recombinant DNA

DNA fragments that have been isolated by PCR or restriction enzymes cannot immediately be cloned and expressed, instead firstly the DNA fragment of interest must be up turned into a form which can be replicated by bacterial host cells. As such the DNA fragment of interest is put into a vector.

2.1.2.1 Vectors

All vectors have two essential traits, firstly they can be combined with DNA fragments (typically from a different organism than the vector DNA - forming recombinant DNA), and they can be capable of replicating autonomously in host cells.⁵² The most commonly used vectors are plasmids, independently replicating circles of DNA in bacteria, and bacteriophage, a virus that can inject its genetic information into bacteria.⁵²

There are three features that all cloning vectors have; (1) an origin of replication, (2) restriction sites and (3) a selectable marker. Replication of the vector is initiated by a particular DNA sequence, termed the origin of replication. Two different restriction enzymes cut both the isolated DNA fragment and the vector, these restriction enzymes are chosen to give compatible 5' and 3'-end to the vector and fragment this ensures not only that the sticky ends of both the vector and the fragment match, but also that the fragment is inserted into the vector in the correct orientation.⁵² DNA ligase then binds the DNA fragment (insert) and the vector together forming the recombinant DNA, termed a construct. Selectable markers

allow the detection of host cells containing the construct, and often take the form of antibiotic resistance. Only cells which contain the vector with antibiotic resistance (also containing the construct) are able to survive when grown on a plate containing the antibiotic, thus allowing for the easy detection of cells containing the construct.⁵² Once the construct has been cloned via a cloning vector, it must then be put into an expression vector to allow for expression of the protein product. The construct is then often introduced into competent cells which are permeable to DNA via transformation. The competent cells (generally bacterial cells) are then grown in a culture dish, and the colonies of clones containing both the DNA insert and antibiotic resistance grow.⁵²

2.2 Protein Expression

Expression of the H122G NDPK mutant used four distinct steps, firstly the genetic insert was generated and amplified from the synthetic gene. In the second step, the expression vector pOPINF was linearised via double digest. Step three involved the in-fusion annealing of the linear pOPINF vector and the amplified insert to form a recombinant plasmid. The plasmid was transformed into BL21(DE3) *E. coli* cells for bacterial overexpression in step 4. Each of these steps will be discussed in detail in the subsections below.

2.2.1 Step 1: Insert Generation

The synthetic gene (pUC57 cloning vector with ampicillin resistance) for H122G NDPK was transferred into Stellar competent cells via heat-shock transformation. The resulting culture was grown over night at 37 °C on a liquid broth (LB)/ agar plate. PCR was then performed using the temperature cycle in table 1

Table 1 PCR temperature cycle

Step	Temperature / °C	Time / s
1 - Initial Denaturation	98	60
2 - Denaturation	98	10
3 - Annealing	62	15
4 - Elongation	72	30
5 - Final Elongation	72	300

Steps 2 - 4 were cycled 30 times before step 5 was completed. After amplification the products were then resolved on agarose gel (1.5 %), the desired product band was

cut out and extracted using NucleoSpin gel clean up (Clonetechn In-Fusion Cloning Kit), after which the insert was stored at -20°C .

2.2.2 Step 2: Linearise Expression Vector

Expression vector pOPINF (ampicillin resistant) in the form of a bacterial stab was grown on LB/ agar plate at 37°C overnight, before undergoing linearisation via double digest. The double digest used HindIII and KpnI, after linearisation the product was analysed on an agarose gel (15 %) which is shown in figure 12.

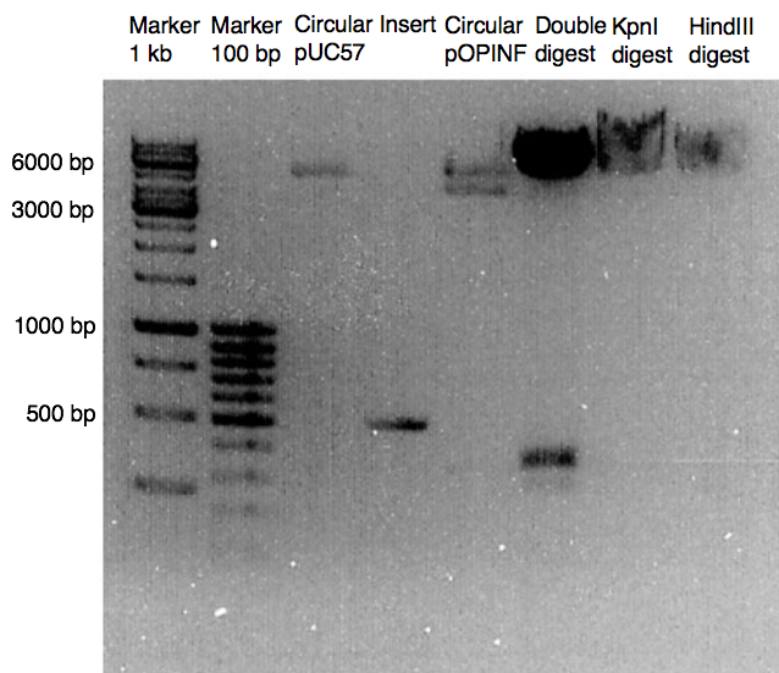


Figure 12 Agarose (15 %) gel of linearised pOPINF

The band containing the digested vector was cut out of the gel and cleaned using the NucleoSpin kit.

2.2.3 Step 3: Vector-Insert Annealing

A linearised vector to insert ratio of 1 : 3 was used, the plasmid was then transformed into Stellar competent cells and grown on a LB/ agar plate overnight at 37°C .

Eight colonies from the plate were used to inoculate LB/ ampicillin ($50\ \mu\text{L}$) mixture, $1\ \mu\text{L}$ of each mixture was then used as a template for PCR following the temperature cycle in table 1. The amplified products were then resolved on an agarose gel (15 %), Figure 13. Colonies 2,3,4 and 8 were shown to carry the 500 bp insert.

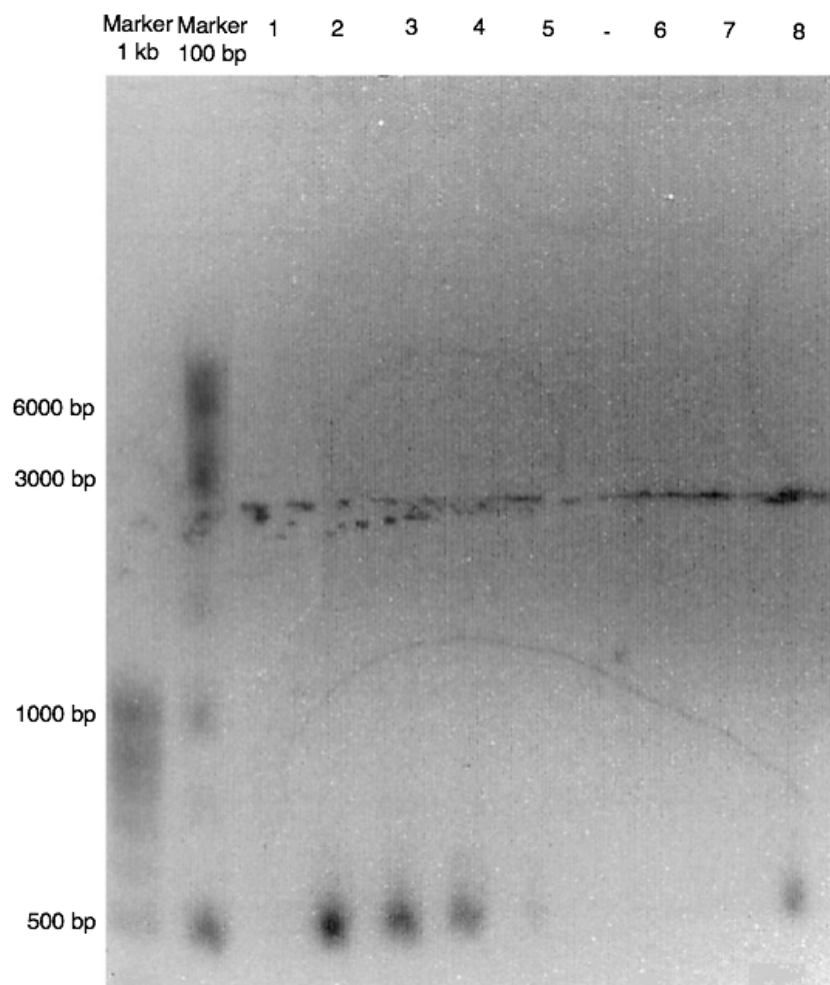


Figure 13 Agarose (15 %) gel of PCR products for eight fusion product colonies

2.2.4 Step 4: Protein Overexpression

After sequencing, to confirm that the insert was present. The plasmid was transformed into BL21(DE3) *E. coli* competent cells, cultures were then grown in super optimal broth (SOB) before being transferred to a LB/ ampicillin and chloramphenicol plate and grown overnight at 37 °C. Colonies from the plate were used to inoculate LB (1 L).

2.3 Protein Purification

This section will discuss firstly the method via which NDPK H122G was purified, before moving on to discuss analysis of the purified fractions and subsequent conformation that the protein of interest had been purified and isolated.

2.3.1 Purification of NDPK H122G

Cell cultures were grown to an optical density (OD) of 0.7, after which isopropyl beta-D-1-thiogalactopyranoside (IPTG) (1 M, 1 mL) was added. After further

growth, the cells were collected and lysed. The supernatant was loaded onto a 1 ml HisTrap column.

The HisTrap column has nickel ions bound to the stationary media, so when cell lysate flows through the column, proteins containing oligohistidine tags coordinate to the nickel ions, thus binding the targeted protein to the column. The binding buffer contains a low concentration of imidazole (30 mM), since imidazole can bind to nickel ions, it competes with proteins which do not contain a oligohistidine tag, thus ensuring that all proteins aside from the target protein cannot bind and are eluted from the HisTrap column. This can be seen during the column wash stage of the chromatograph (figure 14), the peak which eluted after 6 ml of eluent relates to these non-desired proteins. The concentration of elution buffer was increased via a stepwise gradient, from 0, 20, 40, 60, 80 to 100 %. The elution buffer contained 1 M imidazole and so as the % of elution buffer increased so did the imidazole concentration, at approximately 60% elution buffer a large peak was eluted.

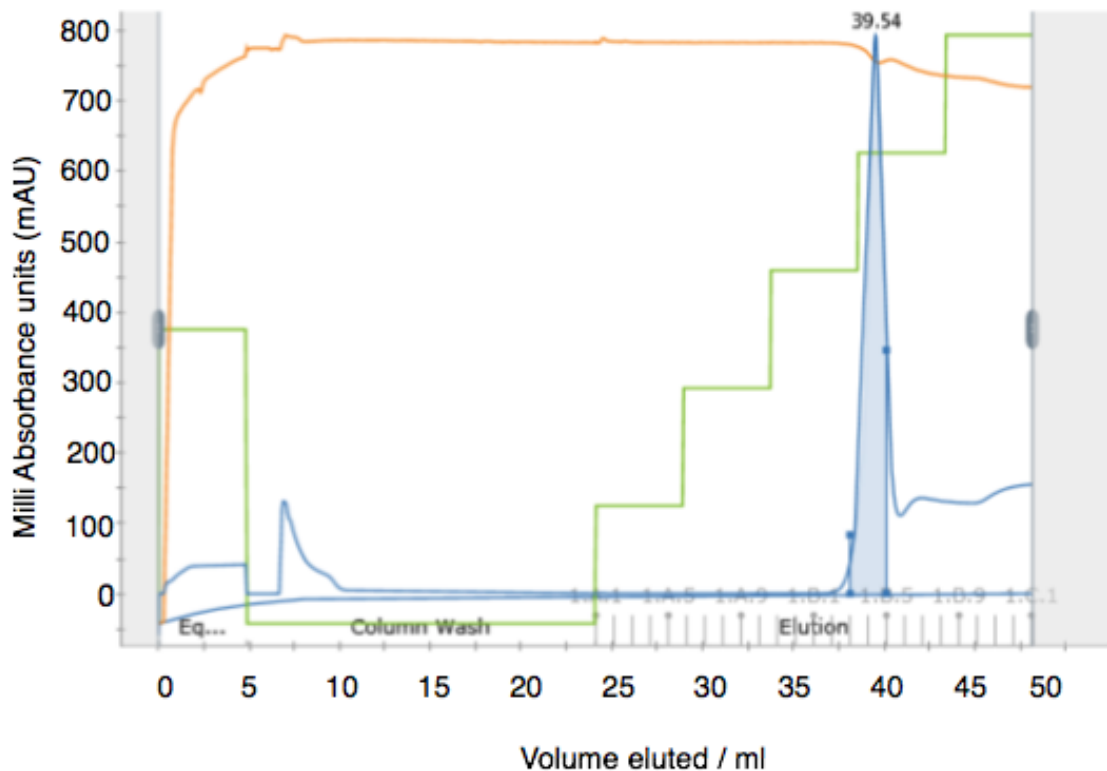


Figure 14 Chromatograph showing the elution of proteins from the HisTrap column. UV absorbance at 280 nm is shown by the blue line, the conductivity is shown by the orange line, while elution buffer concentration is represented by the green line.

Analysis of eluent fractions relating to the large peak was done via SDS-PAGE, to determine if the peak corresponds to the desired NDPK protein. This analysis will be described in Section 2.3.2.

2.3.2 Confirmation of NDPK H122G Purification

Samples of all of the fractions relating to the peaks at retention time 37 - 40 minutes were run, alongside two samples taken from either end of the flow-through to confirm that NDPK binding was successful in non-eluting conditions.

The molecular weight of NDPK H122G is approximately 19 kDa, as can be seen from the gel in Figure 15 fractions 2, 3, 4 and 5 correspond to a protein of this weight, thus we were confident that these fractions contained the desired NDPK protein. The two flow-through samples show no visible bands at 19 kDa, confirming that NDPK protein binding to the HisTrap column was successful. The fractions containing the desired protein were combined and dialysed into HEPES buffer (30 mM, pH 7.5). The dialysed protein was concentrated via centrifugal concentration, the resulting solution had a volume of 1 ml and a protein concentration of 3.61 mg ml⁻¹.

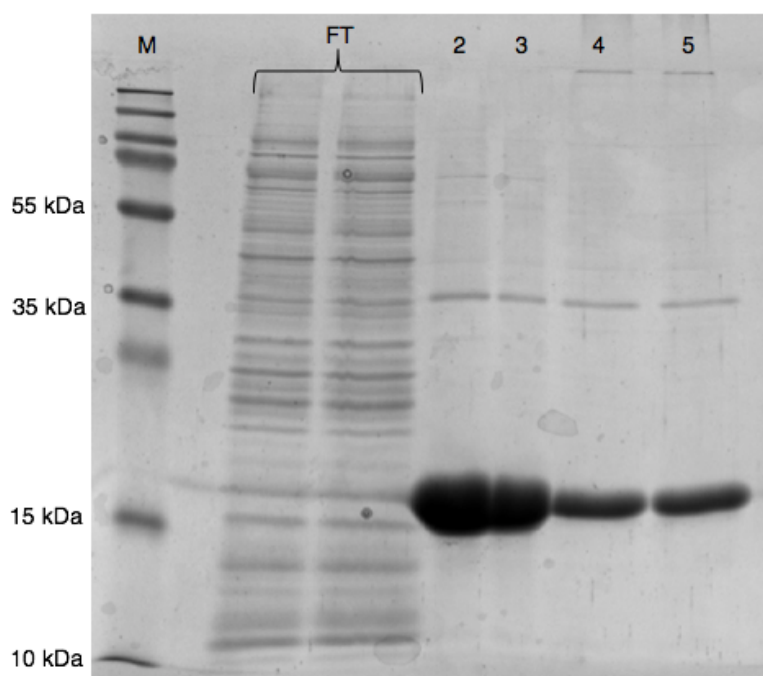


Figure 15 SDS-PAGE of fractions collected during purification of NDPK H122G. Analysed fractions relate to the elution peak shown in Figure 14, M = marker, FT = flow-through.

2.4 Chapter Summary

This chapter discusses the protein expression and purification of the H122G NDPK mutant in detail. Protein expression was a four step procedure performed by Dr Freitag-Pohl; firstly the genetic insert for H122G NDPK was generated and amplified using Stellar competent cells and a 30 cycle PCR method. After the amplified insert had been generated and frozen, the expression vector pOPINF was linearised via double digest using HindIII and KpnI. Annealing of the linearised vector and the insert required a ratio of 1:3 and resulted in the production of a plasmid, which

was transformed in to Stellar competent cells and grown overnight on a LB/ agar plate. Eight of the colonies grown on the plate were subjected to PCR, and of the amplified products; four of the colonies were shown to carry the H122G NDPK insert. Colonies containing the insert were transformed into BL21(DE3) *E. coli* competent cells. These cells were stored at $-20\text{ }^{\circ}\text{C}$.

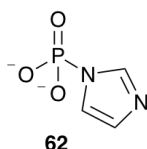
The frozen BL21(DE3) *E. coli* competent cells were defrosted by the author. Cultures were grown in SOB before being transferred to and grown on a LB/ampicillin and chloramphenicol plate. Purification of the cell cultures was done using a HisTrap column, with a 1 M imidazole elution buffer. The eluted fractions which contained the desired protein were combined and dialysed into HEPES buffer.

The methods presented in this chapter show how the H122G NDPK mutant was successfully expressed and purified. After which the mutant was used in the chemo-enzymatic enzymatic method detailed in Chapter 3, to produce NTPs.

3 Phosphorylation of Imidazole

3.1 Introduction

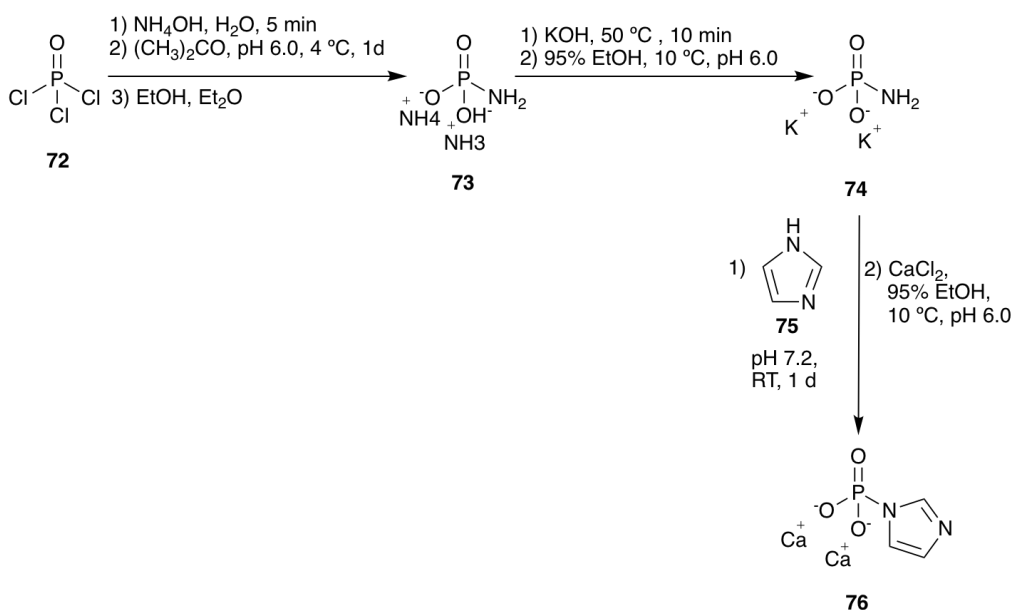
This chapter describes the development and subsequent optimisation of a synthetic route towards phosphoimidazole (**62**). Firstly, known methods of **62** synthesis will be discussed, before moving on to the use of direct aqueous phosphorylation, a method which has been successfully employed by the Hodgson group.⁵³



3.1.1 Known Methods for the Synthesis of Phosphoimidazole

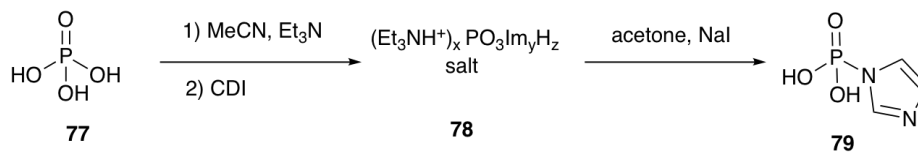
Phosphoimidazole has a half-life of ~ 10 days in neutral conditions thus making it a convenient candidate to serve as a phosphoryl donor. There are currently only two published methods via which phosphoimidazole has been produced.^{47,54,55} Both methods require extensive work up due to a range of phosphorylated imidazole species being produced, thus resulting in arduous and inefficient production of **62**.

In 1956, the Rathlev group produced PIm via a three step reaction procedure (Scheme 15), firstly a phosphoramidate intermediate is formed as the ammonium salt (**73**), which is then converted into the potassium salt (**74**). Imidazole is then reacted with **74** to form a variety of phosphoimidazole species. The purification of the reaction products resulted in a relatively low overall yield of the calcium salt of phosphoimidazole (**76**) ($\sim 9\%$).^{55,56}



Scheme 15 Reaction scheme for the production of PIm via a phosphoramidate intermediate⁵⁶

In 1961, the Cramer group produced PIm via a two step mechanism which produced a crude $(\text{Et}_3\text{NH}^+)_x \text{PO}_3\text{Im}_y\text{H}_z$ salt (Scheme 16). The values of x , y and z are determined by the pH of the reaction.



Scheme 16 Cramer reaction scheme for the production of PIm via a crude $(\text{Et}_3\text{NH}^+)_x \text{PO}_3\text{Im}_y\text{H}_z$ salt

3.1.2 Aqueous Phosphorylation Methods

Most organic reactions that require the use of water-sensitive reagents are performed under scrupulously dry reaction conditions. However our synthetic route towards **62**, utilises the much greater nucleophilicity of amines, when compared to water or hydroxide, to react phosphoryl chloride (which is highly reactive with water) with an amine in aqueous solution.

The potential reaction pathways for the formation of **62** are shown in Figure 16. Currently, the exact reaction pathway through which **62** is formed is unknown. POCl_3 can initially undergo either aminolysis to form dichloro-phosphoimidazole (**80**) or hydrolysis to form phosphodichloridate (**83**).

If hydrolysis is the first step **83** is produced as an intermediate species, **83** is an anionic electrophile and thus can repel attack by hydroxide ions. The greater nucleophilicity of imidazole results in the rate of aminolysis being higher than the rate of hydrolysis for **83**, as such chloro-phosphoimidazole is produced (**86**). ^{31}P NMR studies of the crude reaction mixture produced during phosphorylation of imidazole by POCl_3 showed that 1,1'-phosphodiimidazole (**82**) was produced as a by-product (2%). This suggests that **86** is unselective and so reacts via a dissociative $\text{S}_{\text{N}}1$ like mechanism. A dissociative mechanism means that the nucleophile which reacts with **86** is controlled by the rate of diffusion, and so is dependant on the concentration of the nucleophiles in solution, since water has a much higher concentration (~ 55 M) than imidazole (75 mM) the majority of **86** will undergo hydrolysis to form **62**.

The greater rate of aminolysis compared to hydrolysis means that the first step of the reaction pathway could involve the formation of **80**. Chloride ions are good leaving groups and so the reaction of **80**, like that of **86** is likely to be $\text{S}_{\text{N}}1$ like in nature, as such which nucleophile reacts is controlled by the rate of diffusion and so hydrolysis will be the main reaction pathway due to its higher concentration producing **86**.

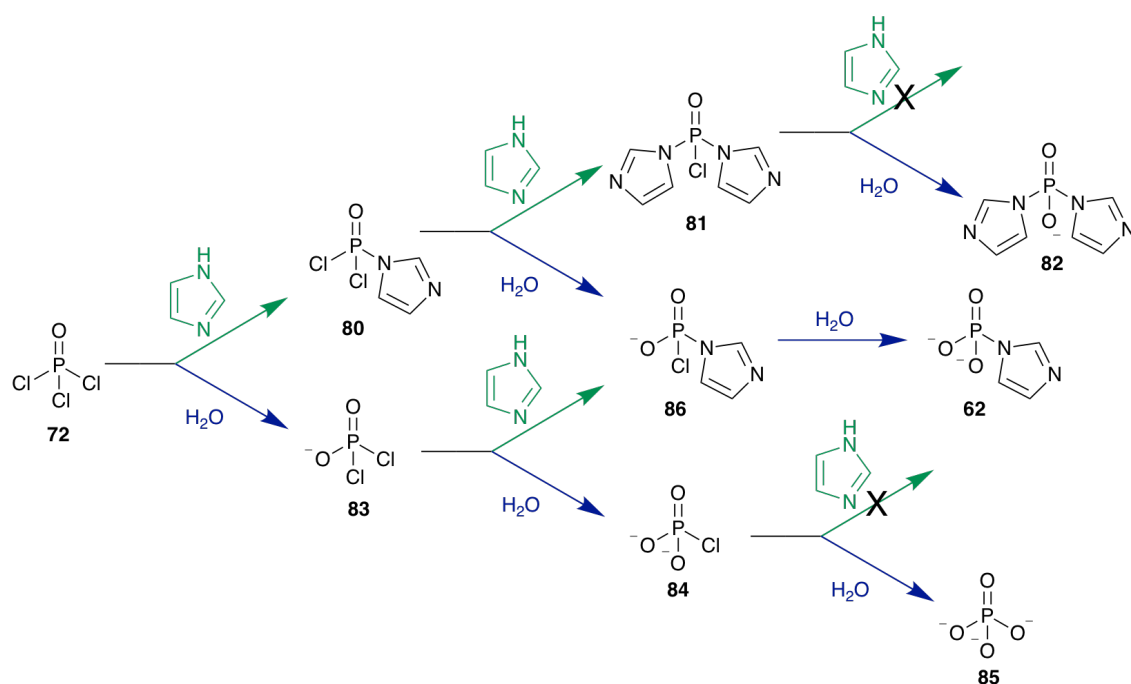
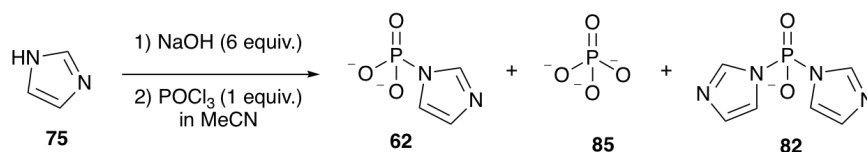


Figure 16 The potential aminolysis and hydrolysis reactions which POCl_3 can undergo during the synthesis of PIm in aqueous media.

3.2 Synthesis of Phosphoimidazole

The method employed to synthesise phosphoimidazole (**Scheme 17**), in this project utilised direct phosphorylation of imidazole by reacting 1 equivalent of POCl_3 in dry acetonitrile with imidazole in basic aqueous solution, predissolved. The POCl_3 stock solution was held under argon, to limit hydrolysis before exposure to the reaction mixture. Six equivalents of sodium hydroxide were used to ensure that the reaction mixture remained basic throughout the phosphorylation reaction, this was essential to limit the hydrolysis of the P-N bond in **62**.



Scheme 17 The method of phosphoimidazole synthesis utilised in this project

In 1971, Benkovic and Sampson conducted a range of experiments into the hydrolysis of phosphoramidate monoanions. The pH-rate profile for the model aliphatic phosphoramidate, N-(*n*-butyl)phosphoramidate is shown in Figure 17, the S-shaped pH-rate graph shown is typical for phosphoramidates in aqueous media.⁵⁷ It is evident that as the pH is lowered, the subsequent protonation of the phosphoramidate results in an increase in the observed rate of hydrolysis. The first rate order constants for the neutral (k_1) and monoanionic (k_2) phosphoramidate species at 36.8 °C are 0.700×10^2 and $0.420 \times 10^2 \text{ min}^{-1}$ respectively, while the second order rate constant associated with hydronium catalysed hydrolysis is $55.5 \times 10^2 \text{ M}^{-1} \text{ min}^{-1}$.^{57,58}

As such to limit scission of the P-N bond via acid hydrolysis, phosphorylation of imidazole was carried out in basic aqueous media.

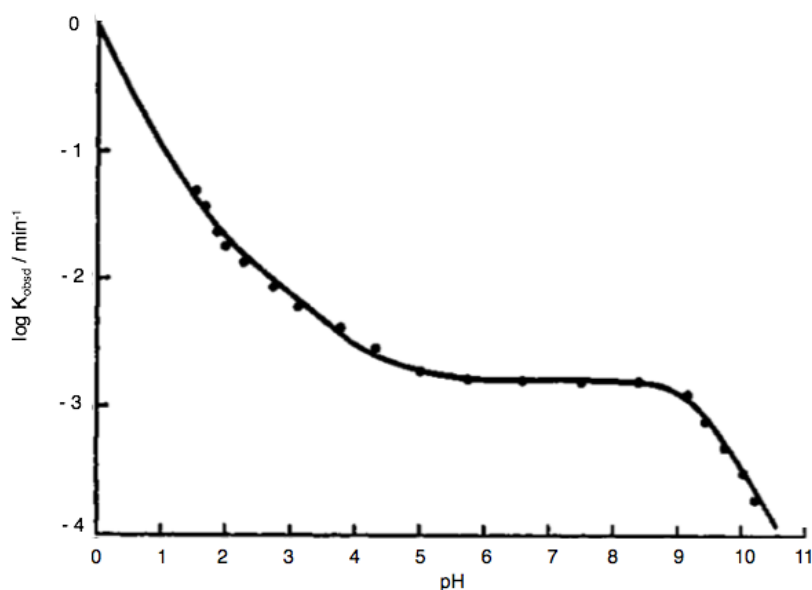


Figure 17 Graph showing the $\log k_{obs}$ -pH rate profile for the hydrolysis of N-(*n*-butyl)phosphoramidate at 55 °C. Adapted from⁵⁷

The ^{31}P NMR spectrum of the crude reaction mixture before purification, contained three signals relating to phosphoimidazole (**62**), inorganic phosphate (**85**) and small levels (2 %) of 1,1'-phosphodiimidazole (**82**) (Figure 18). The presence of inorganic phosphate was confirmed via a 'spike' experiment where trisodium phosphate, was added and the inorganic phosphate signal increased significantly. ^1H NMR spectrum of the crude reaction mixture confirmed the presence of unreacted imidazole.

A purification procedure was adapted from established literature methods by Dr Freitag-Pohl.⁴⁷ Initially, acetonitrile was removed via rotary evaporation followed by freeze drying of the solution, a process which took over 24 h. The crude product was then subjected to centrifugation in the presence of acetone and sodium iodide, resulting in the removal of the unreacted imidazole impurity.⁴⁷

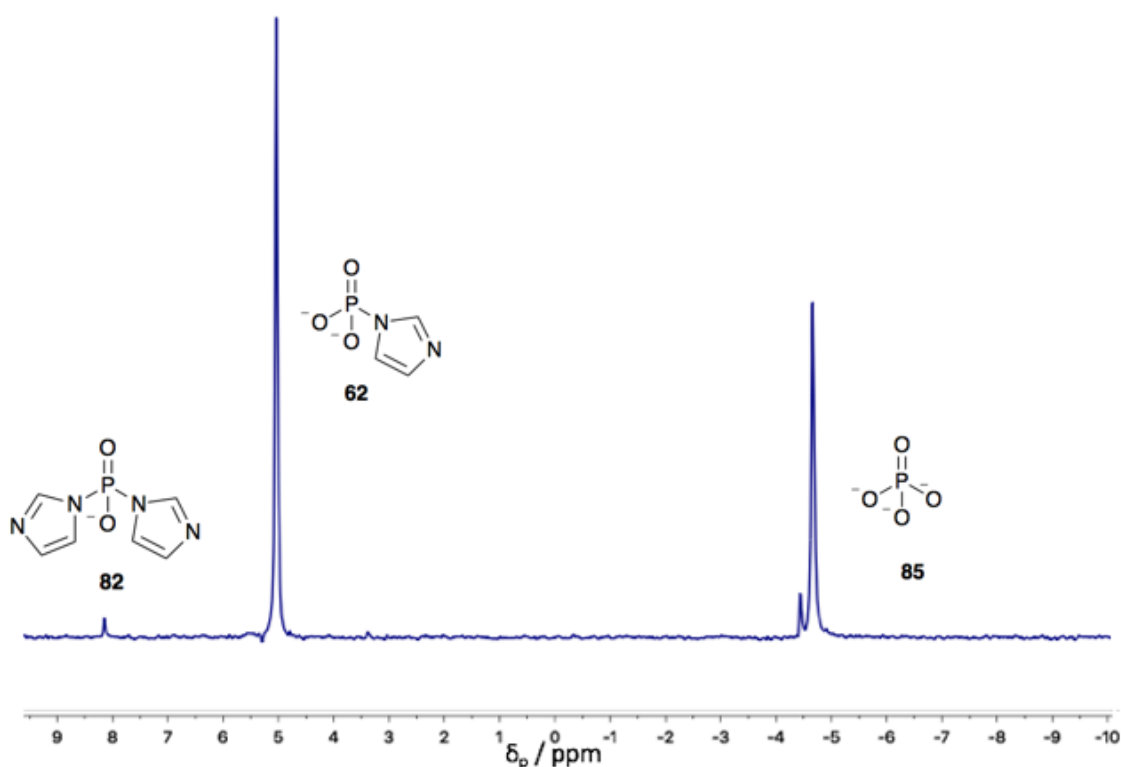


Figure 18 ^{31}P NMR Spectra of PIm crude reaction solution; **85** is at - 4.5 ppm, **62** is a 5.0 ppm and **82** is at 8.2 ppm.

3.3 Optimisation

The following section will firstly describe the experiments that were undertaken to optimise the initial synthesis of phosphoimidazole, before moving on to discuss the purification procedures.

3.3.1 Aqueous Phosphorylation of Imidazole

Initially, the reaction of imidazole with POCl_3 used 50 mM of imidazole in a 1 to 1 ratio with POCl_3 , this gave a crude reaction mixture made up of 45% **62**, 53% **85** and 2% **82** by ^{31}P NMR spectroscopy. The effect of imidazole concentration upon phosphorylation was investigated by varying the starting imidazole concentration between 50 mM and 500 mM, while keeping the molar ratios of imidazole to POCl_3 at 1 to 1. The results were analysed via ^{31}P and ^1H NMR of the crude reaction mixtures.

3.3.1.1 Results and Discussion

Optimal imidazole concentrations were found between 75-250 mM, in this range conversion to **62** was found to be between 53-55 %. In this range, the rate of aminolysis was higher than the rate of hydrolysis of POCl_3 , thus resulting in a greater levels of **62** being produced. Above 250 mM imidazole, both solubility and the exothermicity of the reaction became major issues. Despite both 75 mM

and 250 mM giving 55 % conversion to **62**, 75 mM was chosen as the optimum imidazole concentration, due to the exothermicity of the phosphorylation reaction, at 250 mM the reaction solution began to reflux spontaneously, thus demanding that optimisation of reagent concentration be limited to a value of 75 mM imidazole.

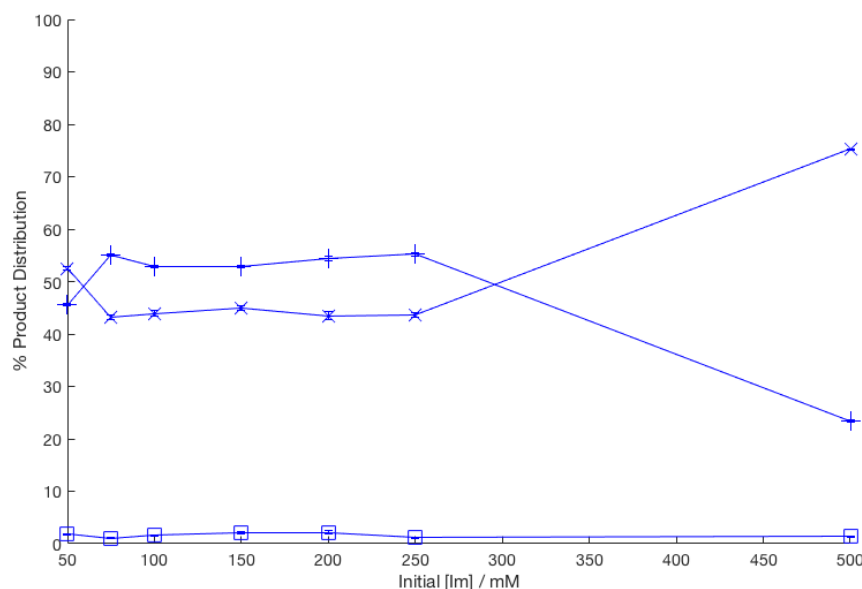


Figure 19 Graph showing the % of **62**, **85** and **82** produced at a range of initial imidazole concentrations. (red - **62**, blue - **85**, green - **82**)

3.3.2 Purification Procedure

The initial purification procedure discussed in section 3.2 was extremely time consuming, due to the use of freeze drying. As such experiments were conducted into a purification method which would allow simple production of pure **62** within 24 hours. One of the key goals of optimising the purification protocol was to remove the use of a freeze-drier from the procedure, as this step was very time inefficient being in excess of 24 h.

3.3.2.1 Results and Discussion

It was found that during the initial rotary evaporation step (to remove acetonitrile), that upon removal of over 80 ml of the 110 ml crude reaction solution (including the removal of some water), a white solid precipitated out of solution. Analysis of the precipitate and solvent showed that the supernatant contained mostly **85** and **82**, while the precipitate was composed of 81 % **62**, 19 % **85** and 1 % **82** by ^{31}P NMR. Thus the precipitate was separated from the supernatant via centrifugation for further purification.

Table 2 The % of **62**, **82** and **85** present in the crude product solution after each of the purification steps by ^{31}P NMR

Purification Step	% Compound		
	62	85	82
1 st Recrystallisation	85	14	1
2 nd Recrystallisation	97	3	0
EtOH Wash	98	2	0

Firstly, the precipitate was recrystallised, initially recrystallisations were performed in water, however later attempts used 10 mM NaOH, as a basic environment should limit the rate of hydrolysis of **62** to **85**. This change in recrystallisation solvent resulted in an increase in the proportion of **62**, from 79 % to 85 %, after the first recrystallisation.

After the second recrystallisation the recovered solid contained 97 % **62** and 2 % **85**. No **82** was detected after the second recrystallisation. ^{31}P NMR was used throughout to monitor how the % of **62**, **85** and **82** changed with each purification step (Figure 20). ^1H NMR revealed that the composition of the recrystallised product was 64 % imidazole to 36 % **62**, removal of the imidazole impurity is imperative, as imidazole has been shown by Admiraal to be a competitive inhibitor in the H122G mutant kinase enzyme.⁴³

Initially, after the second recrystallisation, crystals were dried on the high vacuum line before being washed with ethyl acetate (50 ml) overnight. A ^1H NMR spectrum of the washed crystals showed that the crystals were composed of 73 % **62** and 27 % imidazole. To allow the removal of more imidazole from the final PIm compound, after being dried on the high vacuum line the crystals were ground up with a pestle and mortar before being washed overnight with ethyl acetate (50 ml). After washing the crystals were again dried, after which they were re-subjected to ^1H and ^{31}P NMR, which gave a final product composition of 98 % **62**, 2 % **85** by ^{31}P NMR spectrum and 79 % **62** and 21 % imidazole by ^1H NMR spectrum, as such the purification procedure needs to be further optimised, potential ways to improve purification will be discussed in Section 5.2.1.

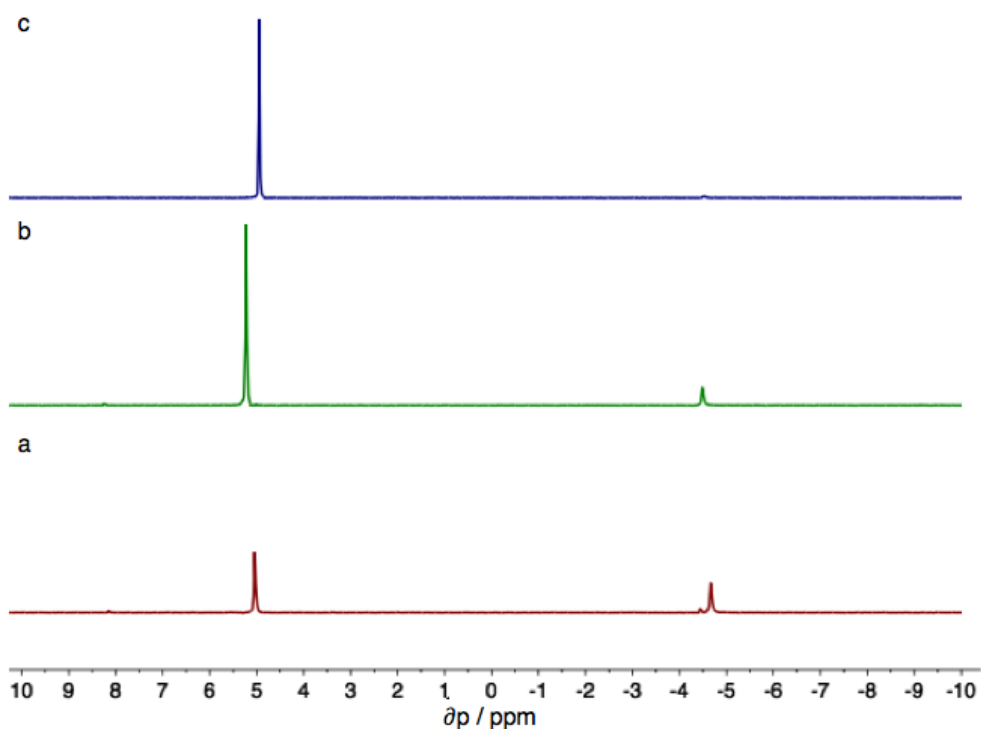


Figure 20 ^{31}P NMR Spectra of PIm (a) crude reaction solution, (b) crystals formed after the first recrystallisation, (c) crystals formed after the second recrystallisation

3.4 Conclusions

Optimisation of both the synthetic route and the purification procedure of phosphoimidazole, has allowed for the production and partial purification of **62** using easy and time efficient methods. Investigations into the optimum concentration for the synthetic pathway allowed for improved conversion to **62**.

Optimisation of the purification procedure, resulted in the reduction of P-N bond scission, via the use of a basic aqueous solvent for recrystallisation. The use of a pestle and mortar to grind up the crystals, produced after the second recrystallisation (thus increasing surface area), resulted in a large decrease in the amount imidazole found in the final compound which is essential for the effective use of **62** with the H122G kinase enzyme.

4 Enzyme Assays and Analysis

This chapter describes firstly, the various high performance liquid chromatography (HPLC) columns and methods used over the course of this project. HPLC was used to monitor the kinetics of the phosphorylation of NDPs by the PIm/ NDPK H122G system. The various enzymatic experiments, investigating the effect of impurities and PIm concentration on the total % conversion of ADP to ATP will be detailed.

4.1 HPLC Analysis

The kinetics of NDP phosphorylation reactions performed over the course of this project were monitored via HPLC. Reactions were monitored using two reverse phase analytical HPLC columns; SUPELCOSIL-LC-18-T and SIELC-Primesep SB columns were used to analyse the conversion of ADP/ATP and GDP/GTP respectively.

4.1.1 HPLC Columns

The development of HPLC methods has allowed for the separation and resolution of a plethora of biological molecules.⁵⁹ Molecules such as proteins, peptides and nucleotides which possess a degree of hydrophobic character, are predominantly separated via reversed phase chromatography.⁶⁰

Two types of reverse phase column were used in this project, a reverse-phase column that is able to run 100 % aqueous eluent (SUPELCOSIL-LC-18-T) and a mixed mode reverse-phase column (SIELC-Primesep SB) that also possesses anionic exchange characteristics. Both of these columns use octadecylsilane (C-18) bonded stationary phase, which allows retention and separation of the nucleotides being analysed.

Analysis of both the ATP/ADP and GTP/GDP systems was investigated with the SUPELCOSIL-LC-18-T column, and it was found that while the nucleotides of the ATP/ADP system had significant retention times and were well separated, the GTP/GDP system eluted at the solvent front. On this basis the SIELC-Primesep SB column was used for the analysis of the GTP/GDP system, as the column was able to retain the nucleotides, allowing for the production of significant retention times and well separated nucleotide peaks.

4.1.1.1 Reverse-Phase Column

Separation of nucleotides by reversed-phase HPLC depends on the strength of the hydrophobic binding interaction between the nucleotides and the immobilised hydrophobic C-18 stationary phase.⁵⁹

Gradient elution systems, which proceed from an initial aqueous buffer to a buffer containing organic solvent, are commonly used for the separation of biologi-

cal molecules. In the initial aqueous mobile phase, there is a high degree of organised water structure around the hydrophobic C-18 ligands and the nucleotides.⁶¹ Reduction of the exposure of these hydrophobic elements to the aqueous mobile phase is entropically favourable, and as such nucleotides and the C-18 ligands bind together.⁶¹ The more phosphate groups that are attached to a nucleotide, the less hydrophobic the nucleotide is and so the shorter its retention time on a reversed phase column. Over the course of the HPLC elution gradient the proportion of organic solvent in the mobile phase is increased. This causes a reduction in the polarity of the mobile phase, allowing for the de-absorption of nucleotides from the C-18 stationary phase.^{61,62}

Nucleotide polarity determines the order in which nucleotides are eluted from the column, NTPs are the most polar, have the shortest (often negligible) retention times and, are eluted first followed by NDPs and NMPs.

4.1.1.2 Reverse-Phase Columns with Ionic Properties

Reverse-phase HPLC is typically performed at low pH, non-polar molecules are retained effectively by the column.⁶³ Acidic molecules, which remain ionised at low pH do not tend to be retained by the column, as such ion pairing reagents are traditionally used to increase retention time.

4.1.1.2.1 Ion Pairing Reagents

Ion pairing reagents have a hydrophilic head and a long hydrocarbon hydrophobic tails, they are added to the mobile phase to increase retention time of charged analytes.⁶³ The hydrophobic tails interacts with the hydrophobic C-18 stationary phase of the column, thus leaving the charged hydrophobic head exposed in the mobile phase, where it can interact with oppositely charged solute molecules.⁶³ These electrostatic interactions result in an increase in retention time. Since nucleotides are anionic, they require the use of cationic ion pairing reagents such as tetra-n-butylammonium hydrogen sulfate $(\text{CH}_3\text{CH}_2\text{CH}_2\text{CH}_2)_4\text{N}(\text{HSO}_4)$.

The use of ion pairing reagents, is not without its drawbacks. Firstly, the use of an elution gradient is difficult due to the need for a long column equilibration time between analytical experiments.⁶⁴ This time is required to ensure the redistribution of the ion pairing reagent after the use of a gradient elution system, and can often be longer than the time required for the elution gradient experiment.⁶³ After the column has been exposed to an ion pairing reagent, due to the strong hydrophobic interactions between the hydrocarbons chains of the stationary phase and the tail of the ion pairing reagent, even after extensive washing of the column the ion pairing reagent cannot be completely removed.⁶³

4.1.1.2.2 Mixed Mode Column

The use of mixed mode columns in place of ion exchange reagents has become more

prevalent in recent years, as they are able to provide both ionic and reverse-phase characteristics^{63, 65}.

Mixed mode columns, unlike traditional reverse-phase and ion exchange columns, allow solutes to interact with the stationary phase of the column via more than one mechanism. They are capable of retaining either basic or acidic compounds, depending on the ionic group used, which cannot be retained by reverse-phase columns. The main interaction mechanism between the solute and the stationary phase is determined by both the elution conditions and the properties of the solute molecule.

Mixed mode columns which display reverse phase and ion exchange characteristics (e.g. SIELC-Primesep SB) can be categorised into four types of stationary phase (Figure 21). Type 1 stationary phases are achieved by mixing particulates of separation media with different chemical properties together, then packing the column with the mixture. Type 2 stationary phases utilises ligands with different functionalities.

Most commercial mixed mode columns are either type 3 or 4, the Primesep SB column used in this project is type 3. The difference between type 3 and 4 lies in the positioning of the ionizable functional group, if the group is positioned close to the surface of the silica gel, and the C-18 tail extends into the mobile phase the functional group is embedded (type 3), if the functional group is positioned at the end of the hydrocarbon chain (tipped) then the stationary phase is type 4.⁶⁶ Hydrogen-bond acceptors such as amide, urea and carbamate are some of the most widely used polar groups used in type 3, reverse phase/ion exchange mixed mode columns.

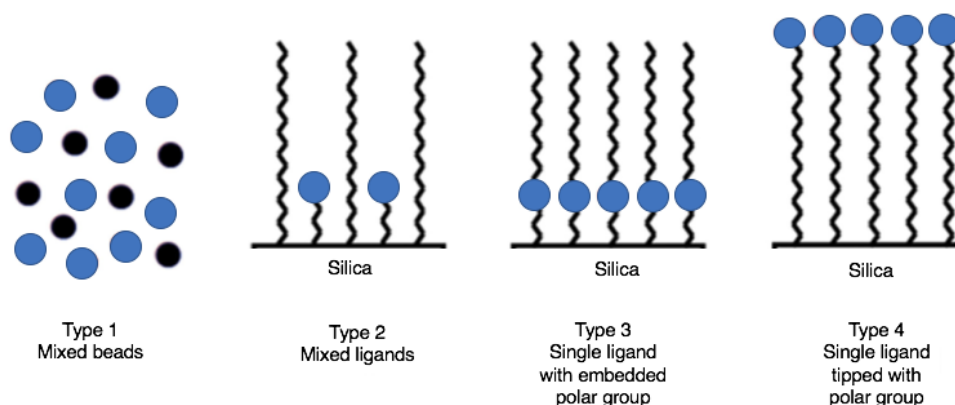


Figure 21 Four types of bimodal column media that can be used in mixed mode reverse-phase/ion exchange columns, blue - ion exchange, black - reverse-phase. Adapted from⁶⁶

4.1.2 Enzymatic Assay Analysis

The conversion of NDP to NTP via H122G NDPK was monitored using analytical HPLC. HPLC of the adenosine system has been performed on a SUPELCOSIL LC-18-T column (250 × 4.6 mm) with a Supelguard LC-18-T guard column, while the

guanine system was analysed using a SIEL-Primesep SB column (150 × 4.6 mm), full column details in sections 6.5.2 and 6.5.3.

4.1.2.1 Conversion to ATP

Kinetics of NDPK H122G catalysed phosphorylation of ADP to ATP was monitored on a SUPELCOSIL LC-18-T column, using UV detection at 254 nm. The initial elution system, used a liner gradient of 0 - 25 % methanol in ammonium acetate (0.05 M, pH 5.9) over the course of 15 minutes.⁶⁷ Chromatographs produced for the analysis of adenosine nucleotides using this elution system, displayed poor peak separation and a high degree of peak tailing. Improvement of the methanol/ ammonium acetate elution system was attempted, firstly to prevent ATP from eluting at the solvent front a stepped gradient elution system was used - this resulted in longer retention times but had no improvement on peak separation and tailing. The effect of changing the pH was investigated using a range from pH 5.5 - 7, no improvement in peak separation or tailing was observed. As such a different literature protocol was investigated, a gradient elution system used again.⁶⁸ The new mobile phase used two phosphate buffers (6.5.1), buffer A = KH_2PO_4 (0.1 M, pH = 6.0) and buffer B = A : methanol (90:10). Analysis of ATP and ADP via this method resulted in well defined peaks, with clear separation as shown in figure 22

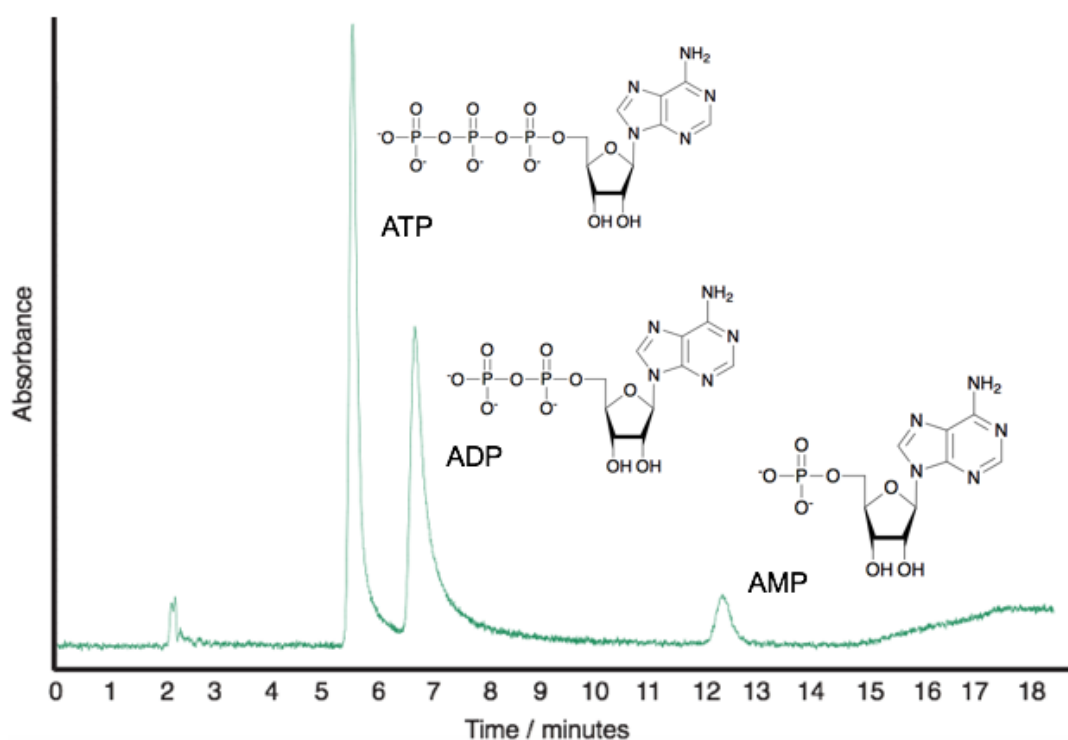


Figure 22 Chromatograph showing the separation of ATP, ADP and AMP over the course of an analytical chromatographic experiment using SUPELCOSIL LC-18-T.

4.1.2.2 Conversion to GTP

Chromatographic experiments monitoring phosphorylation kinetics of GDP to GTP,

were done on mixed mode Primesep SB column using UV detection at 254 nm by Dr Stefanie Freitag-Pohl.

A linear gradient elution system was used to elute the nucleotides over 30 minutes, using two ammonium acetate based buffers. Buffer C = ammonium acetate, (30 mM, pH 4.5) 5 % ACN and buffer D = ammonium acetate (200 mM, pH 4.5), 5 % ACN, the linear gradient went from 70 % C, 30 % D to 100 % D over 30 minutes. Analysis of GTP and GDP via this method resulted in well defined peaks, with clear separation as shown in Figure 23.

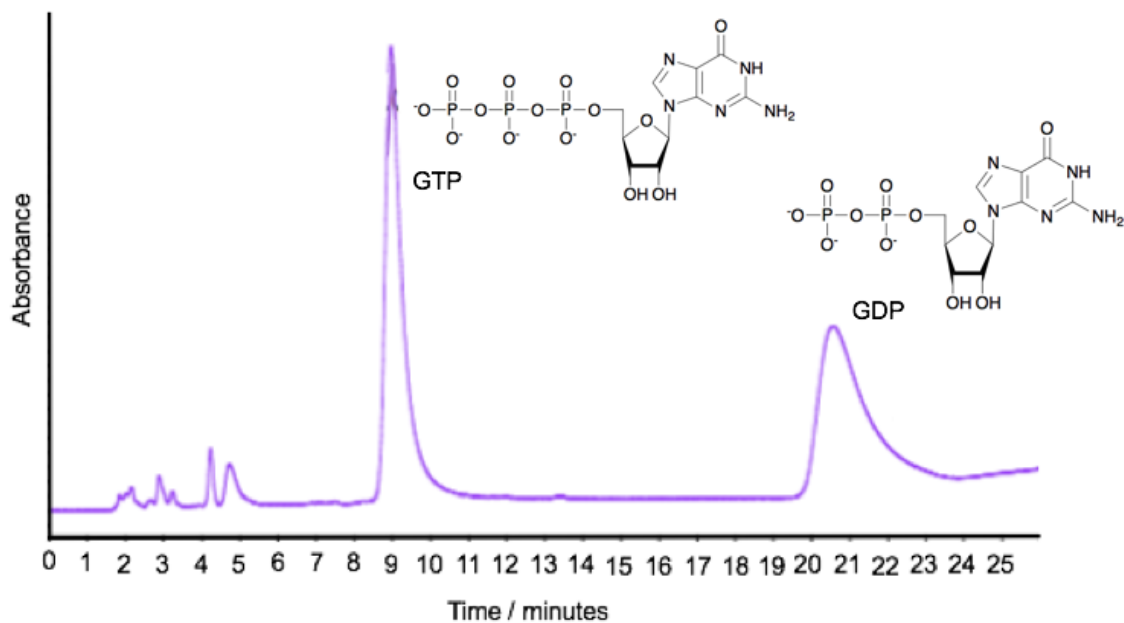


Figure 23 Chromatograph showing the separation of GTP and GDP over the course of an analytical chromatographic experiment using column Primesep SB.

4.2 Enzyme Assays

The key goal of the enzymatic experiments carried out, was firstly to determine whether PIm was capable of rescuing the activity of the H122G mutant kinase, then to investigate the parameters that affect conversion of NDP to NTP.

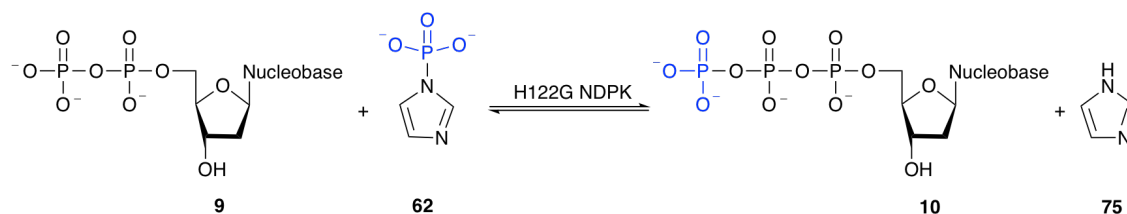


Figure 24 Production of an NTP via the rescue of H122G NDPK mutant activity by the use of phosphoimidazole as a phosphoryl donor.

4.2.1 Pilot Experiment: Dephosphorylation of ATP

Rescue of the activity of the H122G NDPK mutant by imidazole was first demonstrated by the Herschlag group in the late 1990's (scheme 6), the first enzymatic assay undertaken was to repeat this experiment⁶⁹. This was done to ensure that imidazole was able to rescue activity of the NDPK H122G, produced during this project. The principle of microscopic reversibility, means that the reverse reaction using PIm and ADP to produce ATP and imidazole would be possible.

4.2.1.1 Results and Discussion

Three reactions were performed in parallel. Reaction **I** was a positive control experiment and contained ATP, NDPK H122G and imidazole, reactions **II** and **III** were both negative control experiments containing ATP and NDPK H122G or ATP and imidazole, respectively.

Pleasingly, dephosphorylation of ATP only occurred during reaction **I** when all three reactants were present, removal of either the imidazole or the enzyme component resulted in no dephosphorylation reaction occurring, thus no conversion to ADP. Samples from the three parallel reactions were taken at 0, 15, 60 and 90 minutes during the pilot experiment, 15 minutes was chosen over 30 minutes as the rate of dephosphorylation was expected to be higher at the start of the reaction. The samples were analysed via HPLC. Figure 25 clearly shows an increase in the % of ADP in reaction **I** from 0.2 % upon initiation of the reaction to ~ 16 % after 90 minutes.

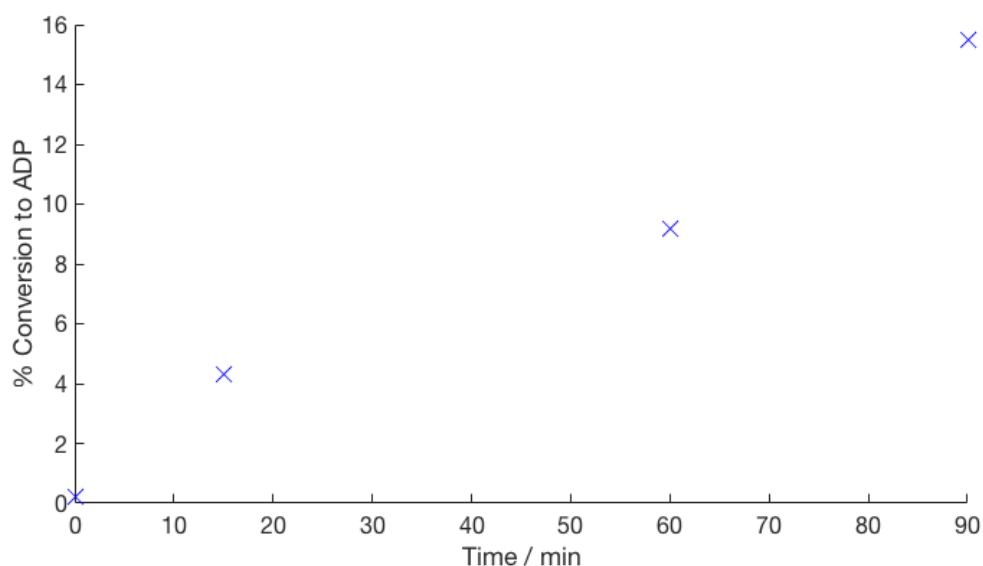


Figure 25 Graph showing dephosphorylation of ATP in positive control experiment **I** to produce ADP during the initial pilot experiment

4.2.2 Initial Enzymatic Phosphorylation Reaction of ADP to ATP

Firstly, the capability of phosphoimidazole to rescue activity of the H122G NDPK mutant had determined. This was done by a performing three reactions in parallel. The compositions of the three reactions are shown in Table 3.

Table 3 Composition of the initial parallel enzymatic experiments

Experiment	Reactant	
	PIm	H122G NDPK
IV	+	+
V	-	+
VI	+	-

4.2.2.1 Results and Discussion

The three parallel experiments were all completed under the same reaction conditions, both **IV** and **VI** used PIm from the same crude stock solution, all three of the reactions were performed at room temperature in HEPES buffer at pH 7.5.

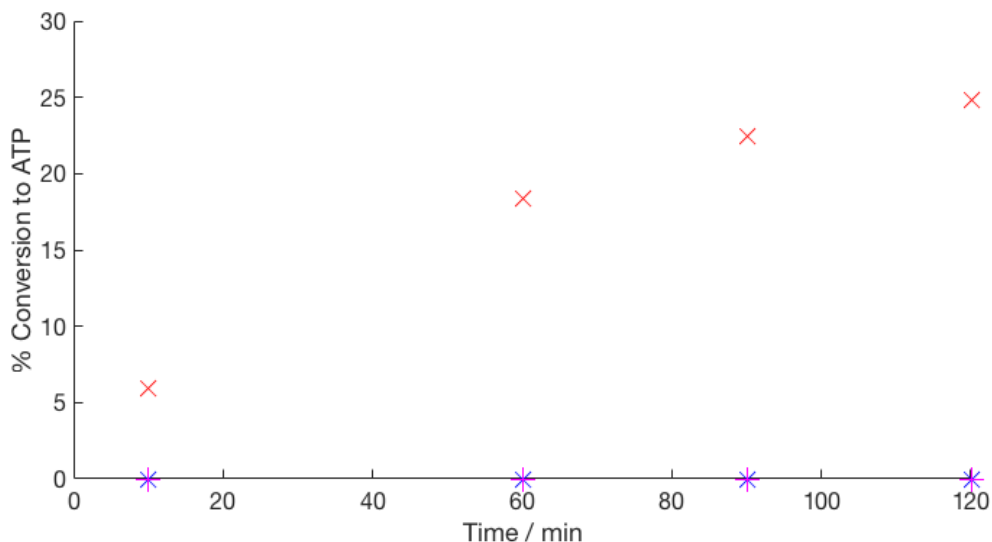


Figure 26 Graph showing the % conversion to ATP in the initial 3 parallel reactions: **IV** (×), **V** (+) and **VI** (×) over the course of a 2 h enzyme catalysed phosphorylation reaction.

Aliquots of all three reaction solutions were taken at time points of; 10, 60, 90 and 120 minutes. The samples were then subjected to centrifugation through a 10 000 kDa molecular weight cut off filter. Which allowed easy and efficient removal of the enzyme from the samples. The samples were then analysed via HPLC, the graph

shown in Figure 26 shows that only **IV** resulted in conversion from ADP to ATP in a time-dependant manner. Both **V** and **VI** displayed no conversion from ADP to ATP over the course of 2 hours, thus showing that under the reaction conditions used, the H122G enzyme is incapable of catalysing the phosphorylation of ADP to ATP.

4.2.3 Effect of Impurities and [PIm] on % Conversion

The enzymatic reactions were carried out under a variety of conditions, to ascertain the effect that both impurities, such as imidazole and acetonitrile, and the initial PIm concentration had on the total conversion of ADP to ATP.

Herschlag showed that at high concentrations imidazole is capable of acting as an inhibitor of NDPK H122G, as such particular emphasis was placed on the study of how the presence of excess imidazole effected the total conversion of ADP to ATP.⁴³ The effect of acetonitrile on ADP phosphorylation was also investigated, to determine if the removal of acetonitrile from crude PIm solutions was imperative.

4.2.3.1 Effect of impurities on % conversion to ATP

The initial crude PIm reaction solution contained acetonitrile and 50 % imidazole by ¹H NMR, to determine if the crude reaction mixture could be used without further purification the effect of these two impurities on total ATP conversion was investigated.

4.2.3.1.1 Results and Discussion

To determine the effect that acetonitrile and imidazole impurities had on the total % conversion of ADP to ATP via H122G NDPK mediated phosphorylation three enzymatic assays were carried out. All of the reactions used the same batch of freshly made crude PIm reaction solution which had been adjusted to pH 7.5; reaction **VII** had deionised water added to the crude PIm, while reaction **VIII** had acetonitrile added to the crude PIm and reaction **IX** had 30 mM imidazole added to the crude PIm (Table 4).

Table 4 Composition of the impurities parallel enzymatic experiments

Experiment	Added Impurities		
	H ₂ O	ACN	IM
VII	+	-	-
VIII	-	+	-
IX	-	-	+

Samples from the three reactions were taken at various time points of; 10, 30, 60, 90 and 120 minutes and analysed via HPLC. Analysis of the three reactions showed that **IX** yielded the largest reduction in conversion after 2 h, this was expected as the Herschlag group has previously shown that for the reverse reaction imidazole acts as an inhibitor at high concentrations.⁴³

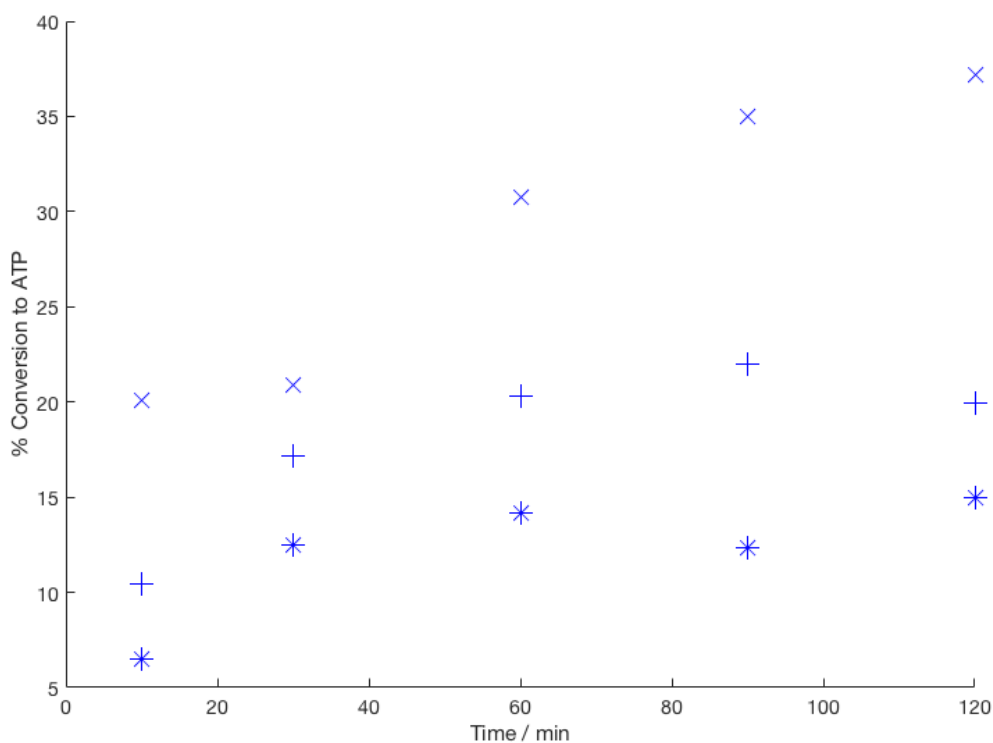


Figure 27 Graph showing the total % conversion to ATP for **VII** (×), **VIII** (+) and **IX** (*) after 2 hours

The % conversion from ADP to ATP for the three reactions over 2 h is shown in Figure 27. Reaction **VII** showed a total conversion of 37 %, reaction **VIII** was 20 % and reaction **IX** was 15 %. The drop in total % conversion of ADP to ATP was 17 % and 22 % for reactions **VIII** and **IX**, respectively when compared to reaction **VII**. The large reduction in total % conversion to ATP showed that, to maximise enzymatic conversion it is imperative that both imidazole and acetonitrile impurities are minimised as much as possible if not completely removed.

4.2.3.2 Effect of [PIm] on % conversion to ATP

The effect of PIm concentration on the total % conversion of ADP to ATP was investigated between 5 - 50 mM PIm, the results were analysed via HPLC (Section 6.5.2).

It should be noted that during the investigation into the effect of initial phosphoimidazole concentration on % conversion to ATP, the reactions were only performed once due to the H122G NDPK enzyme denaturing. This resulted in the investiga-

tion being halted while a new batch of the enzyme was produced, due to the time constraints of the project the investigation was not completed and so a through assessment of the errors associated with the results presented in this section could not be conducted.

4.2.3.2.1 Results and Discussion

It was found that as the concentration of PIm was increased, both the total % conversion to ATP and the initial rate of ATP formation increased.

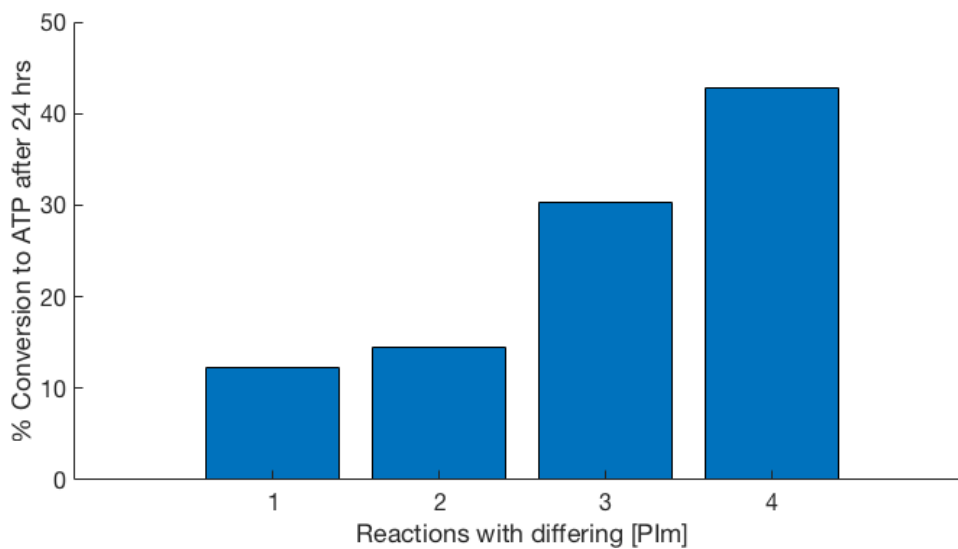


Figure 28 Graph showing the % conversion to ATP after 24 hours for reactions with an initial PIm concentration of 5 mM (1), 10 mM (2), 20 mM (3) and 50 mM (4)

The % conversion after 24 hours were; 12 %, 14 %, 30 % and 43 % for the 5, 10, 20 and 50 mM reactions respectively. Figure 29 shows how the % conversion from ADP to ATP progressed for each of the PIm concentrations over the course of 5 h. The 50 mM PIm reaction produces not only the highest % conversion to ATP after 5 h, but also has the steepest initial gradient implying that it has the greatest initial rate of reaction.

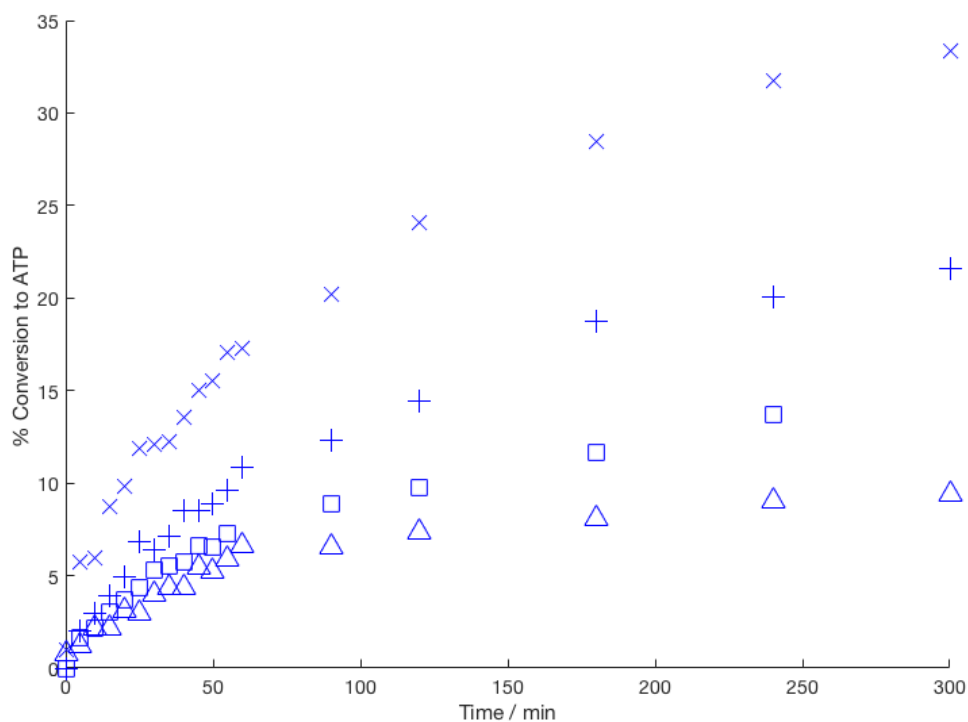


Figure 29 Graph showing the % conversion of ADP (61) to ATP (16) after 5 h for 5 mM (Δ), 10 mM (\square), 20 mM ($+$) and 50 mM (\times) phosphoimidazole

Due to the nature of the enzymatic system and the absence of a fully delineated model, analysis of the kinetics of the formation of ATP was not simple. Due to the complexity of the reaction, the initial gradient from the kinetic results and the % conversion between 10 - 30 minutes were used to give an estimate of the quantitative effect that PIm concentration had on the rate of the enzyme mediated phosphorylation reaction.

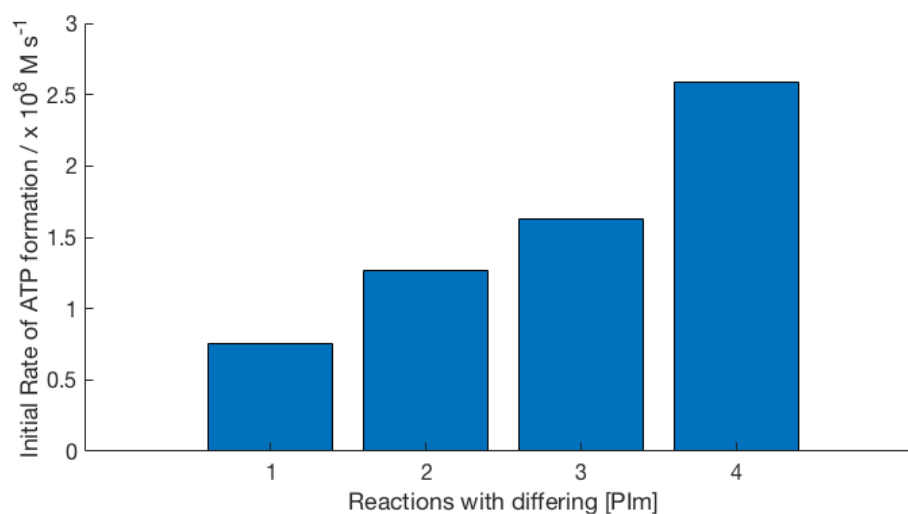


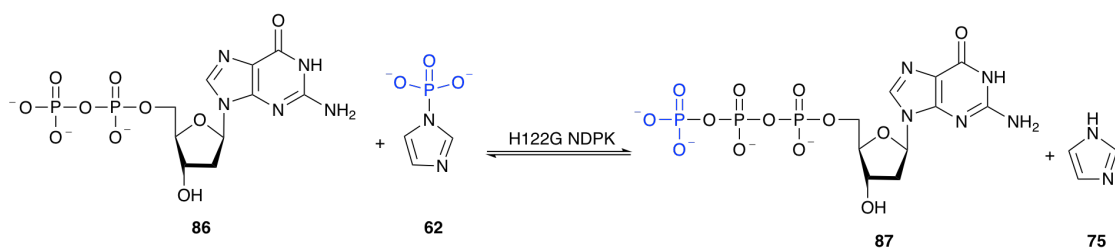
Figure 30 Graph showing how the initial rate of ATP formation changed for various PIm concentrations, 5 mM (1), 10 mM (2), 20 mM (3) and 50 mM (4)

Figure 30 clearly shows a positive relationship between the concentration of PIm and the initial rate of phosphorylation of ADP. The initial rate of the phosphorylation reactions of PIm concentrations: 5 mM, 10 mM, 20 mM and 50 mM are 0.752×10^{-8} , 1.263×10^{-8} , 1.627×10^{-8} and $2.588 \times 10^{-8} \text{ M s}^{-1}$ respectively.

Analysis of both Figure 28 and Figure 30 allowed for the conclusion that both initial velocity and degree of conversion to ATP are positively correlated with PIm concentration.

4.2.4 Enzymatic Phosphorylation of GDP

Enzymatic studies into the phosphorylation of GDP to form GTP were undertaken during the first iteration of this project by Dr. Stefanie Freitag-Pohl at the University of Durham.



Scheme 18 Formation of GTP via H122G NDPK enzyme catalysed phosphorylation of GDP

These experiments established whether H122G NDPK was compatible with guanine based nucleotides and thus whether it could be used to generate GTP. Two reactions were run in parallel: reaction **X** were both PIm and the NDPK H122G enzyme were present in the reaction solution, and reaction **XI** were only PIm was present in the reaction mixture. The composition of the two reactions is shown in Table 5.

Table 5 Composition of the GDP parallel enzymatic experiments

Experiment	Reactant	
	PIm	H122G NDPK
X	+	+
XI	+	-

4.2.4.1 Results and Discussion

The two parallel experiments were completed under the same conditions, using PIm from the same purified batch which had the pH adjusted to 7.5. The reactions were

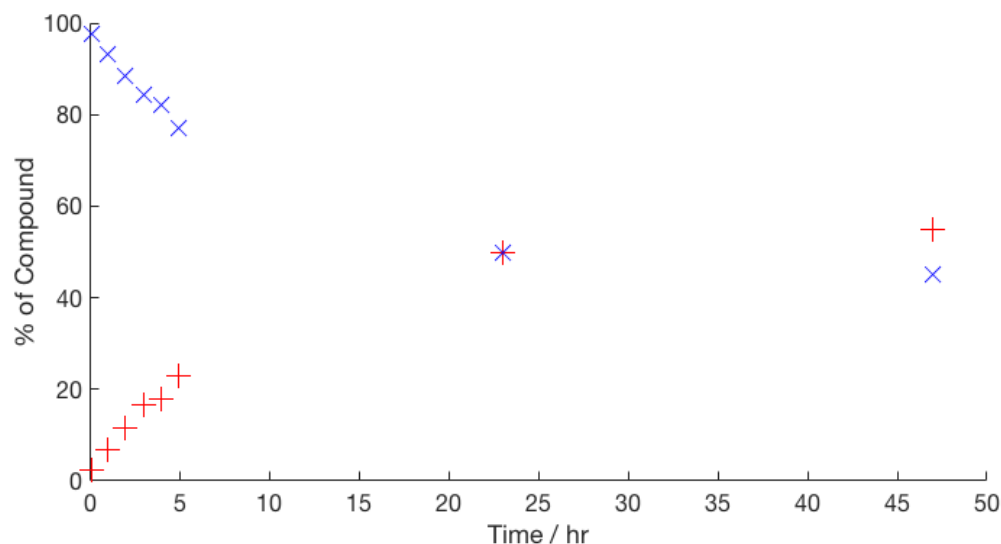


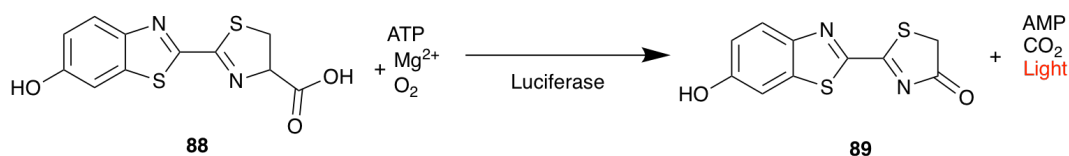
Figure 31 Graph showing % composition of **1** over the course of 47 hours; % GTP (+), % GDP (x)

performed at room temperature and samples were taken and analysed every hour for the first 5 hours, then at 23 h and the final sample was taken at 47 h.

Over the course of the 47 hours, reaction **XI** showed no change in the levels of GDP or GTP, both remained at 100 % and 0 % respectively. Figure 31 clearly shows that this was not the case for reaction **X**, the % of GTP steadily increased from 2 % at 10 minutes up to 55 % after 47 hours. As time progresses the rate of phosphorylation of GDP decreases and, between 23 to 47 hours the equilibrium position seems to be further to the right than it was between 10 minutes and 5 hours, as the % of GTP only increased by 5% over a 24 hour time period where as in the first 5 hours, % GTP increased by 20%.

4.2.5 Bioluminescence Studies

Research into the ability of the H122G enzyme to produce ATP in the presence of a biochemical system that consumes ATP, was undertaken by Dr Hodgson. As discussed in Section 1.4, biocatalysis for cofactor regeneration has become more prevalent in recent years, and the potential capability of the PIm/NDPK H122G for ATP regeneration in the presence of an ATP cofactor dependant enzymatic system was explored.⁵⁰

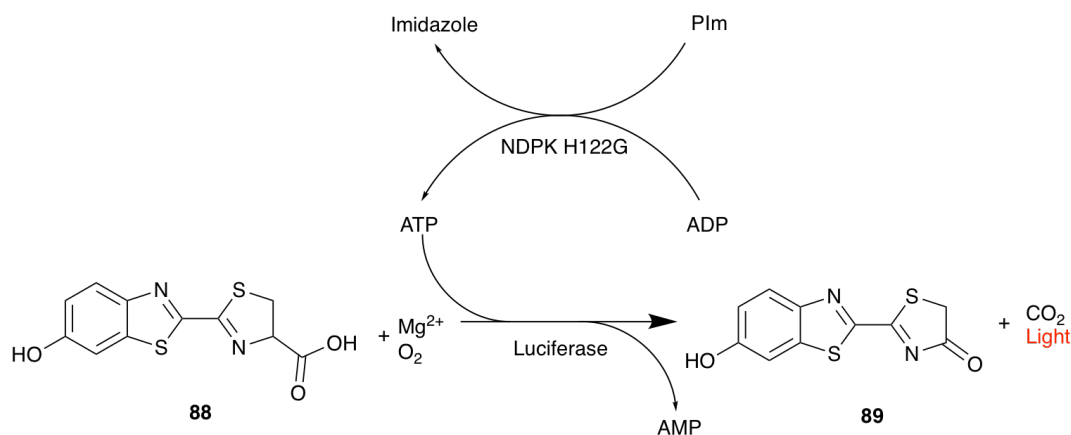


Scheme 19 ATP-dependant bioluminescence reaction, catalysed by firefly luciferase.

The ATP test kit was chosen, due to the sensitivity and simplicity of the luciferase

reaction (Scheme 19), which uses the luciferase enzyme to catalyse the reaction of D-luciferin (**88**) to oxy-luciferin (**89**). The test kit is capable of detecting the presence of ATP at low concentrations (10^{-12} M).

To test the compatibility of the H122G mutant with the luciferase enzyme, instead of adding ATP to the luciferase enzyme, H122G NDPK, PIm and ADP were added.



Scheme 20 Phosphorylation of ADP by NDPK H122G to form ATP, an essential co-factor for the luciferase catalysed reaction.

A series of reactions were carried out by Dr Hodgson, each of the reactions used a stock reaction solution (Section 6.4.2) crude PIm and NDPK H122G (0.2 mg ml^{-1}) stock solution.

An initial pilot reaction (**XII**), and reaction to assess the effect of increased PIm concentration **XIII** were undertaken by Dr Hodgson. Each of the reactions used a stock reaction solution (Section 6.4.2) of crude PIm and NDPK H122G (0.2 mg ml^{-1}) stock solution.

Both of the reactions consisted of five experiments which were run in parallel, the components present in each of the five experiments are given in Table 6.

Table 6 Composition of the five bioluminescent assays

Component	Experiment				
	a	b	c	d	e
ADP	-	+	+	+	-
PIm	-	+	+	-	+
H122G	-	+	-	+	+

4.2.5.1 Reaction XII: Positive Control Experiment

Initially, a positive control experiment was carried out to confirm that in the absence of ADP (100 mM), NDPK H122G or PIm, the luciferase catalysed reaction did not give a luminescent signal above background level.

4.2.5.1.1 Results and Discussion

The reaction solution (100 μL) was pipetted into wells of a black bodied microtiter plate, and 1 μL of ADP, PIm and NDPK H122G was added depending on the experiment being performed.

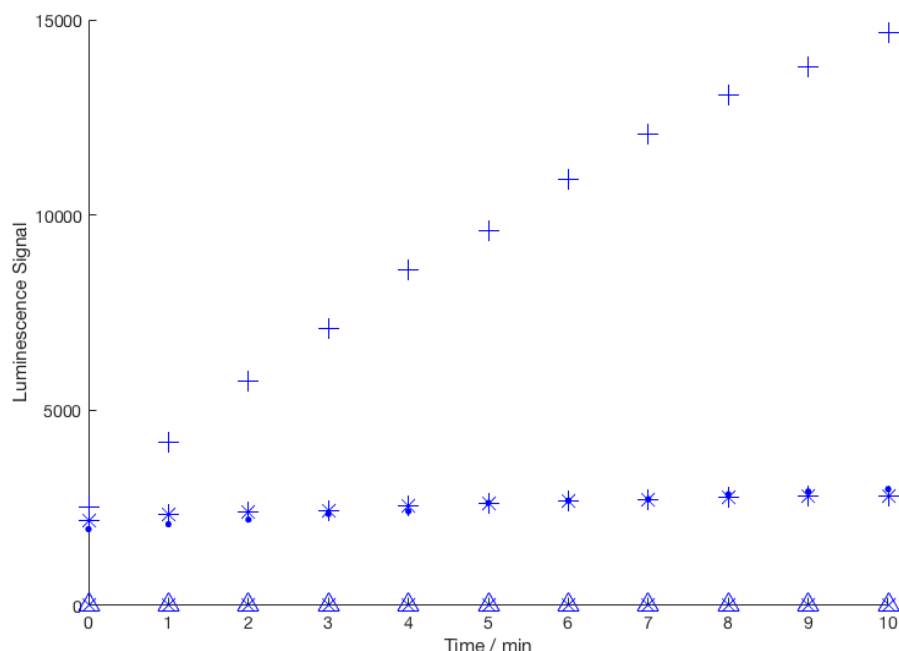


Figure 32 Luminescence signals of the 5 experiments performed during reaction **XII**. Reaction **a** (\times), **b** ($+$), **c** ($*$), **d** (\bullet), **e** (Δ)

The largest luminescent signal was seen in experiment **XIIb**, which contained ADP, PIm and NDPK H122G. The background luminescent signals for **XIIc** and **XIId** are significantly larger than those seen in **XIIa** and **XIIe**, this is most likely due to ATP contamination of the ADP stock solution. Commercial nucleotides such as ADP are generally extracted from whole organisms, and as such are prone to low levels of contamination by other nucleotides.

4.2.5.2 Reaction XIII: Increased PIm Concentration

The effect of PIm concentration on the rate of ATP generation was also explored. The 5 parallel experiments were conducted using using a higher concentration of PIm and NDPK H122G.

4.2.5.2.1 Results and Discussion

The reaction solution (100 μL) was pipetted into wells of a black bodied microtiter plate, where necessary water (18 Ω) was added to maintain reagent concentration across all 5 parallel experiments

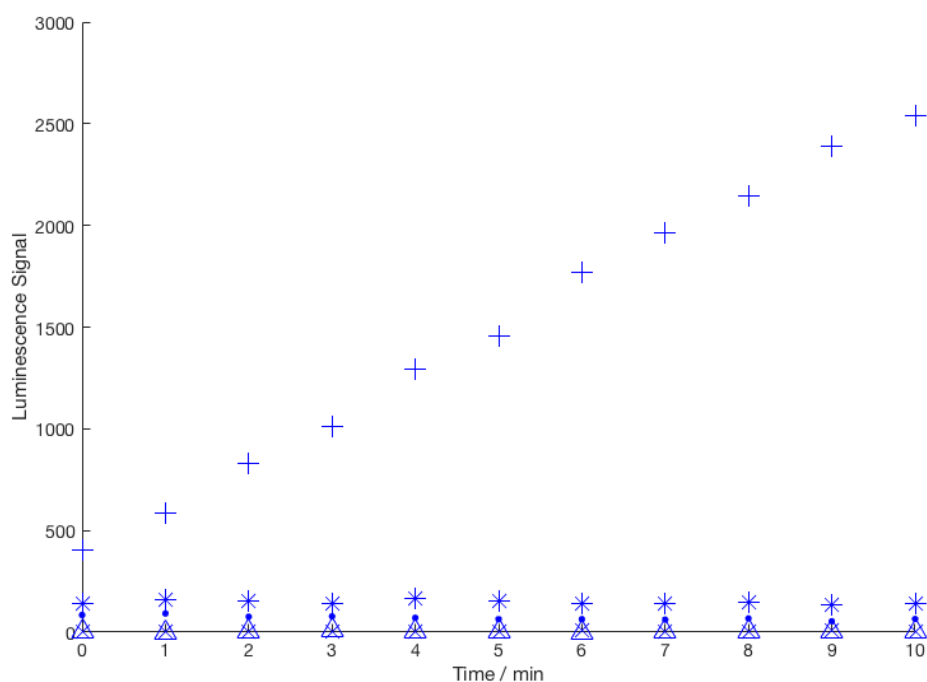


Figure 33 Luminescence signals of the 5 experiments performed during reaction **XIII**. Reaction **a** (\times), **b** ($+$), **c** ($*$), **d** (\bullet), **e** (\triangle)

Over the course of the reaction, a significant increase in the luminescent signal from reaction **XIIIb** can clearly be seen in figure. This increase is indicative of a build up of ATP, produced via the enzymatic phosphorylation of ADP by NDPK H122G. The background luminescence signals, for **XIIIc** and **XIIId** relating to contamination of ATP, remained constant over the course of the reaction.

4.2.5.3 Analysis of Bioluminescent Reactions at Later Time Points

Luminescent signals resulting from contamination of the ADP stock solution by ATP, such as experiments **XIIIc** and **XIIId** were expected to decrease as reaction time increased owing to the consumption of the ATP contaminant. While the luminescent signal produced by the positive control was expected to either increase or remain steady, as NDPK H122G catalysed the production of more ATP.

4.2.5.3.1 Results and Discussion

Reaction **XIII** was re-analysed 0.25 h after initiation of the reaction, Figure 34 shows a decrease in the luminescent signals for negative control reactions **XIIIc** and **XIIId**, indicating that the ATP contaminant in both of **XIIIc** and **XIIId** is being used up. Luminescent signals for **XIIIb**, are higher than those observed in the original analysis, this is due to the increased concentration of ATP, produced by the NDPK H122G enzymatic phosphorylation reaction.

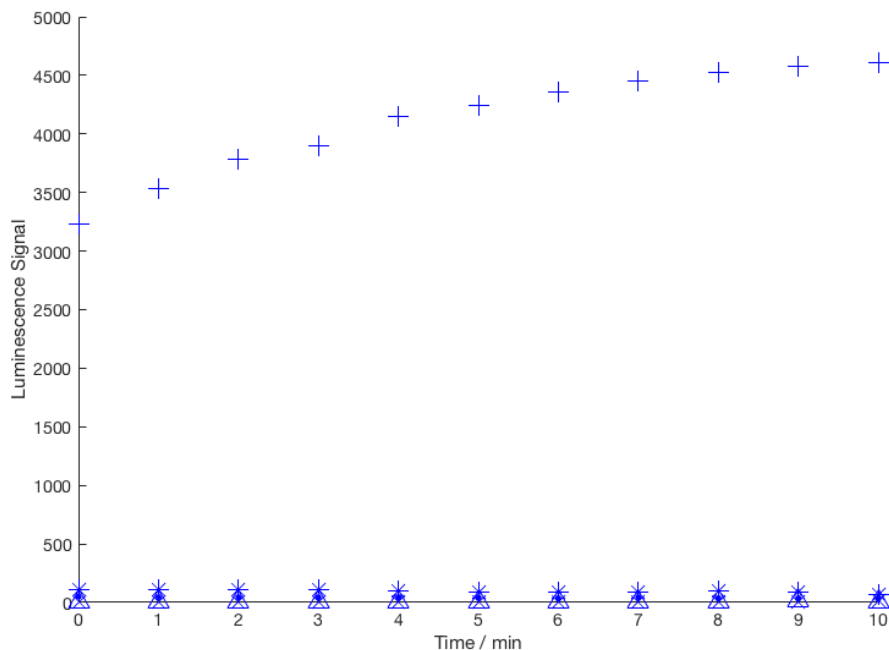


Figure 34 Luminescence signals of the 5 experiments performed during reaction **XIII** 0.25 h after initiation. Reaction **a** (\times), **b** ($+$), **c** ($*$), **d** (\bullet), **e** (\triangle)

The longevity of the reactions was investigated. The reactions were stored at 4 °C overnight, and then allowed to equilibrate to room temperature before being analysed at a single time point (Table 7).

Table 7 Luminescence signals for all 4 reactions after being kept at 4 °C overnight

Reaction	Luminescence Signal				
	a	b	c	d	e
XII	8	6173	90	336	4
XIII	4	1787	5	14	5

Experiments **XIIc** and **XIId**, both show a significant reduction in luminescence signal, with signal intensities $\sim 3\%$ and $\sim 11\%$ of those recorded 10 minutes after reaction initiation, while the luminescent signal for **XIIb** has only decreased 2-fold. Reaction **XII** shows large luminescent signals for the positive control reaction **XIIb**, and low background luminescent signals for the negative control reactions. Experiment **XIIb**, shows a large signal, which is $\sim 70\%$ of that recorded 10 minutes after reaction initiation, and $\sim 39\%$ of the signal recorded 0.25 h after initiation. Luminescent signal recorded for **XIIb** is also ~ 250 -fold above background luminescence.

Analysis of the results of the two reactions, shows that only the positive control reactions (**XIIb** and **XIIIb**) displayed luminescence signals significantly above background luminescent levels, after overnight storage. The luminescence signal due to ATP contamination had significantly reduced after overnight storage, to the level

of background luminescence. The increase in the luminescence signal of **XIIIb** was due to ATP produced *in situ* by the NDPK H122G catalysed phosphorylation reaction. These results confirm that the NDPK H122G system is compatible with the luciferase system, and can be used as an ATP generation system.

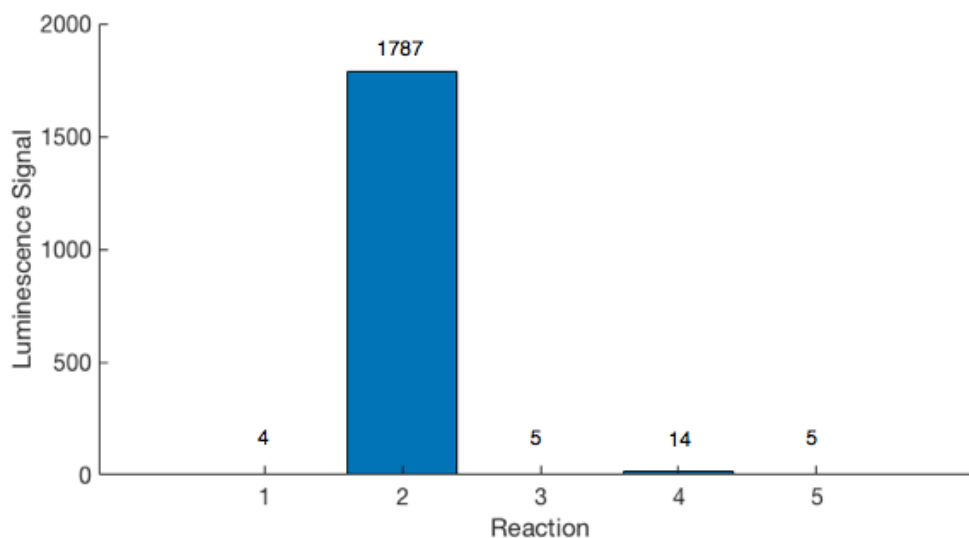


Figure 35 Luminescence signals of the 5 experiments performed during reaction **XIII** after overnight storage

4.3 Conclusions

Firstly, the development of HPLC protocols for both the SUPELCOSIL-LC-18-T and Primesep SB columns allowed for the clear separation and resolution of their respective nucleotide series, thus allowing for the kinetics of NDPK H122G catalysed phosphorylation reactions to be monitored.

Initial experiments confirmed that the H122G mutant was capable of using PIm to rescue enzyme activity, the use of negative control experiments showed that without PIm present phosphorylation of the NDP did not occur. The effect of imidazole and acetonitrile on the total % conversion of the enzymatic reaction was investigated, the presence of imidazole and acetonitrile in the reaction mixture was shown to be detrimental to % conversion. As such, optimisation of the PIm purification procedure was done, to minimise the amount of these impurities present in the reaction solution (Section 3.3.2).

The effect of % conversion to ATP was investigated between 5-50 mM PIm, these experiments clearly showed a positive relationship between concentration of PIm and the total % conversion to ATP after 24 h. Initial rate of phosphorylation was calculated, to give an indication of how PIm concentration effected the initial rate, it was found that as PIm concentration increased so did initial rate of phosphorylation

with PIm concentrations 5, 10, 20 and 50 mM showing initial rates of 0.752×10^{-8} , 1.263×10^{-8} , 1.627×10^{-8} and $2.588 \times 10^{-8} \text{ M s}^{-1}$ respectively.

Biocatalysis for the regeneration of cofactors, such as ATP *in situ* with other ATP dependant enzymatic reactions has gained traction in both academia and industry in recent years.⁴⁴ As such the PIm/NDPK H122G system was used in the presence of the luciferase catalysed reaction of D-luciferin to oxy-luciferin, which produces a luminescent signal which was monitored for the initial 10 minutes after reaction initiation and after overnight storage at 4 °C. Negative controls were used in each iteration of these experiments, which allowed for the identification of ATP contamination present in the ADP stock solution. After overnight storage, only the positive control reactions remained significantly above background levels, thus showing the ATP contaminant had been consumed and the luciferase reaction in the positive control experiment was using ATP produced *in situ* by the PIm/NDPK H122G system.

5 Conclusions and Future Work

This chapter will firstly discuss the salient points and conclusions of this project, before considering the available scope for further work. Particular emphasis will be placed on the preliminary work done on the synthesis of thio-phosphoimidazole (PSIm) performed by the author and Dr Freitag-Pohl.

5.1 Conclusions

5.1.1 Optimised Synthesis of Phosphoimidazole

The synthesis of phosphoimidazole (**62**, Scheme 17) from cheap, readily available reagents is detailed in Chapter 3. The method for the production of **62**, a phosphoryl donor, was streamlined and optimised which resulted in the production of high purity **62**. The optimisation process examined the optimum initial imidazole (**75**) concentration and the steps used in the purification procedure of crude **62**.

Investigation into the initial concentration of **75** resulted in an increase in the % of **62** present in the crude reaction solution. The original reaction used 50 mM **75** in a 1 to 1 reaction ratio with POCl₃ (**72**), which resulted in a crude reaction solution of **62**, inorganic phosphate (**85**) and 1,1'-phosphodiimidazole (**82**) with a composition of 45, 53 and 2%, respectively. The % of **62** found in the crude reaction solution was 55%, when the concentration of **75** was increased to 75 mM (Table 8).

Table 8 The % of **62**, **82** and **85** present in the crude product solutions produced by reactions with different initial concentrations of imidazole (³¹P NMR)

	% Compound		
[75] /mM	62	85	82
50	45	53	2
75	55	43	2

The original purification procedure involved freeze drying the reaction solution, a process which took 24 h. The crude product was then dissolved in acetone containing sodium iodide, to facilitate the removal of the imidazole impurity. Phosphoimidazole is a time-sensitive compound and as such the main goal of purification optimisation was to remove the use of a freeze-drier.

Rotary evaporation of the crude reaction solution lead to the formation of a white precipitate, upon analysis via ³¹P NMR the precipitate was found to consist of 81% **62**, 19% **85** and 1% **82**. The precipitate was then recrystallised twice in 10 mM sodium hydroxide, after the second recrystallisation the recovered solid contained 97% **62** and 3% **85**. The precipitate was then ground up and washed overnight using

EtOH, after drying the final product consisted of 98% **62** and 2% **85** by ^{31}P NMR. Analysis of the final product via ^1H NMR gave a product composition of 79% **62** and 21% **75**.

5.1.2 Use of Phosphoimidazole in Biocatalytic Reactions

The principal goal of the enzymatic experiments was to determine whether **62** was capable of behaving as a phosphoryl donor, and thus capable of rescuing the activity of the mutant H122G NDPK enzyme (Chapter 4). The initial phosphorylation reaction (Section 4.2.2) of ADP was conducted using a crude reaction solution containing 45% **62**, after 2 h the % conversion from ADP to ATP was 25%.

The effect of impurities and initial **62** concentration was investigated (Section 4.2.3). Three reactions were ran in parallel to determine the effect that acetonitrile and imidazole impurities had on the % conversion from ADP to ATP. After 2 h, the % conversion to ATP was 37%, 20% and 15% for the reactions containing no added impurities, added acetonitrile and imidazole, respectively. The significant drop in the % conversion to ATP when acetonitrile or imidazole impurities were present, gave a clear indication that the removal of these impurities was essential to maximise enzymatic conversion from ADP to ATP. The effect of the concentration of **62** on % conversion to ATP was investigated, after 24 h the % conversion to ATP for the reactions with initial **62** concentrations of 5, 10, 20 and 50 mM was 12, 14, 30 and 43%, respectively.

The promiscuity of the H122G NDPK enzyme was demonstrated by the production of ATP by the author and GTP by Dr Freitag-Pohl, both reactions used **62** to rescue the activity of the mutant enzyme.

Biocatalysis for the *in situ* generation of cofactors such as ATP, has become more popular in recent years. The potential of the **62**/ H122G NDPK system to be used as a ATP generation system in the presence of an ATP cofactor dependant enzymatic system was investigated by Dr Hodgson. The results of these experiments clearly showed that the **62**/ H122G NDPK system was capable of producing ATP in the presence of the luciferase enzyme, which in turn used the ATP to produced a bioluminescent signal.

5.2 Future Work

5.2.1 Further Optimisation of the Production of PIm

Further optimisation of the conditions of both the synthetic reaction and the purification procedure, would increase the efficiency of PIm synthesis by increasing both the overall yield and the purity of the final PIm product.

5.2.1.1 Optimisation of the Reaction Conditions of PIm Synthesis

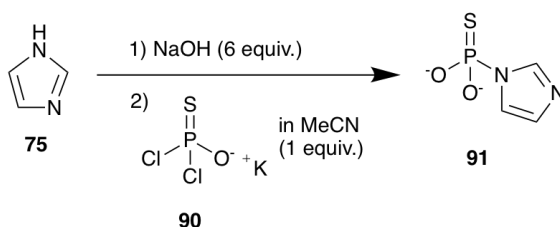
Optimal imidazole concentrations were found between 75 - 250 mM (Section 3.3.1), the highest conversions were achieved by 75 mM and 250 mM with a total conversion to PIm for 55 %. Due to the exothermic nature of the reaction, 75 mM imidazole was chosen as the optimum imidazole concentration. In a future iteration of this project the effect of performing the phosphorylation of imidazole reaction on ice should be investigated, as this may allow the use of higher initial % of imidazole to be used, which allow for a greater mass of PIm to be produced.

5.2.1.2 Optimisation of PIm Purification Procedures

The purification procedure of PIm described in Sections 3.2 and 6.3.1, achieved a partially pure product. ^{31}P NMR spectra gave a final product composition of 98 % PIm, 2 % P_i , while ^1H NMR spectra gave a final composition of 79 % PIm and 21 % imidazole. Since imidazole has been shown to behave as an inhibitor of NDPK H122G, the removal of the imidazole impurity is imperative to achieve the highest % conversion from NDP to NTP using the mutant enzyme.⁴³

Further optimisation of the purification procedure could be done by investigating the effect of washing the final compound with acetone and sodium iodine, this method was used by Crammer in 1961 to remove the imidazole impurity after the production of PIm.⁴⁷

5.2.2 Thiophosphorylation of Imidazole



Scheme 21 The method of γ -thio-phosphoimidazole synthesis utilised in this project

The use of γ -thio-nucleoside 5'-triphosphates ($\text{NTP}\gamma\text{S}$), is a well established method of investigating the mechanistic pathways of nucleotides.⁷⁰ In more recent years, $\text{NTP}\gamma\text{S}$ have been used to clarify the roles of a variety of protein kinases, via identification of substrates and elucidation of the effect that phosphorylation has on substrate function.⁷¹ $\text{ATP}\gamma\text{S}$ has found particular use in investigative roles involving the function of protein kinases. $\text{ATP}\gamma\text{S}$ behaves as a phosphate donor, producing thiophosphorylated proteins which unlike their phosphorylated analogues are resistant to protein phosphatases.⁷¹ The inclusion of the unnatural P-S bond into the phosphorylated product, allows for the modification and subsequent detection of the thiophosphorylated product.

Preliminary investigations into synthesis of PSIm (Scheme 21), have been performed as detailed in Section 6.3. Purification of the crude reaction solution proved difficult and due to time constraints investigations into the production of PSIm were halted. Due to the importance of NTP γ S in research, the ability to produce them via a simple and cost efficient method is essential, as such further investigations into the production of PSIm should be carried out, with a view to use PSIm as a thio-phosphoryl donor in the enzymatic production of NTP γ Ss by H122G NDPK .

6 Experimental

6.1 General Instrumentation and Materials

The biological materials and buffer components were commercially available, all solutions and buffers were prepared directly before use. The chemical syntheses undertaken during the project, utilised raw commercial materials which did not require further purification unless specifically stated.

NMR samples were prepared in deuterium oxide or with the use of a deuterium oxide lock tube. ^1H NMR spectra at 400.13 MHz and ^{31}P NMR spectra at 161.98 MHz were recorded on Bruker Ultrashield 400, Varian Mercury 400 spectrometers in Durham University. NMR data are represented as follows: chemical shift, integral, multiplicity (s = singlet, d = doublet, t = triplet, q = quartet, m = multiplet), coupling constants in Hertz (Hz), and assignment. The ^{31}P NMR spectra presented in section 6.3 have relaxation delays of 2.00 s, number of points for each spectrum is 32768, spectral width is 49019.6 Hz and a limit of resolution of 1.49 Hz. The ^1H NMR spectra presented in section 6.3 have relaxation delays of 1.00 s, number of points for each spectrum is 32768, spectral width is 8012.8 Hz and a limit of resolution of 0.24 Hz.

pH values (± 0.03) of buffered solutions were determined at 25 °C using a Meter-Lab PHM 290 electrode, which was standardized for measurement between between pH 4-7 or pH 7-12.46, depending on the pH of the buffered solution.

Moisture sensitive components were manipulated under an argon atmosphere using glassware that had been dried over night at 95°C.

6.2 Enzyme Expression

6.2.1 Protein Expression

The mutant NDPK H122G produced and overexpressed during this project was an N-terminal fusion of H122G with a His₆ tag (blue); with the following sequence: **MAHHHHHSSGLEVLFGQP**-MSTNKVNKERTFLAVKPDGVARGLVGEIIARYEKKGFVLVGLKQLVPTKDLAESHYAEHKERPFFGGLVSFITSGPVVAMVFEGKGVVASARLMIGVTNPLASAPGSIRGDFGVDVGRNIIGGSDSVESANREIALWFKPEELLTEVKPNPNLYE.

Four key steps were performed during the expression of H122G NDPK mutant; insert generation, linearisation of the expression vector, vector-insert annealing and finally protein overexpression. Each of these steps will be discussed in subsections below. Only protein overexpression was performed by the author, the rest were performed by Dr Freitag-Pohl but have been included for completeness.

6.2.1.1 Step 1: Insert Generation

Synthetic pUC57 (cloning vector) plasmid, it was centrifuged at 6000 rpm at 4 °C

for 1 minute, and then stored at $-20\text{ }^{\circ}\text{C}$. The plasmid and Stellar competent cells were thawed before use. Plasmid ($0.5\text{ }\mu\text{L}$, 50 ng) was added to Stellar competent cells ($50\text{ }\mu\text{L}$), the mixture was then incubated on ice for 30 minutes, then placed in a water bath ($42\text{ }^{\circ}\text{C}$) for 45 seconds, before being returned to the ice box for 2 minutes. Warmed SOC media ($450\text{ }\mu\text{L}$, $37\text{ }^{\circ}\text{C}$) was added to the competent cell/plasmid solution, the mixture was then shaken at 200 rpm for 45 minutes at $37\text{ }^{\circ}\text{C}$. Cell culture ($50\text{ }\mu\text{L}$) was added to fresh warmed SOC media ($50\text{ }\mu\text{L}$, $37\text{ }^{\circ}\text{C}$) and grown on a LB/ agar plate. One colony from the plate was used to inoculate LB media ($10\text{ ml LB} + 10\text{ }\mu\text{L ampicillin}$) and grown overnight at $37\text{ }^{\circ}\text{C}$, 5 ml of the pre-culture was centrifuged at 5500 rpm for 2 minutes.

The pellet was resuspended in buffer ($250\text{ }\mu\text{L}$, $25\text{ mM Tris-HCL pH }8$, 10 mM EDTA), after which alkaline lysis buffer ($50\text{ }\mu\text{L }400\text{ mM NaOH}$, $50\text{ }\mu\text{L }2\% \text{ SDS}$) was added to the solution and mixed via inversion producing a viscous solution. The lysate was neutralised with potassium acetate (5 M , $\text{pH }5.5$), after which the solution appeared cloudy. The solution was subjected to centrifugation at $14\text{ }000\text{ rpm}$ for 5 minutes, producing a white precipitate. The supernatant was loaded onto a spin column and spun for 1 minute, the flow through was discarded. Wash solution ($500\text{ }\mu\text{L}$) was added to the plasmid and then centrifuged again for 1 minute, the flow through was discarded. Buffer ($50\text{ }\mu\text{L}$) was added to the plasmid, the mixture was incubated at room temperature for 2 minutes before being centrifuged for 2 minutes at $14\text{ }000\text{ rpm}$, the isolated plasmid was stored at $-20\text{ }^{\circ}\text{C}$.

PCR was preformed using CloneAmp HiFi PCR Premix, the PCR mix ($25\text{ }\mu\text{L}$) was made up of the components shown in the table below.

Reagent	Volume / μL
HiFi PCR Mix	12.5
Template	1
Forward Primer	2.5
Reverse Primer	2.5
DMSO	0.25
Water	6.25

The template used for PCR was the protein in the isolated pUC57, the forward primer was $5' - \text{AAGTTCTGTTTCAGGGCCCGATGTCCACAAATAAAGTAAACAAAG}$ and the reverse primer was $5' - \text{ATGGTCTAGAAAGCTTTATTATTCGTATAAATTTGGGTTTGG}$. The temperature cycle for PCR is displayed in the table below, a $14\text{ }^{\circ}\text{C}$ gradient used during step 3 annealing.

Step	Temperature / °C	Time / s
1 - Initial Denaturation	98	60
2 - Denaturation	98	10
3 - Annealing	62	15
4 - Elongation	72	30
5 - Final Elongation	72	300

After amplification of the insert via PCR, the product was ran on a 1.5 % agarose gel. A NucleoSpin Gel and PCR kit was used to extract the insert from the agarose gel. The contents of the NucleoSpi kit are listed in the table below.

Reagent	Volume / mL
Binding Buffer NT1	10
Wash Buffer NT3	6
Elution Buffer NE	13

Elution buffer (NE) was Tris/HCl (5 mM, pH 8.5), before use of the wash buffer it was diluted with ethanol (24 ml).

The band containing the amplified insert was cut out of the agarose gel, the gel (100 mg) was dissolved in NT1 buffer (200 μ L). The sample was incubated for 10 minutes at 50 °C, vortexing briefly every 2 minutes until the gel had dissolved. The sample was pipetted into a spin column and the volume made up to 700 μ L with NT1, the column was then centrifuged at 11 000 g for 30 seconds. The flow through was discarded and buffer NT3 (700 μ L) was added to the column, which was again centrifuged at 11 000 g for 30 seconds. After washing with NT3 the column was centrifuged at 11 000 g for 1 minute, elution buffer (15 μ L) was added to the sample and then incubated at room temperature for 1 minute. The sample was then centrifuged for 1 minute at 11 000 g.

6.2.1.2 Step 2: Linearise Expression Vector

Expression vector pOPINF was a bacterial stab, as such it was grown on a LB/agar (with ampicillin) plate. One colony from the plate was used to inoculate LB media (10 ml LB + 10 μ L ampicillin) and grown overnight at 37 °C, 5 ml of the pre-culture was centrifuged at 5500 rpm for 2 minutes.

The pellet was resuspended in buffer (250 μ L, 25 mM Tris-HCL pH 8, 10 mM EDTA), after which alkaline lysis buffer(50 μ L 400 mM NaOH, 50 μ L 2 % SDS)

was added to the solution and mixed via inversion producing a viscous solution. The lysate was neutralised with potassium acetate (5 M, pH 5.5), after which the solution appeared cloudy. The solution was subjected to centrifugation at 14 000 rpm for 5 minutes, producing a white precipitate. The supernatant was loaded onto a spin column and spun for 1 minute, the flow through was discarded. Wash solution (500 μL) was added to the plasmid and then centrifuged again for 1 minute, the flow through was discarded. Buffer (50 μL) was added to the plasmid, the mixture was incubated at room temperature for 2 minutes before being centrifuged for 2 minutes at 14 000 rpm, producing isolated pOPINF plasmids.

The isolated pOPINF plasmids were linearised via a double digest, the components involved in the digest are detailed in the table below.

Reagent	Volume / mL
pOPINF plasmid	22
HindIII	4
KpnI	1
10 \times KpnI buffer	3

The product was shaken over night at 37 $^{\circ}\text{C}$, and then ran on 15 % agarose gel to confirm the presence of linear pOPINF. The band relating to linear pOPINF was cut out of the gel and extracted using a NucleoSpin Gel and PCR kit, the same method as used in section 6.2.1.1 was again used to extract the linear pOPINF from the agarose gel.

6.2.1.3 Step 3: Vector - Insert Annealing

The amplified and isolated insert (42 ng μL^{-1}) generated in step 1 and the isolated linear pOPINF vector (78.8 ng μL^{-1}) were bound together using a vector to insert ratio of 1 : 2. The reaction components are detailed in the following table.

Reagent	Volume / mL
linear pOPINF	2
insert	1
5 \times in-fusion enzyme	2
H ₂ O	5

The solution was then incubated at 50 $^{\circ}\text{C}$, for 15 minutes. The recombinant plasmid was transformed into Stellar competent cells using the same method as

described in section 6.2.1.1. Eight colonies were removed from the LB/agar plate and mixed with LB/ ampicillin (50 μL), 1 μL of these mixture was then used as a DNA template for PCR, using the temperature cycle below, without a gradient during the annealing step.

Step	Temperature / $^{\circ}\text{C}$	Time / s
1 - Initial Denaturation	98	60
2 - Denaturation	98	10
3 - Annealing	62	15
4 - Elongation	72	30
5 - Final Elongation	72	300

The PCR products of the eight colonies were ran on 15 % agarose gel, colonies found to contain the 500 pb insert were used for overexpression of the protein.

6.2.1.4 Step 4: Protein Overexpression

The recombinant plasmid was transformed into *e.coli* expression cells BL21(DE3). Recombinant plasmid (1 μL) was added to competent BL21(DE3) cells (10 μL), the resulting mixture was incubated on ice for 30 minutes, then a water bath (42 $^{\circ}\text{C}$) for 45 seconds which was followed by 2 minutes on ice. Warmed SOC media (900 μL , 37 $^{\circ}\text{C}$) was added to the solution, which was then shaken (37 $^{\circ}\text{C}$) at 200 rpm for 1 h. A LB/agar plate contaminating ampicillin and chloramphenicol was inoculated with 150 μL of the mixture and grow overnight at 37 $^{\circ}\text{C}$. The remaining solution was centrifuged for 5 minutes at 6000 g, the pellet was resuspended in SOC media (150 μL) and grown overnight on a LB/agar plate contaminating ampicillin and chloramphenicol at 37 $^{\circ}\text{C}$.

Colonies from the plate were used to inoculate LB media (250 ml), which was grown overnight at 37 $^{\circ}\text{C}$. 40 ml of the overnight culture was added to LB (1 L) with ampicillin (1 ml, 100 mg ml^{-1}), and grown at 37 $^{\circ}\text{C}$ to an optical density of 0.7 The mixture was induced by IPTG (1 ml, 1M) and grown overnight at 20 $^{\circ}\text{C}$. The culture was centrifuges at 4000 rpm for 20 minutes and the pellet re-suspended in lysis \times binding buffer (50 ml) with a protease inhibitor tablet. Cells were then lysed by sonication (cycle 2 \times 10 % on ice for 2 minutes at 40 % power), before undergoing centrifugation at 21000 rpm for 30 minutes.

6.2.2 Protein Purification

A HisTrap (1 ml) column was equilibrated with water, then with lysis \times binding buffer. The supernatant from the centrifuged lysate cells was loaded onto the His-

Trap column. Purification of the enzyme required the use of two buffers; lysis × binding buffer and an elution buffer.

Components of the lysis × binding buffer are shown in the table below.

Reagent	Concentration / mM
Tris-HCl pH 7.5	50
NaCl	500
imidazole	30
β -mercaptoethanol	2

Components of the elution buffer are shown in the table below.

Reagent	Concentration / mM
Tris-HCl pH 7.5	50
NaCl	500
imidazole	1000
β -mercaptoethanol	2

Protein purification was carried out using an Amersham Biosciences ÄKTAprime protein purification system, equipped with fraction collector. ÄKTA lines were firstly washed with MilliQ water (18.2 Ω) then line A was purged with lysis + binding buffer, line B was purged with elution buffer. The program washes the column for 20 minutes, with 100 % lysis + binding buffer at a rate of 1 ml min⁻¹. After the column wash stage was completed the % of elution buffer was increased from 0, 20 40, 60, 80 and 100 %, via a step up every 5 minutes, flow rate remained at 1 ml min⁻¹ and 2 ml were collected. The procedure was complete when 100% elution buffer was passing through the column and no further protein was eluting. Fractions which related to the signal on the chromatograph were kept for further analysis.

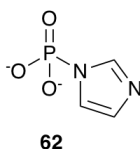
6.2.2.1 Confirmation of NDPK H122G Purification

Fractions of interest and samples from either end of the flow through, were analysed via SDS-PAGE. Samples were boiled in loading buffer at 100 °C for 5 min to denature the proteins, before being loaded on to the gel. After loading then gel was run in 1 × SDS-PAGE running buffer at 150 V until the dye-front reached the bottom of the gel plate. After the gel had been run it was removed from the tank and washed

with MilliQ water (18.2 Ω), after which it was covered with Coomassie Blue staining solution. The gel was left in the Coomassie Blue solution with agitation for 30 min, before the solution was decanted, destained and the gel was examined.

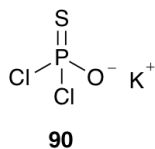
6.3 Chemical Synthesis

6.3.1 Synthesis of Phosphoimidazole **62**



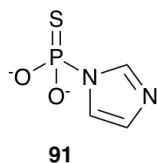
Imidazole (**75**) (0.51 g, 7.48 mmol) was dissolved in sodium hydroxide solution (100 ml, 450 mM) under an inert nitrogen atmosphere. Dry acetonitrile (10 ml) was added to phosphoryl chloride (**72**) (699 μ L, 7.48 mmol) in a dropping funnel, under an argon atmosphere. The phosphoryl chloride solution was added to the imidazole solution via dropwise addition over 10 minutes, the reaction mixture was then stirred vigorously for 1 h. The reaction mixture was then subjected to rotary evaporation, which resulted in the formation of a white precipitate. The precipitate and solution were then separated via centrifugation (4000 rpm, 10 minutes). The precipitate was then recrystallised twice from sodium hydroxide (3 ml, 10 mM), after which the precipitate was dried on the high vacuum line. Once dry, the crystals were ground up before being subjected to overnight extraction with ethyl acetate (50 ml). The crystals were then dried on the high vacuum line to yield the final product of phosphoimidazole (**62**) (0.49 g, 44 %). δ_H (400 MHz; D_2O-d_2) 6.92 (1H, dd, J 4, 8), 7.16 (1H, dd, J 4, 8), 7.72 (1H, s) δ_P (162 MHz; D_2O-d_2) 4.42 (1P, s)

6.3.2 Synthesis of Potassium Thiophosphodichloridate **90**



Thiophosphoryl chloride (1.410 g, 8.33 mmol) in dry acetonitrile (25 ml) was added to oven-dried potassium hydrogen carbonate (1.675 g, 0.0167 mol), under an argon atmosphere. The mixture was stirred for 12 h and, the potassium chloride by-product was removed via filtration, to give a final product solution of 0.33 M potassium thiophosphodichloridate in dry acetonitrile. Potassium thiophosphodichloridate **90** was freshly made and used immediately for the attempted synthesis of thiophosphoimidazole. δ_P (162 MHz; D_2O-d_2) 39.8 (1P, s)

6.3.3 Synthesis of Thiophosphoimidazole **91**



Imidazole **75** (0.34 g, 4.99 mmol) was dissolved in sodium hydroxide solution (100 ml, 300 mM) in an inert nitrogen atmosphere. Potassium thiophosphodichloridate **90** in dry acetonitrile (15.15 ml, 0.33 M) was added to the imidazole solution via dropwise addition over 10 minutes, the reaction mixture was then stirred vigorously for three hours. The reaction mixture was then subjected to rotary evaporation, which resulted in the formation of a off-white precipitate. The precipitate and solution were then separated via centrifugation (4000 rpm, 10 minutes). The thiophosphoimidazole **91** proved difficult to purify further , as such the NMR is of the crude material. δ_H (400 MHz; D₂O-*d*₂) 6.92 (1H, d, *J* 4), 7.25 (1H, dd, *J* 4, 8), 7.81 (1H, s) δ_P (162 MHz; D₂O-*d*₂) 34.6 (1P, s)

6.4 Enzyme Assay

6.4.1 Reactions involving Adenosine Nucleotides

Four series of studies involving either ADP (**61**) or ATP (**16**) as a substrate were performed over the course of this project: dephosphorylation of **16**, phosphorylation of **61**, effect of impurities on phosphorylation level/rate of **61** from crude phosphoimidazole **62** and effect of **62** concentration on level/rate of conversion to **16** (from purified **62**), the protocol for each of these reactions will be discussed in detail. All references to HEPES reaction buffer are referencing the buffer detailed in the table below.

Reagent	Concentration / mM
HEPES	30
MgCl ₂	10
NaCl	150

HEPES buffer was made by combining 1 ml of HEPES (300 mM, pH 7.5), with 1ml MgCl₂ (100 mM) and 1 ml of NaCl (1.5 M), 6 ml Milli Q (18.2 Ω) was then added to the solution. The pH was then monitored and adjusted to pH 7.5 using HCl or NaOH as required, the total volume of the HEPES stock solution was 10 ml.

6.4.1.1 Dephosphorylation of 16

16 (5 μL , 100 mM) and imidazole (**75**) (1 ml, 30 mM, pH 7.5) were added to HEPES reaction buffer (1 ml, pH 7.5). H122G NDPK (2 μL , 9.5 mg ml⁻¹) was then added to the reaction solution, which was then inverted to ensure mixing of all reaction components. Immediately after inversion, a 100 μL sample was taken, and then 100 μL samples were taken at time points of; 0, 15, 60 and 90 minutes. The samples were subjected to centrifugation at 13.5 rpm for 15 minutes in an Amicon Ultra-0.5 Centrifugal Filter Unit (10 kDa), to allow for the removal of H122G enzyme from each sample. The samples were then subjected to HPLC analysis.

6.4.1.2 Phosphorylation of 61 from 62

Phosphoimidazole (**62**) (75 mg, 0.5 mmol) was added to HEPES reaction buffer (1 ml, pH 7.5) the pH was then adjusted back to 7.5 with HCl (37 %). **61** (5 μL , 100 mM) was then added to the reaction solution along with H122G NDPK (2 μL , 9.5 mg ml⁻¹), the solution was then inverted to ensure mixing of all reaction components. Immediately after inversion, a 100 μL sample was taken, and then 100 μL samples were taken at time points of; 0, 15, 60 and 90 minutes. The samples were subjected to centrifugation at 13.5 rpm for 15 minutes in Amicon Ultra-0.5 Centrifugal Filter Unit (10 kDa), to allow for the removal of H122G enzyme from the sample. The samples were then subjected to HPLC analysis.

6.4.1.3 Effect of Impurities on Phosphorylation of 61

Crude **62** reaction mixture was subjected to rotary evaporation, which resulted in the removal of acetonitrile, giving a clear colourless crude solution of **62**. The pH of the crude **62** was adjusted from 10.76 to 7.51 using HCl (0.5 M). Three reactions were done in parallel using this crude **62** solution. All of the reactions used the same basic reagent composition: crude **62** (2.02 mL), HEPES reaction buffer (1 mL, pH 7.5), textcolorblack**61** (5 μL , 100 mM). MilliQ water (18.2 Ω , 0.5 mL), **75** (30 mM, 0.5 mL, pH 7.5) or acetonitrile (0.5 mL) were then added to reactions; textcolorblack**VII**, textcolorblack**VIII** and textcolorblack**IX** respectively. H122G NDPK (2 μL , 9.5 mg ml⁻¹) was then added to each of the reaction solutions, which were then inverted to ensure mixing of all reaction components. 100 μL samples were taken at time points of; 10, 30, 60, 90 and 120 minutes. The samples were subjected to centrifugation at 13.5 rpm for 15 minutes in Amicon Ultra-0.5 Centrifugal Filter Unit (10 kDa), to allow for the removal of H122G enzyme from the sample. The samples were then subjected to HPLC analysis.

6.4.1.4 Effect of [62] on Degree of Conversion to 16

Purified **62** (0.1920 g) was dissolved in MilliQ water (18.2 Ω , 8 mL) and the pH adjusted to 7.5 with HCl (37 %), MilliQ water was then added to give a total **62**

stock solution (100 mM) of volume 10 ml. All experiments used this common **62** stock solution. The volumes used in each of the four reactions are detailed in the table below.

Reaction [62] / mM	Volume of 62 stock / μL	Volume of Water / μL
5	100	900
10	200	800
20	400	600
50	1000	0

All four of the reactions had the same basic procedure, firstly the **62** and water were added to a 15 mL falcon tube, then HEPES reaction buffer (989 μL , pH 7.5) and **61** (100 mM, 5 μL) were added. H122G NDPK (6 μL , 3.6 mg ml⁻¹) was then added to the reaction solution, which was then inverted to ensure mixing of all reaction components. Immediately after inversion, a 100 μL sample was taken and quenched with Na-EDTA (15 μL , pH 7.5). 100 μL samples were then taken and quenched with Na-EDTA at time points of; 0, 5, 10, 15, 20, 25, 30, 35, 40, 45, 50, 55, 60, 90, 120, 180, 240, 300 and 1440 minutes. The samples were subjected to centrifugation at 13.5 rpm for 15 minutes in Amicon Ultra-0.5 Centrifugal Filter Unit (10 kDa), to allow for the removal of H122G enzyme from the sample. The samples were then subjected to HPLC analysis.

6.4.2 Bioluminescent Assays

Two distinct bioluminescent reactions were carried out by Dr Hodgson using a Molecular Probes/Invitrogen **16** detection kit (A22066), all reactions consisted of one positive control experiment and four negative control experiments. The test kit contained; D-luciferin (**88**)(3 mg), luciferase (5 mg ml⁻¹), dithiothreitol, **16** (5 mM) and 20 \times reaction buffer (500 mM Tricine buffer, pH 7.8, 100 mM MgSO₄, 2 mM EDTA and 2 mM sodium azide). Stock solutions of **88** (1 ml, 10 mM) and dithiothreitol (1.62 ml, 100 mM) were made. A standard reaction solution (10 ml) was made according to the manufactures instructions, the dithiothreitol and **88** stock solutions were used, components of the standard reaction solution are displayed in the table below.

Reagent	Volume / mL
H ₂ O	8.9
20× reaction buffer	0.5
Dithiothreitol	0.1
D-luciferin	0.5
Luciferase	0.0025

The **16** test kit was calibrated as per the suppliers instructions, by adding 10 μL of 5 μM , 0.5 μM , 50 nM, 5 nM and 0.5 nM to 100 μL of the assembled standard reaction solution. All concentrations, except 0.5 nM which appears to give a signal below the background level of our instrument, gave a proportional luminescent response. All experiments were carried out in the wells of a black-bodied microtiter plate at 28 °C. Standard stock solutions of NDPK H122G (0.2 mg ml⁻¹), crude **62** and were used throughout the experiments.

All experiments were performed in a black bodied microtiter plate, using standard reaction solution (100 μL). Reaction **XII** used 100 mM **61** (μL), 1 μL crude **62** and 1 μL NDPK H122G (0.2 mg ml⁻¹). Reaction **XIII** used 1 mM **61** (μL), 4 μL crude **62** and 1 μL NDPK H122G (0.2 mg ml⁻¹).

The luminescence signal was measured every minute for the first ten minutes after initiation, both reactions were then stored overnight at 4 (°)C, the reaction solutions were allowed to warm to room temperature then luminescence was measured again at a single time point.

6.5 HPLC Conditions and Retention Times

This section will firstly describe the protocol for the preparation of the eluent buffers used throughout the project, then there will be an in-depth description of the parameters used for both of the columns and results of HPLC analysis.

A PerkinElmer Series 200 HPLC system was used for all of the kinetic experiments analysed through HPLC. TotalChrom Chromatography software from PerkinElmer was used to process the chromatographs on Microsoft Windows XP. The SUPELCOSIL-18-T and SIELC-Primesep SB columns were purchased from Sigma-Aldrich and SIECL, respectively.

6.5.1 Buffer Preparation

A variety of elution buffers were required for the analysis of the nucleotides on the two columns. Phosphate buffers were used for the elution of adenosine nucleotides, while ammonium acetate buffers were utilised for the guanosine series.

6.5.1.1 General Procedure for Phosphate Buffers

A gradient elution method requiring two phosphate buffers, adapted from the literature procedure, was used for the elution of the adenosine series.⁶⁸ buffer A - KH_2PO_4 , 0.1 M, pH = 6.00, buffer B - 90 % buffer A : 10 % methanol, pH = 6.00 .

6.5.1.1.1 Buffer A

KH_2PO_4 (13.6 g) was dissolved in ~ 900 ml MilliQ water (18.2 Ω), the pH of the buffer was then adjusted from 4.55 to 6.00 through the addition of potassium hydroxide solution (5 M). The total volume was made up to the 1 L mark in a volumetric flask. The buffer was then vacuum filtered.

6.5.1.1.2 Buffer B

The preparation of buffer B follows that of A, until filtration, methanol (100 ml) was added to a 1 L volumetric flask which was then made up to the 1 L mark with buffer A, to give a total volume of 1 L. The buffer was then vacuum filtered.

6.5.1.2 General Procedure for Acetate Buffers

The guanosine series used two ammonium acetate based buffers to elute the nucleotides. Buffer C (30 mM ammonium acetate, 5 % acetonitrile, pH 4.50) and buffer D (200 mM ammonium acetate, 5 % acetonitrile, pH 4.50).

6.5.1.2.1 Buffer C

Ammonium acetate (2.31 g) was dissolved in ~ 800 ml of MilliQ water (18.2 Ω), the pH was adjusted to 4.50 with glacial acetic acid. Acetonitrile (50 ml) was pipetted into a 1 L volumetric flask and the ammonium acetate solution was added, the flask was then topped up to 1 L with water, after which buffer C was filtered.

6.5.1.2.2 Buffer D

Ammonium acetate (15.42 g) was dissolved in ~ 800 ml of MilliQ water (18.2 Ω), the pH was adjusted to 4.50 with glacial acetic acid. Acetonitrile (50 ml) was pipetted into a 1 L volumetric flask and the ammonium acetate solution was added, the flask was then topped up to 1 L with water, after which buffer D was filtered.

6.5.2 SUPELCOSIL-LC-18-T Column Protocol

Experiments involving adenosine nucleotides were completed, with a SUPELCOSIL-LC-18-T column measuring 250 mm in length and 46 mm in diameter, surface coverage $3.1 \mu\text{mol m}^{-2}$, matrix silica gel (spherical particle platform), particle size $5 \mu\text{m}$ and a surface area of $170 \text{ m}^2 \text{ g}^{-1}$. The parameters and elution method below, were used for all HPLC analysis performed on the SUPELCOSIL-LC-18-T column.

Parameter	Value	Unit
Injection Volume	10	μL
Detector	254	nm

Step	Time / min	Flow / mlmin^{-1}	% A	% B	Curve
0	6	1.3	100	0	0
1	9	1.3	100	0	0
2	4	1.3	0	100	1
3	4	1.3	0	100	0
4	1.5	1.3	100	0	1

Compound	Retention Time / min
ATP	5.5
ADP	6.8
AMP	12.0

6.5.3 SIELC-Primesep SB Column Protocol

Experiments involving guanosine nucleotides were completed, with a SIELC-Primesep SB column measuring 150 mm in length and 4.6 mm in diameter, particle size 5 μm . The parameters and elution method below, were used for all HPLC analysis performed on the SIELC-Primesep SB column.

The column was found to be very prone shifting peak retention time subsequently, a cleaning step was added in to the protocol, running at 40 % acetonitrile and 60 % buffer C.

Parameter	Value	Unit
Injection Volume	10	μL
Detector	254	nm

Step	Time / min	Flow /mlmin ⁻¹	% C	% D	ACN	Curve
0	5	1	70	30	0	0
1	30	1	0	100	0	1
2	5	1	0	100	0	0
3	5	1	70	0	30	1
4	15	1	60	0	40	1
5	5	1	70	30	0	1
6	5	1	70	30	0	0

Compound	Retention Time / min
----------	----------------------

GDP	10
GTP	22

References

- [1] H. Lodish, A. Berk, S. L. Zipursky, P. Matsudaira, D. Baltimore and J. Darnell, *Molecular Cell Biology*, 4th edition, 2000.
- [2] L. Weinschenk and C. Meier, in *Chemical Synthesis of Nucleoside Analogues*, John Wiley & Sons, Ltd, 2013, pp. 209–227.
- [3] A. Varki and N. Sharon, in *Essentials of Glycobiology*, Cold Spring Harbor, 2nd edn., 2009.
- [4] K. Colley, J. Esko and A. Varki, in *Essentials of Glycobiology*, Cold Spring Harbor, 2nd edn., 2009.
- [5] H. Freeze and A. Elbein, in *Essentials of Glycobiology*, Cold Spring Harbor, 2nd edn., 2009.
- [6] P. A. Frey, *The FASEB Journal*, 1996, **10**, 461–470.
- [7] H. M. Holden, I. Rayment and J. B. Thoden, *J. Biol. Chem.*, 2003, **278**, 43885–43888.
- [8] Z. Lazar, H. Gamboa-Meléndez, A.-M. C. Le Coq, C. Neuvéglise and J.-M. Nicaud, *Biotechnol Biofuels*, 2015, **8**, year.
- [9] J. A. Adams, *Chem. Rev.*, 2001, **101**, 2271–2290.
- [10] G. Manning, D. B. Whyte, R. Martinez, T. Hunter and S. Sudarsanam, *Science*, 2002, **298**, 1912–1934.
- [11] S. Hanks, A. Quinn and T. Hunter, *Science*, 1988, **241**, 42–52.
- [12] *Encyclopedia of Immunology*, ed. P. J. Delves and I. M. Roitt, Academic Press, San Diego, 2nd edn., 1998.
- [13] D. Knighton, J. Zheng, L. Teneyck, V. Ashford, N. Xuong, S. Taylor and J. Sowadski, *Science*, 1991, **253**, 407–414.
- [14] M. N. Levit, B. M. Abramczyk, J. B. Stock and E. H. Postel, *J. Biol. Chem.*, 2002, **277**, 5163–5167.
- [15] D. R. W. Hodgson and Martin Schröder, *Chem. Soc. Rev.*, 2011, **40**, 1211–1223.
- [16] C. Dumas, I. Lascu, S. Morera, P. Glaser, R. Fourme, V. Wallet, M. L. Lacombe, M. Veron and J. Janin, *EMBO J.*, 1992, **11**, 3203–3208.
- [17] M. Valiev, J. Yang, J. A. Adams, S. S. Taylor and J. H. Weare, *J. Phys. Chem. B*, 2007, **111**, 13455–13464.
- [18] P. A. Frey, in *The Enzymes*, ed. D. S. Sigman, Academic Press, 1992, vol. 20, pp. 141–186.
- [19] P. V. Attwood and T. Wieland, *Naunyn-Schmiedeberg's Arch Pharmacol*, 2015, **388**, 153–160.
- [20] S. Schaertl, M. Konrad and M. A. Geeves, *J. Biol. Chem.*, 1998, **273**, 5662–5669.
- [21] B. Roy, A. Depaix, C. Périgaud and S. Peyrottes, *Chem. Rev.*, 2016, **116**, 7854–7897.
- [22] R. Wolfenden, *Annu. Rev. Biochem.*, 2011, **80**, 645–667.
- [23] M. Tetas and J. M. Lowenstein, *J. Biochem.*, 1963, **2**, 350–357.
- [24] R. B. Stockbridge and R. Wolfenden, *J. Biol. Chem.*, 2009, **284**, 22747–22757.
- [25] M. Yoshikawa, T. Kato and T. Takenishi, *Tetrahedron Lett*, 1967, **8**, 5065–5068.
- [26] K. Burgess and D. Cook, *Chem. Rev.*, 2000, **100**, 2047–2060.
- [27] J. Ludwig, *Biochim. Biophys. Acta. Bioenerg.*, 1981, **16 (3-4)**, 131 – 134.

- [28] J. W. Kozarich, A. C. Chinault and S. M. Hecht, *Biochemistry*, 1973, **12**, 4458–4463.
- [29] I. Gillerman and B. Fischer, *Nucleosides Nucleotides Nucleic Acids*, 2010, **29**, 245–256.
- [30] J. G. Moffatt and H. G. Khorana, *J. Am. Chem. Soc.*, 1961, **83**, 649–658.
- [31] D. E. Hoard and D. G. Ott, *J. Am. Chem. Soc.*, 1965, **87**, 1785–1788.
- [32] H. Takaku, T. Konishi and T. Hata, *Chem. Lett.*, 1977, **6**, 655–658.
- [33] R. B. Merrifield, *J. Am. Chem. Soc.*, 1963, **85**, 2149–2154.
- [34] P. H. Toy and K. D. Janda, *Acc. Chem. Res.*, 2000, **33**, 546–554.
- [35] R. K. Gaur, B. S. Sproat and G. Krupp, *Tetrahedron Lett*, 1992, **33**, 3301–3304.
- [36] V. C. Tonn and C. Meier, *Chem.: Eur. J.*, 2011, **17**, 9832–9842.
- [37] C. Crauste, C. Périgaud and S. Peyrottes, *J. Org. Chem.*, 2009, **74**, 9165–9172.
- [38] S. Peyrottes, C. Perigaud and C. CRAUSTE, 2009.
- [39] A. Depaix, J.-Y. Puy, B. Roy and S. Peyrottes, *New J. Chem.*, 2018, **42**, 16441–16445.
- [40] M. Hölzl, A. Tinazli, C. Leitner, C. D. Hahn, B. Lackner, R. Tampé and H. J. Gruber, *Langmuir*, 2007, **23**, 5571–5577.
- [41] W. Wu, D. E. Bergstrom and J. V. Davisson, *J. Org. Chem.*, 2003, **68**, 3860–3865.
- [42] W. Wu, D. E. Bergstrom and J. V. Davisson, *Curr Protoc Nucleic Acid Chem*, 2004, **Chapter 13**, Unit 13.2.
- [43] S. J. Admiraal, B. Schneider, P. Meyer, J. Janin, M. Véron, D. Deville-Bonne and D. Herschlag, *Biochemistry*, 1999, **38**, 4701–4711.
- [44] S. Kara, J. H. Schrittwieser, F. Hollmann and M. B. Ansorge-Schumacher, *Appl. Microbiol. Biotechnol.*, 2014, **98**, 1517–1529.
- [45] H. Zhao and W. A. van der Donk, *Current Opinion in Biotechnology*, 2003, **14**, 583–589.
- [46] D. C. Crans, R. J. Kazlauskas, B. L. Hirschbein, C.-H. Wong, O. Abril and G. M. Whitesides, in *Methods in Enzymology*, Academic Press, 1987, vol. 136 of Immobilized Enzymes and Cells, Part C, pp. 263–280.
- [47] F. Cramer, H. Schaller and H. Staab, *Chem. Ber*, 1961, **94**, 1612 – 1619.
- [48] S. M. Resnick and A. J. B. Zehnder, *Appl. Environ. Microbiol.*, 2000, **66**, 2045–2051.
- [49] A. Kameda, T. Shiba, Y. Kawazoe, Y. Satoh, Y. Ihara, M. Munekata, K. Ishige and T. Noguchi, *J. Biosci. Bioeng.*, 2001, **91**, 557–563.
- [50] J. N. Andexer and M. Richter, *ChemBioChem*, 2015, **16**, 380–386.
- [51] J. D. Watson and F. H. C. Crick, *Nature*, 1953, **171**, 737–738.
- [52] Matt Carter and J. Schieh, in *Guide to Research Techniques in Neuroscience*, Elsevier Inc, 2010, pp. 207 – 227.
- [53] L. Conway, R. J. Delley, J. Neville, G. Freeman, H. Maple, V. Chan, A. J. Hall and D. Hodgson, *RSC Adv.*, 2014, **4**, year.
- [54] E. S. Orth, E. H. Wanderlind, M. Medeiros, P. S. M. Oliveira, B. G. Vaz, M. N. Eberlin, A. J. Kirby and F. Nome, *J. Org. Chem.*, 2011, **76**, 8003–8008.
- [55] T. Rathlev and T. Rosenberg, *Arch. Biochem. Biophys.*, 1956, **65**, 319–339.

- [56] Y.-F. Wei and H. R. Matthews, in *Methods in Enzymology*, Academic Press, 1991, vol. 200 of Protein Phosphorylation Part A: Protein Kinases: Assays, Purification, Antibodies, Functional Analysis, Cloning, and Expression, pp. 388–414.
- [57] S. J. Benkovic and E. J. Sampson, *J. Am. Chem. Soc.*, 1971, **93**, 4009–4016.
- [58] J. D. Chanley and E. Feageson, *J. Am. Chem. Soc.*, 1963, **85**, 1181–1190.
- [59] B. Nikolin, B. Imamović, S. Medanhodžić-Vuk and M. Sober, *Bosn. J. Basic Med. Sci.*, 2004, **4**, 5–9.
- [60] S. Winkel Pettersson, in *Protein Purification: Principles, High Resolution Methods and Applications*, John Wiley & Sons, 3rd edn., 2011, pp. 135 – 164.
- [61] A. Biosciences, *Reversed Phase Chromatography: Principles and Methods*, 1999.
- [62] S. Lindsay, *High Performance Liquid Chromatography*, John Wiley & Sons, 2nd edn., 1992.
- [63] C. K Yerneni, *Journal of Analytical & Pharmaceutical Research*, 2017, **4**, year.
- [64] J. Zhang, T. Raglione, Q. Wang, B. Kleintop, F. Tomasella and X. Liang, *J Chromatogr Sci*, 2011 Nov-Dec, **49**, 825–831.
- [65] K. Zhang and X. Liu, *Journal of Pharmaceutical and Biomedical Analysis*, 2016, **128**, 73–88.
- [66] X. Liu and C. A. Pohl, *J. Sep. Sci.*, 2010, **33**, 779–786.
- [67] J. Kowalska, M. Lewdorowicz, E. Darzynkiewicz and J. Jemielity, *Tetrahedron Lett*, 2007, **48**, 5475–5479.
- [68] S. Aldrich, *Bulletin 913: Rapid, Reliable Nucleotides Analyses, Using SUPELCOSIL LC-18-T HPLC Columns*.
- [69] S. J. Admiraal, P. Meyer, B. Schneider, D. Deville-Bonne, J. Janin and D. Herschlag, *Biochemistry*, 2001, **40**, 403–413.
- [70] H. J. Korhonen, L. P. Conway and D. R. W. Hodgson, *Curr. Opin. Chem. Biol.*, 2014, **21**, 63–72.
- [71] S. E. Lee, L. M. Elphick, H. B. Kramer, A. M. E. Jones, E. S. Child, A. A. Anderson, L. Bonnac, N. Suwaki, B. M. Kessler, V. Gouverneur and D. J. Mann, *ChemBioChem*, 2011, **12**, 633–640.